Supporting Information

Customising excitation properties of polycyclic aromatic hydrocarbons by rational positional heteroatom doping: the peri-xanthenoxanthene (PXX) case

Cataldo Valentini,[a] Duncan Gowland,[b] C. Grazia Bezzu,[a] Deborah Romito,[c] Nicola Demitri,[d] Nicola Bonini[b,*] and Davide Bonifazi[a,c,*]

[a]*School of Chemistry, Cardiff University, Main Building, Park Place, Cardiff CF10 3AT, United Kingdom*

[b]*Department of Physics, King's College London, Strand, London, WC2R 2LS, United Kingdom; Email: nicola.bonini@kcl.ac.uk*

[c]*Institute of Organic Chemistry, Faculty of Chemistry, University of Vienna, Währinger Str. 38, 1090, Vienna, Austria; E-mail: davide.bonifazi@univie.ac.at*

[d]*Elettra - Sincrotrone Trieste, S.S. 14 Km 163.5 in Area Science Park, 34149 Basovizza - Trieste, Italy*

1. General remarks

1.1 Instrumentation

Thin layer chromatography (TLC) was conducted on pre-coated aluminium sheets with 0.20 mm Merk Millipore Silica gel 60 with fluorescent indicator F254.

Column chromatography was carried out using Merck Gerduran silica gel 60 (particle size 40-63 μm).

Melting points (mp) were measured on a Gallenkamp apparatus in open capillary tubes and have not been corrected.

Nuclear magnetic resonance: (NMR) spectra were recorded on a Bruker Fourier 300 MHz spectrometer equipped with a dual (^{13}C, ^{1}H) probe, a Bruker AVANCE III HD 400MHz NMR spectrometer equipped with a Broadband multinuclear (BBFO) SmartProbeTM or a Bruker AVANCE III HD 500MHz Spectrometer equipped with Broadband multinuclear (BBO) Prodigy CryoProbe. ^{1}H spectra were obtained at 300, 400 or 500 MHz, ^{13}C spectra were obtained at 75, 100 or 125 MHz NMR. All spectra were measured at r.t. if not otherwise stated. Chemical shifts were reported in ppm relative to tetramethylsilane using the solvent residual signal as an internal reference (CDCl3: δ_H = 7.26 ppm, δ_C = 77.16 ppm; THF: δ_H = 1.73 ppm, δ_C = 25.30 ppm; DMSO-d_6: δ_H = 2.50 ppm, δ_C = 39.52 ppm, CD_2Cl_2: δ_H = 54.00 ppm, δ_C = 40.45 ppm). Coupling constants (*J*) were given in Hz. Resonance multiplicity was described as s (singlet), d (doublet), t (triplet), q (quartet) and broad (broad signal). Carbon spectra were acquired with a complete decoupling for the proton. The Attached Proton Test (APT) experiments were used to determine C-H multiplicities in carbon spectra and the peaks assigned as singlet (s) for quaternary and doublet (d) for tertiary carbon atoms.

Infrared spectra (IR) were recorded on a Shimadzu IR Affinity 1S FTIR spectrometer in ATR mode with a diamond mono-crystal. Selected absorption bands are reported by wavenumber (cm^{-1}).

Mass spectrometry: (i) High-resolution ESI mass spectra (HRMS) were performed on a Waters LCT HR TOF mass spectrometer in the positive or negative ion mode. (ii) High-resolution MALDI mass spectra (HRMS) were performed on a Waters Synapt G2-Si QTOF mass spectrometer, all these analyses were carried out at Cardiff University.

Photophysical analysis: Absorption spectra of compounds were recorded on air equilibrated solvents at room temperature with Agilent Cary 5000 UV-Vis spectrophotometer, using quartz HELLMA cells with path length of 1.0 cm. Emission spectra were recorded on Agilent Cary Eclipse fluorescence spectrofluorometer. Emission lifetime measurements were performed on a JobinYvon-Horiba FluoroHub single photon counting module, using Nano-LED pulsed source at 405 nm or 280 nm. Quantum yield values were calculated using Coumarin 153 in air equilibrated ethanol (Φ = 0.53) or rhodamine 6G in Ethanol (Φ = 0.94), following the method of Demas and Crosby.[11]

Electrochemical characterization: Cyclic voltammetry experiments were performed at room temperature in dry nitrogen-purged ortho-dichlorobenzene (ODCB), CH_2Cl_2 or CH_3CN (previously filtered on alumina, 50 - 200 µm), with a Model 800 potentiostat (CH Instruments). The working electrode used is a glassy carbon S3 electrode (3 mm diameter), the counter electrode was a Pt spiral and an Ag wire was used as quasi-reference electrode (AgQRE). Working electrode and quasi-reference electrodes were polished on a felt pad with 0.05 or 0.3 µm alumina suspension and sonicated in deionized water for 1 minute before each experiment; the Pt wire was flame-cleaned. Tetrabutylammonium hexafluorophosphate ($TBAPF_6$) were added to the solution as supporting electrolytes at concentrations typically 2 orders of magnitude higher than the electroactive analyte. The couple ferrocene/ferrocenium was used as internal reference ($E_{1/2}^{ox}$=0.45 V in ODCB, $E_{1/2}^{ox}$=0.37 V in CH_2Cl_2). HOMO and LUMO energies were calculated from the first formal redox potentials (halfwave potentials) using equations: $E_{HOMO} = -\left(E_{1/2}^{ox} + 5.1\ eV\right)$; $E_{LUMO} = -\left(E_{1/2}^{red} + 5.1\ eV\right)$. In the cases where oxidation or reduction waves were not detected by means of cyclic voltammetry, HOMO or LUMO levels are calculated using the optical gap E_{opt}, considering the crossing point between normalised absorption and emission spectra, recorded with the same experimental conditions, in the same solvent. The corresponding eV were calculated following equation: E_{opt} = 1240 / λ_{cross} (nm).

X-ray measurements: Crystallographic studies were undertaken on single crystal mounted onto a MiTiGen Microloop TM using paratone oil and studied on an Agilent SuperNova Dual three-circle diffractometer using Cu-Kα (λ = 1.540598 Å) or Mo-Kα (λ = 0.7093187 Å) radiation and a CCD detector. Measurements were typically made at 150(1) K with temperatures maintained using an Oxford Cryostream unless otherwise stated. Data were collected, integrated and corrected for absorption using a numerical absorption correction based on gaussian integration over a multifaceted crystal model within CrysAlisPro. The structures were solved by direct methods and refined against F2 within SHELXL-2013.

1.2 Materials and General Methods

Chemicals were purchased from *Sigma Aldrich*, *Acros Organics*, *TCI, Apollo Scientific*, *Alfa Aesar* and *Fluorochem* and were used as received unless specified otherwise. Solvents were purchased from *Fluorochem*, *Sigma Aldrich* and *Acros Organics*. Deuterated solvents were purchased from *Eurisotop* and *Sigma Aldrich*. THF, Et_2O and CH_2Cl_2 were dried on a *Braun* MB SPS-800 solvent purification system. Et_3N was distilled on CaH_2 and then stored over KOH. DMF and pyridine were dried on molecular sieves 4 Å and then stored over molecular sieves 4 Å. Sulfuric acid (H_2SO_4 >95%) was purchased from *Fluorochem*. Low temperature baths were prepared using different solvent mixtures depending on the desired temperature: -84 °C with ethyl acetate/liq. N_2, -78 °C with acetone/dry ice and 0 °C with ice/H_2O. Anhydrous conditions were achieved by flaming two necked flasks with a heat gun under vacuum and purging with N_2. The inert atmosphere was maintained using N_2-filled balloons equipped with a syringe and needle that was used to penetrate the rubber stoppers used to close the flask's necks. Additions of liquid reagents were performed using dried plastic or glass syringes. All reactions were performed in dry conditions and under inert atmosphere unless otherwise stated.

2. Synthetic procedures and spectral data

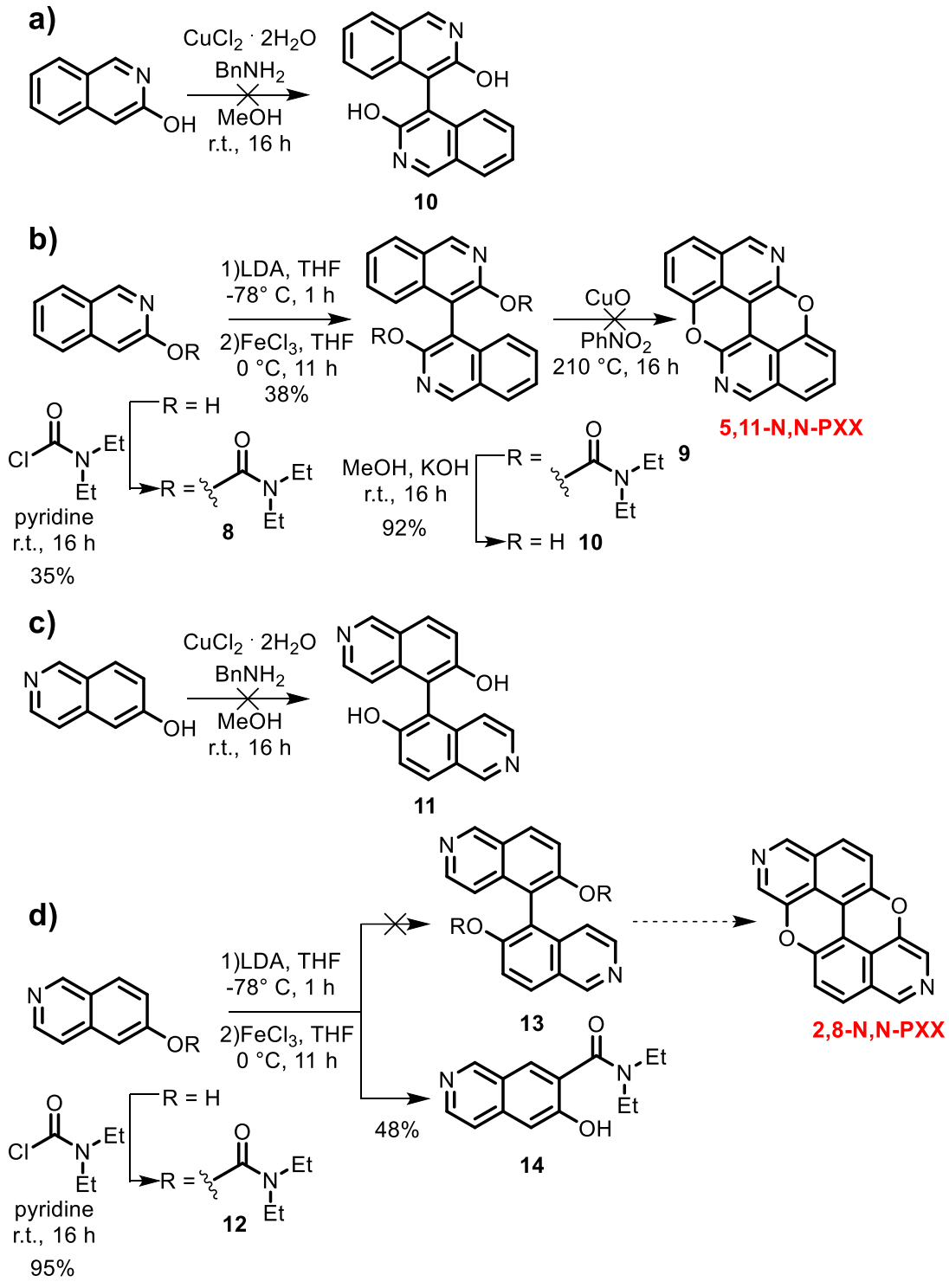

Scheme S1. Synthetic approaches for the synthesis of **5,11-N,N-PXX** (a and b) and **2,8-N,N-PXX** (c and d).

Synthesis of [8,8'-biisoquinoline]-7,7'-diol 2

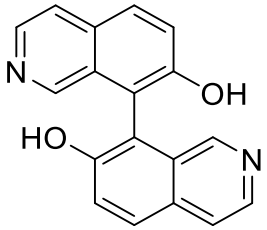

2

To a stirred solution of $CuCl_2 \cdot 2H_2O$ (2.82 g, 16.53 mmol) in MeOH (130 mL) was added a solution of benzylamine (5.91 mg, 55.11 mmol) in MeOH (30 mL) and the reaction mixture was stirred for 5 min. A solution of 7-hydroxylisoquinoline (1 g, 6.89 mmol) in MeOH (30 mL) was added and the reaction mixture stirred at rt for 16 h. During this period the colour of the mixture turned from green to brown. The reaction solvent was halved. The brown precipitate filtered and washed with MeOH. The crude was dissolved in a 5 mL of HCl 37 % aqueous solution and reprecipitated upon addition of 10 mL of NH_3 35% aqueous solution. The brown precipitate was filtered and washed with 30 mL of H_2O and 5 mL of methanol yielding **2** as pure brown solid (614 mg, 63 %).

mp 170–175°C. IR (neat): cm^{-1} 417, 440, 494, 540, 579, 656, 702, 741, 779, 826, 934, 972, 1049, 1096, 1165, 1234, 1273, 1288, 1319, 1366, 1404, 1435, 1504, 1597, 1705, 1867, 1960, 2006, 2554, 2600, 2632, 3001, 3063. ^{1}H-NMR (500 MHz, DMSO-d_6) δ: 9.86 (s, 2H), 8.33 (broad d, *J* = 18.0 Hz, 4H), 7.98 (d, *J* = 9.0 Hz, 2H), 7.80 (s, 2H), 7.60 (d, *J* = 9.0 Hz, 2H). ^{13}C-NMR (125 MHz, DMSO-d_6) δ 154.6, 149.2, 140.4, 130.7, 128.7, 123.5, 114.1. HRMS (ES+): m/z $[M+H]^+$ calcd for ($C_{18}H_{13}N_2O_2$): 289.0977; found: 289.0977.

Synthesis of 1,7-diaza peri-xanthenoxanthene 1,7-N,N-PXX

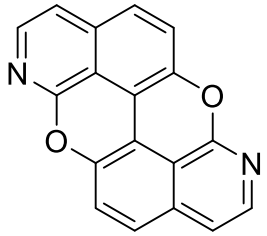

1,7-N,N-PXX

In a round bottomed flask, **2** (200 mg, 0.69 mmol) and CuO (496.6 mg, 6.24 mmol) were suspended in 3 mL of $PhNO_2$. The reaction mixture was stirred at 200 °C for 10 h. The solvent was evaporated under reduced pressure and the reaction mixture dissolved in hot THF (50 mL), then filtered on celite. The organic phase was concentrated under reduced pressure. The crude was purified through column chromatography on silica gel with eluent (toluene/THF 9:1) to give product as a yellow solid (103 mg, 52%)

m.p. 182-185 °C. IR (neat): cm^{-1} 494, 525, 586, 679, 725, 772, 833, 941, 1065, 1227, 1319, 1427, 1474, 1582, 1620, 1697, 1744, 1805, 1906, 2855, 2916, 2955, 3040. ^{1}H-NMR (500 MHz, $CDCl_3$): δ 7.91 (d, *J* = 6.0 Hz, 2H), 7.50 (d, *J* = 9.0 Hz, 2H), 7.42 (d, *J* = 9.0, 2H), 7.09 (d, *J* = 6.0 Hz, 2H). ^{13}C-NMR (125 MHz, $CDCl_3$): δ 142.8, 125.6, 121.7, 115.9, 113.5, four carbon peaks are missing. HRMS (ES+): m/z $[M+H]^+$ calcd for ($C_{18}H_9N_2O_2$): 285.0664; found: 285.0670

Synthesis of [5,5'-biquinoline]-6,6'-diol 1

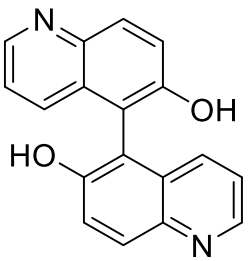

1

To a stirred solution of $CuCl_2 \cdot 2H_2O$ (2.82g, 16.53 mmol) in MeOH (130 mL) was added a solution of benzylamine (5.91 mg, 55.11 mmol) in MeOH (30 mL) and the solution was stirred for 5 min. A solution of quinoline-6-ol (1 g, 6.89 mmol) in MeOH (30 mL) was added and the reaction mixture was stirred at r.t. for 16 h. During this period the colour of the mixture turned from green to brown. The reaction solvent was halved, and the brown precipitate filtered and washed with MeOH. The crude was dissolved in 5 mL of HCl 37 % solution and reprecipitated by adding 10 mL of NH_3 35%. The brown precipitate was filtered and washed with 30 mL of water and 5 mL of MeOH yielding product **1** as a brown solid (550 mg, 55 %).

mp 174–176°C. ^{1}H-NMR (500 MHz, DMSO-d) δ: 9.63 (s, 2H), 8.66 (s, 2H), 7.99 (d, *J* = 8.6 Hz, 2H), 7.56 (d, *J* = 8.6 Hz, 2H), 7.33 (m, 4H). ^{13}C-NMR (125 MHz, DMSO-d) δ 153.7, 147.2, 143.3, 132.8, 130.6, 129.3, 122.3, 121.8, 114.6. HRMS (EI+): m/z $[M]^+$ calcd for ($C_{18}H_{12}N_2O_2$): 288.0899; found: 288.0897 Characterization in accordance with literature.[42]

Synthesis of 3,9-diaza peri-xanthenoxanthene 3,9-N,N-PXX

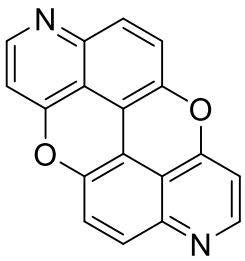

3,9-N,N-PXX

In a round bottomed flask, **1** (50 mg, 0.174 mmol) and CuO (137.9 mg, 1.73 mmol) were suspended in 1 mL of $PhNO_2$. The reaction mixture was stirred at 200 °C for 16 h. The solvent was distilled off under reduced pressure, the reaction mixture dissolved in hot THF (50 mL) and filtered on celite. The organic phase was concentrated under reduced pressure. The crude was purified through silica gel column chromatography (toluene/THF 7:3) to give product as orange solid (12 mg, 23%).

m.p. 176-181 °C. IR (neat): cm^{-1} 408.9, 447.4, 486.0, 516.9, 563.2, 594.5, 663.5, 735.9, 756.1, 779.2, 825.5, 894.9, 941.2, 1080.1, 1134.1, 1211.3, 1257.6, 1342.6, 1404.2, 1465.9, 1573.9, 620.2, 1720.5, 1905.6, 1975.1, 2854.6, 2916.3, 3055.2, 3086.1. ^{1}H-NMR (500 MHz, $CDCl_3$): δ 8.46 (d, *J* = 5.3 Hz, 2H), 7.64 (d, *J* = 9.3 Hz, 2H), 7.24 (d, *J* = 9.3 Hz, 2H), 6.61 (d, *J* = 5.3 Hz, 2H). ^{13}C-NMR (125 MHz, $CDCl_3$): δ 153.3, 143.3, 127.9, 120.6, 116.7, 111.9, 105.2, two carbon peaks missing. HRMS (ES+): m/z $[M+H]^+$ calcd for ($C_{18}H_9N_2O_2$): 285.0664; found: 285.0668

Synthesis of molecule 3

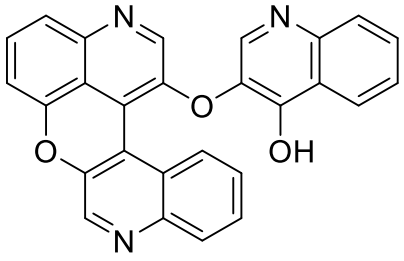

3

In a round bottomed flask, quinolin-3-ol (100 mg, 0.69 mmol) and CuCl (68 mg, 0.69 mmol) were dissolved in 1 mL of DMSO. The reaction mixture was stirred at 120 °C for 16 h. The reaction mixture was quenched with 3 mL of NH_4Cl aq. sat. solution, the organic phase extracted with AcOEt (10 mL x 3) and washed with brine (20 mL x 5). The organic phase was dried over $NaSO_4$ and evaporated under reduce pressure. The crude material was purified through column chromatography on silica gel with eluent (CH_2Cl_2/AcOEt 7:3) to give product **3** as a yellow solid (18 mg, 30%).

m.p. 186-189 °C. IR (neat): cm^{-1} 418.5, 432.0, 459.0, 484.1, 538.1, 563.2, 592.1, 611.4, 628.7, 688.5, 715.5, 759.9, 788.8, 817.8, 864.1, 883.4, 910.4, 945.1, 987.5, 1001.0, 1029.9, 1047.3, 1068.5, 1114.8, 1147.6, 1220.9, 1232.5, 1257.5, 1269.1, 1303.8, 1338.6, 1363.6, 1413.8, 1465.9, 1473.6,

1496.7, 1556.5, 1598.9, 1624.0, 2924.0, 2981.9, 3064.8, 3396.6. ^{1}H-NMR (500 MHz, $CDCl_3$): δ 8.97 (s, 1H), 8.79 (dd, *J* = 8.6, 0.8 Hz, 1H), 8.53 (s, 1H), 8.34 (s, 1H), 8.22 (dd, *J* = 8.2, 1.1 Hz, 1H), 8.02 (dd, *J* = 8.3, 0.9 Hz, 1H), 7.76 – 7.70 (m, 1H), 7.69 – 7.60 (m, 4H), 7.48 (ddd, *J* = 8.4, 6.9, 1.3 Hz, 1H), 7.41 (ddd, *J* = 8.1, 6.9, 1.1 Hz, 1H), 7.28 (dd, *J* = 6.9, 1.8 Hz, 1H).^{13}C-NMR (125 MHz, $CDCl_3$): δ 148.9, 148.49, 145.9, 144.7, 144.6, 144.6, 142.7, 135.0, 133.6, 132.1, 129.2, 128.5, 128.4, 128.2, 126.6, 126.4, 125.5, 123.7, 123.7, 121.9, 119.7, 119.5, 118.5, 115.7, 109.4, 107.0 (1 carbon peak is missing). LRMS (ASAP+): m/z $[M+H]^+$ calcd for ($C_{27}H_{16}N_3O_3$): 430.12; found: 430.12.

Synthesis of quinolin-3-yl diethylcarbamate 4

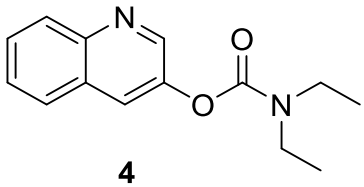

4

To a stirred solution of quinolin-3-ol (0.69 mmol, 100 mg) in 1 mL of dry pyridine at r.t. under N_2 was added diethylamino carbonyl chloride (0.69 mmol, 0.16 mL). The resulting brown solution was heated to 100 °C and stirred for 16 h. After this time the mixture was allowed to cool to r.t. and partitioned between EtOAc (15 mL) and H_2O (10 mL). The pH of the aqueous layer was adjusted to 9 by the addition of aq. $NaHCO_3$ sat. solution and the layers were shaken and separated. The aqueous phase was extracted with EtOAc (15 mL x 3) and the combined organic dried on Na_2SO_4 and concentrated in vacuo. The crude residue was further purified in a silica gel column chromatography (EtOAc) yielding **4** as a colourless oil (160.00 mg, 95%).

IR (neat): cm^{-1} 428.2, 482.2, 555.5, 615.2, 748.3, 759.9, 827.4, 908.4, 920.0, 956.6, 1001.0, 1045.4, 1076.2, 1093.6, 1147.6, 1207.4, 1255.6, 1307.7, 1352.1, 1409.9, 1425.4, 1463.9, 1498.6, 1568.1, 1604.7, 1641.4, 1714.7, 2873.9, 2931.8, 2974.2, 3059.1.^{1}H-NMR (300 MHz, $CDCl_3$): δ 8.67 (broad s, 1H), 8.02 (broad d, *J* = 8.5 Hz, 1H), 7.88 (d, *J* = 2.5 Hz, 1H), 7.70 (dd, *J* = 8.2, 1.5 Hz, 1H), 7.57 (ddd, *J* = 8.5, 6.9, 1.5 Hz, 1H), 7.44 (ddd, *J* = 8.2, 6.9, 1.1 Hz, 1H), 3.37 (m, 4H), 1.16 (m, 6H).^{13}C-NMR (75 MHz, $CDCl_3$): δ 153.6, 146.2, 145.7, 144.9, 129.3, 128.6, 128.3, 127.6, 127.1, 125.9, 42.5, 42.1, 14.3, 13.4. HRMS (ES+): m/z $[M+H]^+$ calcd for ($C_{14}H_{17}N_2O_2$): 245.1290; found: 245.1296

Synthesis of [4,4'-biquinoline]-3,3'-diyl bis(diethylcarbamate) 5

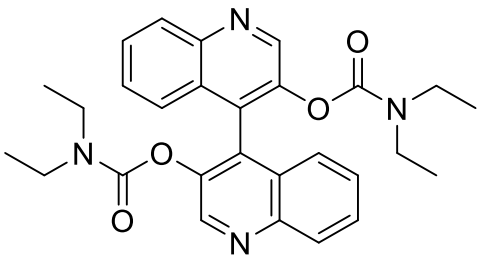

5

To a stirred solution of **4** (2.70 mmol, 660 mg) in 5 mL of dry THF was cooled down at -78 °C and LDA (3.51 mmol, 3.51 mL) added dropwise. The dark brown solution was stirred for 30 min, at –78 °C. In parallel, anhydrous $FeCl_3$ (2.70 mmol, 440 mg) was suspended in dry THF (5 mL) and cooled at -78 °C (dry powdered $FeCl_3$ had been previously dried at 120 °C at 0.5 mmHg for 16 h). The suspension of $FeCl_3$ was carefully added to the dark brown solution. The resulting dark brown mixture was allowed to warm to 0 °C and stirred for 11 h. The mixture was quenched with NH_4Cl aq. sat. and diluted EtOAc with H_2O (2 mL) and extracted with EtOAc (20 mL x 3) and the combined organic phase dried on Na_2SO_4 and concentrated in *vacuo*. The crude residue was purified a silica gel column chromatography (petroleum ether/EtOAc 7:3) yielding **5** as a colourless oil (340 mg, 52%).

IR (neat): cm^{-1} 425.2, 486.3, 549.6, 617.3, 750.4, 757.5, 828.6, 908.5, 923.0, 957.5, 1008.4, 1043.4, 1077.2, 1095.6, 1145.7, 1202.9, 1254.9, 1308.2, 1355.1, 1411.2, 1425.9, 1468.0, 1405.8, 1571.1, 1601.4, 1649.4, 1718.8, 2877.0, 2932.8, 2976.1, 3060.1. ^{1}H-NMR (500 MHz, $CDCl_3$): δ 9.04 (s, 2H), 8.21 (broad dd, *J* = 8.1 Hz, 2H), 7.69 (broad m, 2H), 7.43 (broad m, 2H), 7.32 (broad dd, 2H), 3.09 (m, 4H), 2.75 (m, 4H), 0.88 (t, *J* = 7 Hz, 6H) 0.43 (t, *J* = 7 Hz, 6H). ^{13}C-NMR (75 MHz, $CDCl_3$): δ 152.6, 147.3, 145.5, 142.9, 129.8, 129.6, 128.9, 127.6, 127.1, 125.5, 42.3, 4.7, 13.2, 13.0. HRMS (ES+): m/z $[M+H]^+$ calcd for ($C_{28}H_{31}N_4O_4$): 487.2345; found: 487.2341

Synthesis of [4,4'-biquinoline]-3,3'-diol 6

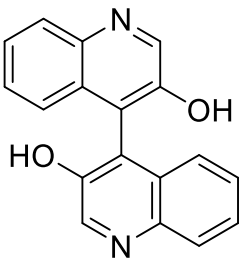

6

A solution of diaryl-dicarbamate **5** (140 mg, 0.288 mmol) in 10 wt.% methanolic KOH (7 mL) was stirred at reflux for 18 h. The resulting solution was cooled to r.t. and concentrated in *vacuo*. The residue was dissolved in H_2O (5 mL) and the pH adjusted to 7 by the careful addition of 2 M aq. HCl. The aqueous phase was saturated with NaCl and the formed precipitate filtered and washed with H_2O and cold EtOH. The precipitate was dried under *vacuo* yielding **6** as a white solid (80 mg, 98%).

m.p. 176-179 °C. IR (neat): cm^{-1} 403.1, 418.5, 457.1, 466.7, 480.2, 514.9, 563.2, 655.8, 669.3, 719.4, 746.4, 808.1, 844.8, 883.4, 920.0, 954.7, 1062.7, 1103.2, 1136.0, 1151.5, 1195.8, 1220.9, 1296.1, 1330.8, 1388.7, 1446.6, 1490.9, 1506.4, 1573.9, 1600.9, 1627.9, 1716.6, 1749.4, 2358.9, 2926.0, 2980.0, 3080.3. ^{1}H-NMR (500 MHz, DMSO-d_6): δ 10.1 (s, 2H), 8.8 (s, 2H), 8.03 (dd, *J* = 8.4 Hz, *J* = 0.9 Hz, 2H), 7.53 (ddd, *J* = 8.3 Hz, *J* = 6.8 Hz, *J* = 1.4 Hz, 2H), 7.35 (ddd, *J* = 8.2 Hz, *J* = 6.9 Hz, *J* = 1.2 Hz, 2H), 7.03 (dd, *J* = 8.3 Hz, *J* = 1.0 Hz, 2H). ^{13}C-NMR (125 MHz, DMSO-d_6): δ 148.6, 143.6, 142.6, 129.2, 127.9, 127.0, 125.8, 124.2, 120.3. HRMS (ES+): m/z $[M+H]^+$ calcd for ($C_{18}H_{13}N_2O_2$): 289.0977; found: 289.0982

Synthesis of 4,10-diaza peri-xanthenoxanthene 4,10-N,N-PXX

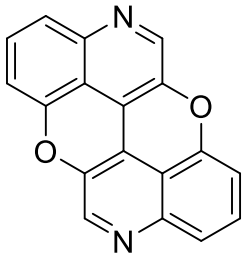

4,10-N,N-PXX

In a round bottomed flask, **6** (50 mg, 0.174 mmol) and CuO (137.9 mg, 1.73 mmol) were suspended in 1 mL of $PhNO_2$. The reaction mixture was stirred at 200 °C for 16 h. The solvent was evaporated under reduced pressure and the reaction mixture dissolved in hot THF (50 mL) and filtered on celite. The organic phase was concentrated under reduced pressure. The crude was purified through column chromatography on silica gel with eluent (toluene/THF 9:1) to give product as orange solid (10 mg, 20%).

m.p. 180-184 °C. IR (neat): cm^{-1} 403.1, 418.5, 457.1, 466.7, 480.2, 514.9, 563.2, 655.8, 669.3, 719.4, 746.4, 808.1, 844.8, 883.4, 920.0, 954.7, 1062.7, 1103.2, 1136.0, 1151.5, 1195.8, 1220.9, 1296.1, 1330.8, 1388.7, 1446.1, 1465.9, 1490.9, 1506.4, 1573.9, 1600.9, 1627.9, 1683.8, 1716.6, 1749.4, 2358.9, 2926.0, 2980.0, 3080.3.^{1}H-NMR (500 MHz, $CDCl_3$): δ 8.53 (s, 2H), 7.48 (m, 4H), 6.91 (dd, *J* = 7.2, J = 1.2 Hz, 2H) ^{13}C-NMR (125 MHz, $CDCl_3$): δ 151.3, 145.2, 141.8, 141.4, 130.5, 122.2, 116.7, 115.8, 110.2. HRMS (ES+): m/z $[M+H]^+$ calcd for ($C_{18}H_9N_2O_2$): 285.0664; found: 285.0667

Synthesis of 1,9-diaza peri-xanthenoxanthene 1,9-N,N-PXX

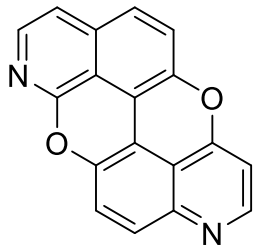

1,9-N,N-PXX

To a stirred solution of $CuCl_2 \cdot 2H_2O$ (564 mg, 3.31 mmol) in MeOH (20 mL) was added a solution of benzylamine (1.18 g, 11.02 mmol) in MeOH (20 mL) and the solution was stirred for 5 min. A solution of quinolin-6-ol (100 mg, 0.69 mmol) and isoquinolin-7-ol (100 mg, 0.69 mmol) in MeOH (40 mL) was added and the reaction mixture was stirred at r.t. for 16 h. During this period the colour of the mixture turned from green to brown. The reaction solvent was halved, and the brown precipitate filtered and washed with MeOH. The crude was dissolved in 5 mL of HCl 37 % solution and reprecipitate by adding 10 mL of NH_3 35%. The brown precipitate was filtered and washed with 30 mL of water and 5 mL of MeOH. The brown solid and CuO (1.08 g, 13.60 mmol) were suspended in 1 mL of $PhNO_2$. The reaction mixture was stirred at 200 °C for 16 h. The solvent was evaporated under reduced pressure, the reaction mixture dissolved in hot THF (50 mL) and filtered on celite. The organic phase was concentrated under reduced pressure. The crude was purified by silica gel column chromatography (toluene/THF 7:3) to give product as orange solid (12 mg, 5%).

m.p. 178-185 °C. IR (neat): cm^{-1} 422.2, 458.2, 467.1, 483.0, 515.0, 559.5, 657.2, 673.0, 717.5, 747.7, 8012.1, 834.3, 886.1, 921.5, 961.0, 1059.7, 1107.8, 1134.9, 1155.5, 1196.2, 1215.6, 1298.1, 1333.7, 1395.3, 1453.3, 1488.0, 1495.3, 1505.0, 1577.5, 1603.2, 1628.5, 1678.5, 2361.2, 2933.5, 2978.5, 3083.0.^{1}H-NMR (500 MHz, $CDCl_3$): δ 8.52 (d, *J* = 5.2 Hz, 1H), 7.87 (d, *J* = 6.0 Hz, 1H), 7.71 (d, *J* = 9.3 Hz, 1H), 7.38 (d, *J* = 9.0 Hz, 1H), 7.38 (d, *J* = 9.3 Hz, 1H), 7.25 (d, *J* = 9.0 Hz, 1H), 7.02 (d, *J* = 6.0 Hz, 1H), 6.65 (d, *J* = 5.2 Hz, 1H).^{13}C-NMR (125 MHz, $CDCl_3$): δ 160.5, 159.7, 153.5, 146.8, 144.7, 144.6, 143.0, 135.4, 128.8, 125.1, 121.3, 121.0, 116.8, 115.8, 115.8, 115.1, 110.3, 105.2. HRMS (AP+): m/z $[M+H]^+$ calcd for ($C_{18}H_9N_2O_2$): 285.0664; found: 285.0666.

Synthesis of isoquinolin-3-yl diethylcarbamate 8

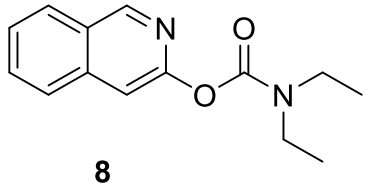

8

To a stirred solution of isoquinolin-3-ol (0.69 mmol, 100 mg) in 1 mL of dry pyridine at r.t. under N_2 was added dethylaminocarbonyl chloride (1.38 mmol, 0.16 mL). The resulting brown solution was heated to 100 °C and stirred for 16 h. After this time the mixture was allowed to cool to r.t. and partitioned between EtOAc (15 mL) and H_2O (10 mL). The pH of the aqueous layer was adjusted to 9 by the addition of $NaHCO_3$ aq. sat. solution and the layers were shaken and separated. The aqueous phase was extracted with EtOAc (15 mL x 3) and the combined organic dried on Na_2SO_4 and concentrated in vacuo. The crude residue was further purified in a silica gel column chromatography (EtOAc) yielding **12** as a yellow oil (59.00 mg, 35%).

IR (neat): cm^{-1} 426.2, 481.2, 557.5, 617.2, 756.3,759.9, 827.5, 901.4, 923.0, 956.7, 1006.5, 1051.47, 1074.8, 1096.9, 1149.9, 1207.4, 1265.2, 1301.0, 1363.1, 1409.5, 1433.2, 1455.2, 1520.6, 1578.1, 1609.1, 1646.9, 1730.0, 2886.0, 2935.1, 2965.3, 3063.1.^{1}H-NMR (300 MHz, $CDCl_3$): δ 9.08 (s, 1H), 7.96 (dd, *J* = 8.1, 0.9, 1H), 7.79 (dd, *J* = 8.3, 0.9, 1H), 7.66 (ddd, *J* = 8.3, 6.8, 0.9 Hz, 1H), 7.52 (ddd, *J* = 8.1, 6.8, 0.9 Hz, 1H), 7.47 (s, 1H), 3.46 (q, *J* = 7.1 Hz, 2H), 3.36 (q, *J* = 7.1, Hz, 2H), 1.24 (t, *J* = 7.0 Hz, 3H), 1.23 (t, *J* = 7.1, 3H).^{13}C-NMR (75 MHz, $CDCl_3$): δ 154.8, 154.0, 151.6, 138.6, 130.8, 127.6, 127.4, 126.6, 126.5, 110.8, 42.3, 42.1, 14.3, 13.4.HRMS (ES+): m/z $[M+H]^+$ calcd for ($C_{14}H_{17}N_2O_2$): 245.1290; found: 245.1299

Synthesis of [4,4'-biisoquinoline]-3,3'-diyl bis(diethylcarbamate) 9

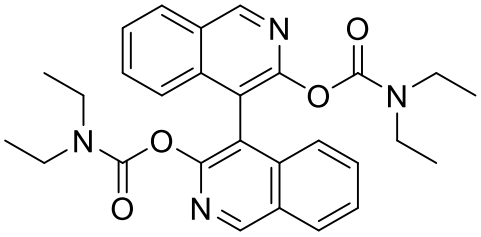

9

To a stirred solution of **8** (2.70 mmol, 660 mg) in 5 mL of dry THF was cooled down at -78 °C and LDA (3.51 mmol, 3.51 mL) added dropwise. The dark brown solution was stirred for 30 min, at –78 °C. In parallel, anhydrous $FeCl_3$ (2.70 mmol, 440 mg) was suspended in dry THF (5 mL) and cooled at -78 °C (powdered $FeCl_3$ had been previously dried at 120 °C at 0.5 mmHg for 16 h). The suspension of $FeCl_3$ was carefully added to the dark brown solution. The resulting dark brown mixture was allowed to warm to 0 °C and stirred for 11 h. The mixture was quenched with sat. aq. NH_4Cl and diluted EtOAc with H_2O (2 mL) and extracted with EtOAc (20 mL x 3) and the combined organic phase dried on Na_2SO_4 and concentrated in *vacuo*. The crude residue was purified by silica gel column chromatography (petroleum ether/EtOAc 7:3) yielding **9** as a colourless oil (252 mg, 38%).

IR (neat): cm^{-1} 430.2, 487.3, 551.6, 616.5, 753.9, 753.6, 825.6, 905.1, 925.5, 960.5, 1010.2, 1048.33, 1072.8, 1097.7, 1165.5, 1208.0, 1254.1, 1310.2, 1357.1, 1419.2, 1465.2, 1451.2, 1408.8, 1575.1, 1606.4, 1653.5, 1721.5, 2875.5, 2933.0, 2977.3, 3062.1.^{1}H-NMR (300 MHz, $CDCl_3$): δ 9.22 (s, 2H), 8.09 – 8.00 (m, 2H), 7.61 – 7.48 (m, 4H), 7.40 – 7.33 (m, 2H), 3.27 – 2.77 (m, 8H), 0.79 (t, *J* = 7.1 Hz, 6H), 0.64 (t, *J* = 7.0 Hz, 6H).^{13}C-NMR (75 MHz, $CDCl_3$): δ 153.2, 152.9, 152.2, 138.1, 131.2, 127.8, 127.3, 126.8, 125.4, 115.4, 42.0, 41.8, 13.5, 13.0. HRMS (ES+): m/z $[M+H]^+$ calcd for ($C_{28}H_{31}N_4O_4$): 487.2345; found: 487.2347.

Synthesis of [4,4'-biisoquinoline]-3,3'-diol 10

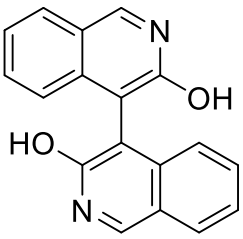

10

A solution of **9** (50 mg, 0.1 mmol) in 10 wt.% methanolic KOH (10 mL) was stirred at reflux for 18 h. The resulting solution was cooled to r.t. and concentrated in *vacuo*. The residue was dissolved in H_2O (7 mL) and the pH adjusted to 7 by a careful addition of 2 M aq. HCl. The aqueous phase was

saturated with NaCl and the formed precipitate filtered and washed with H_2O and cold EtOH. The precipitate was dried under *vacuo* yielding **10** as a yellow solid (27 mg, 92%).

m.p. 177-180 °C. IR (neat): cm^{-1} 405.1, 421.0, 455.3, 468.7, 482.0, 511.9, 563.5, 659.8, 667.8, 721.5, 743.3, 805.0, 845.2, 888.0, 921.1, 953.2, 1068.0, 1105.4, 1136.9, 1151.5, 1197.6, 1233.2, 1293.1, 1338.0, 1386.8, 1448.5, 1493.2, 1502.9, 1571.8, 1605.4, 1625.2, 1717.8, 1754.8, 2352.2, 2930.1, 2983.6, 3082.4. ^{1}H-NMR (500 MHz, DMSO-d_6): δ 10.81 (s, 2H), 9.01 (s, 2H), 8.03 (d, *J* = 8.2 Hz, 2H), 7.41 (m, 2H), 7.31 (m, 2H), 6.96 (d, *J* = 8.6 Hz, 2H).^{13}C-NMR (125 MHz, DMSO-d_6): δ 158.4, 138.5, 130.6, 128.2, 123.2, 123.1, (3 carbon peaks are missing). HRMS (ES+): m/z $[M+H]^+$ calcd for ($C_{18}H_{13}N_2O_2$): 289.0977; found: 289.0981.

Synthesis of quinolin-3-yl diethylcarbamate 12

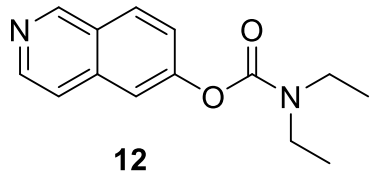

12

To a stirred solution of isoquinolin-6-ol (0.69 mmol, 100 mg) in 1 mL of dry pyridine at r.t. under N_2 was added with dethylaminocarbonyl chloride (1.38 mmol, 0.16 mL). The resulting brown solution was heated to 100 °C and stirred for 16 h. After this time the mixture was allowed to cool to r.t. and partitioned between EtOAc (15 mL) and H_2O (10 mL). The pH of the aqueous layer was adjusted to 9 by the addition of sat. aq. solution $NaHCO_3$ and the layers were shaken and separated. The aqueous phase was extracted with EtOAc (15 mL x 3) and the combined organic dried on Na_2SO_4 and concentrated in vacuo. The crude residue was further purified by silica gel column chromatography (EtOAc) yielding **12** as a yellow oil (151.00 mg, 89%).

IR (neat): cm^{-1} 423.2, 478.3, 566.8, 623.5, 751.7, 755.4, 828.7, 905.1, 922.3, 959.0, 1022.1, 1015.9, 1075.5, 1089.0, 1150.2, 1208.4, 1252.3, 1312.5, 1358.1, 14011.0, 1423.9, 1458.4, 1496.7, 1552.85, 1603.5, 1648.3, 1716.6, 2879.0, 2933.5, 2974.5, 3072.1. ^{1}H-NMR (300 MHz, $CDCl_3$): δ 9.29 (s, 1H), 8.54 (d, *J* = 4.7 Hz, 1H), 7.97 (d, *J* = 8.9 Hz, 1H), 7.62 (d, *J* = 4.7 Hz, 1H), 7.58 (d, *J* = 2.2 Hz, 1H), 7.40 (dd, *J* = 8.9, 2.2 Hz, 1H), 3.66 – 3.17 (m, 4H), 1.35 –1.17 (m, 6H). ^{13}C-NMR (75 MHz, $CDCl_3$): δ 153.7, 152.7, 152.0, 143.4, 136.7, 129.2, 126.5, 123.3, 120.4, 117.0, 42.4, 42.1, 14.3, 13.4. HRMS (ES+): m/z $[M+H]^+$ calcd for ($C_{14}H_{17}N_2O_2$): 245.1290; found: 245.1292

Synthesis of 5-hydroxyisoquinolin-6-yl diethylcarbamate 14

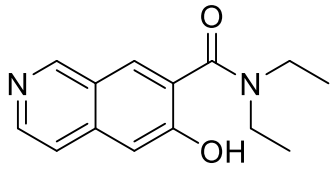

14

To a stirred solution of **12** (0.49 mmol, 120 mg) in 5 mL of dry THF was cooled down at -78 °C and LDA (0.64 mmol, 0.64 mL) added dropwise. The dark brown solution was stirred for 30 min at –78 °C. In parallel, anhydrous $FeCl_3$ (0.49 mmol, 79.7 mg) was suspended in dry THF (5 mL) and cooled at -78 °C (powdered $FeCl_3$ had been previously dried at 120 °C at 0.5 mmHg for 16 h). The suspension of $FeCl_3$ was carefully added to the dark brown solution. The resulting dark brown mixture was allowed to warm to 0 °C and stirred for 11 h. The mixture was quenched with sat. aq. NH_4Cl and diluted EtOAc with H_2O (2 mL) and extracted with EtOAc (20 mL x 3) and the combined organic phase dried on Na_2SO_4 and concentrated in *vacuo*. The crude residue was purified with a silica gel column chromatography (petroleum ether/EtOAc 7:3) yielding **14** as a colourless oil (58 mg, 48%).

m.p. = 86-93 °C. IR (neat): cm^{-1} 405.0, 410.8, 416.6, 443.6, 472.5, 530.4, 545.8, 578.6, 640.3, 665.4, 721.3, 736.8, 750.3, 771.5, 815.8, 864.11, 896.9, 941.2, 972.1, 1033.8, 1068.5, 1095.5, 1155.3, 1166.9, 1186.2, 1217.0, 1234.4, 1274.9, 1290.3, 1311.5, 1336.6, 1359.8, 1379.1, 1409.9, 1427.3, 1475.5, 1616.3, 2933.7, 2978.0. ^{1}H-NMR (300 MHz, CD_3OD): δ 10.63 (s, 1H), 9.85 (d, *J* = 6.0 Hz, 1H), 9.50 (s, 1H), 9.18 (d, *J* = 6.0 Hz, 1H), 8.75 (s, 1H), 5.17 (m, 2H), 4.82 (m, 2H), 2.85 (t, *J* = 6.7 Hz, 3H), 2.67 (t, *J* = 6.8 Hz, 3H), one proton peak is missed. ^{13}C-NMR (75 MHz, CD_3OD): δ 172.8, 154.9, 145.6, 142.3, 133.6, 131.3, 127.2, 123.3, 111.5, 47.2, 43.3, 16.7, 15.6, (1 carbon is missed). HRMS (ES+): m/z $[M+H]^+$ calcd for ($C_{14}H_{17}N_2O_2$): 245.1290; found: 245.1292

3. Lifetime measurements

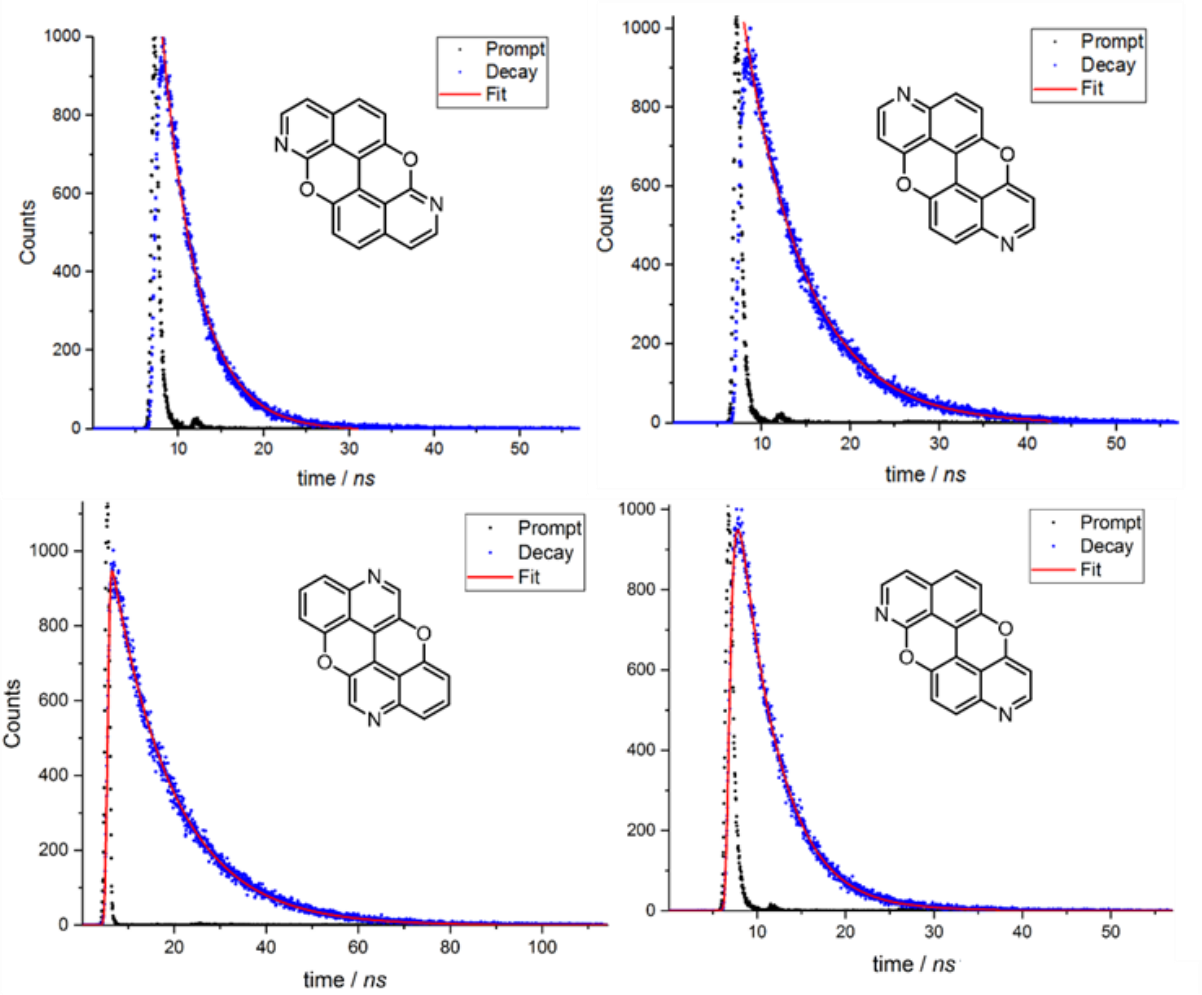

Figure S1. Fluorescence emission lifetime decays (blue dots), relative fittings (red lines) and decay of excitation source (black line).

4. Cyclic Voltammetry

Cyclic Voltammetry of 1,7-diaza peri-xanthenoxanthene

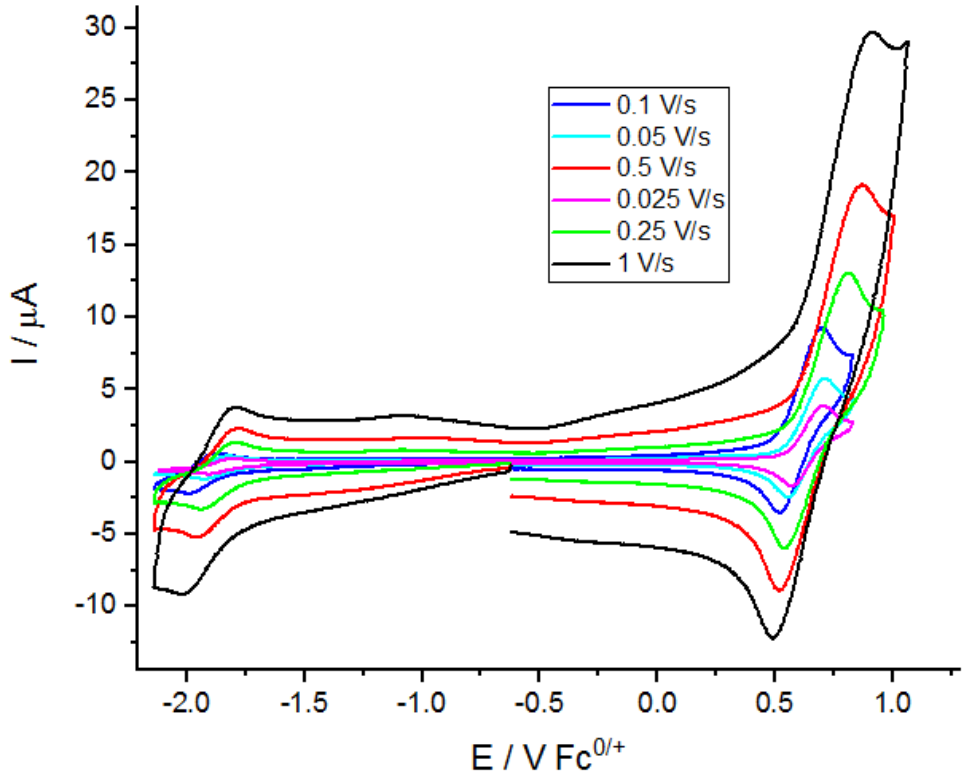

Figure S2. Cyclic voltammograms of **1,7-N,N-PXX** in ODCB (ca. 0.70 mM) at different scan rates. $TBAPF_6$ (0.08 M) is used as a supporting electrolyte; ferrocene/ferrocenium redox couple (Fc/Fc^+) is used as reference.

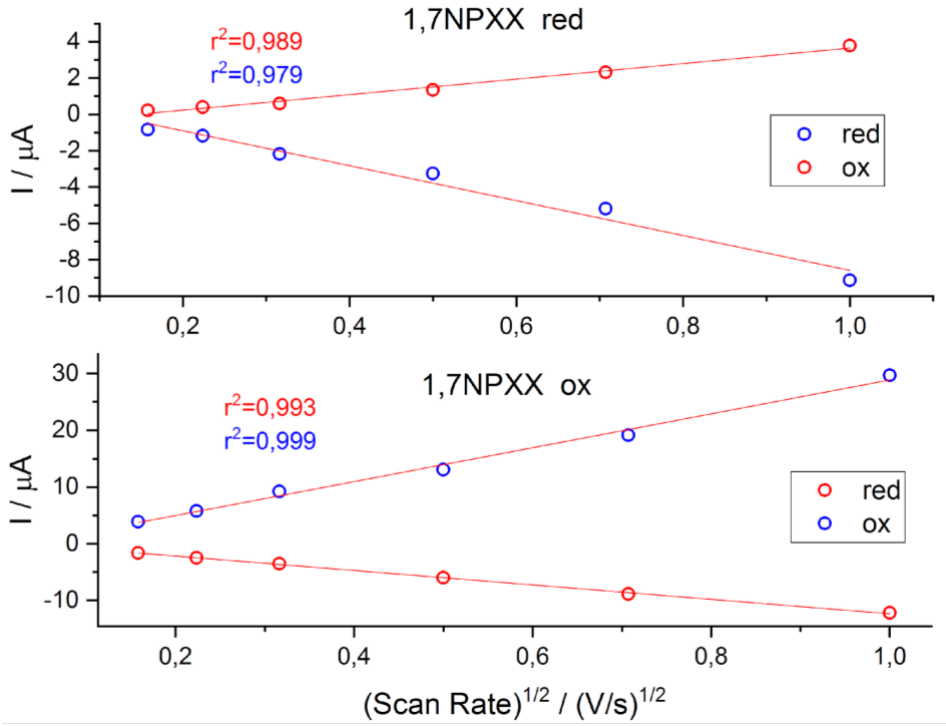

Figure S3. Linear dependence between anodic or cathodic peak currents and scan rate$^{1/2}$.

Cyclic Voltammetry of 3,9-diaza peri-xanthenoxanthene

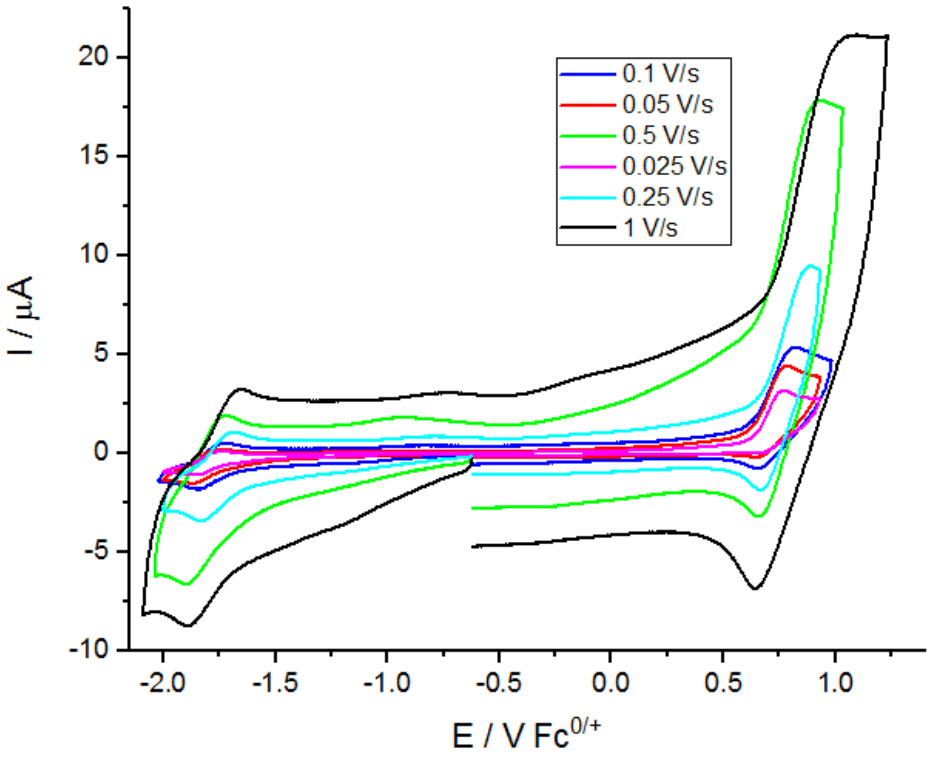

Figure S4. Cyclic voltammograms of **3,9-N,N-PXX** in ODCB (ca. 0.70 mM) at different scan rates. $TBAPF_6$ (0.08 M) is used as a supporting electrolyte; ferrocene/ferrocenium redox couple (Fc/Fc^+) is used as reference.

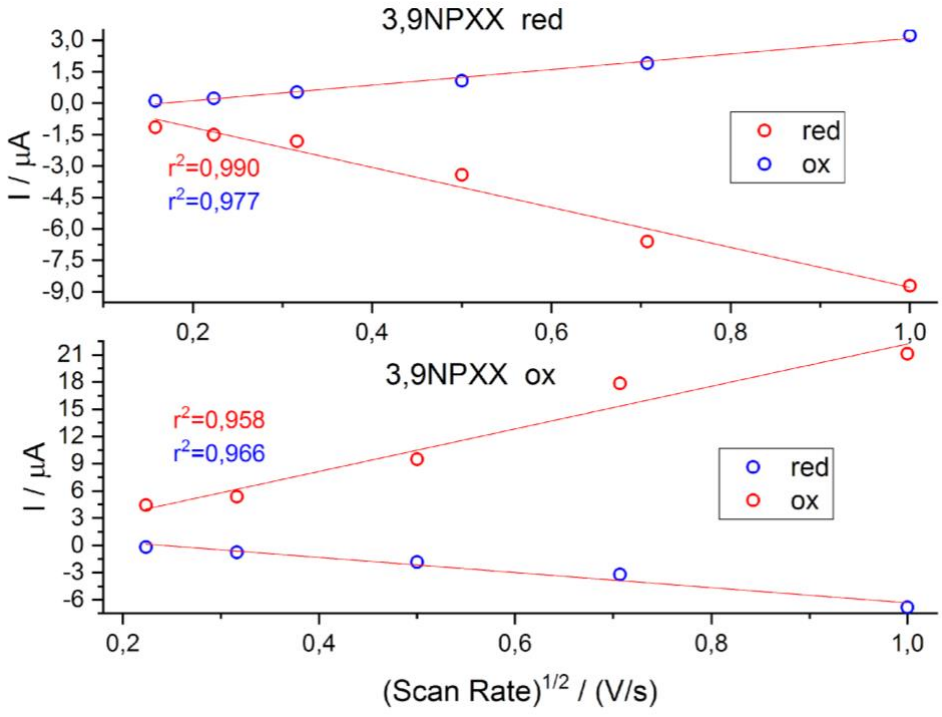

Figure S5. Linear dependence between anodic or cathodic peak currents and scan rate$^{1/2}$.

Cyclic Voltammetry of 4,10-diaza peri-xanthenoxanthene

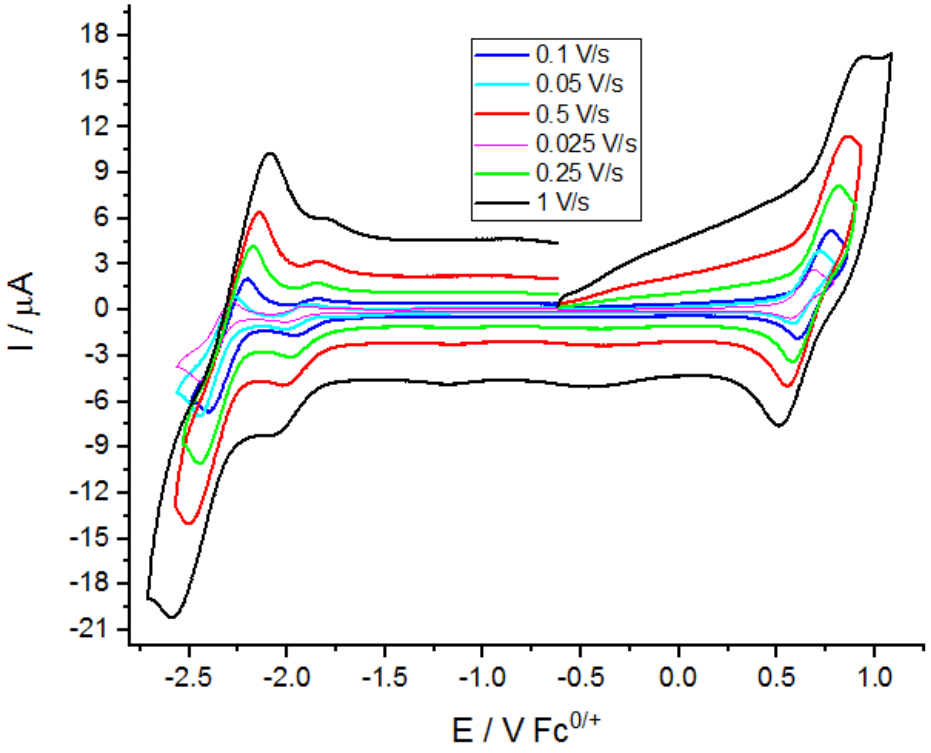

Figure S6. Cyclic voltammograms of **4,10-N,N-PXX** in ODCB (ca. 0.70 mM) at different scan rates. $TBAPF_6$ (0.08 M) is used as a supporting electrolyte; ferrocene/ferrocenium redox couple (Fc/Fc^+) is used as reference.

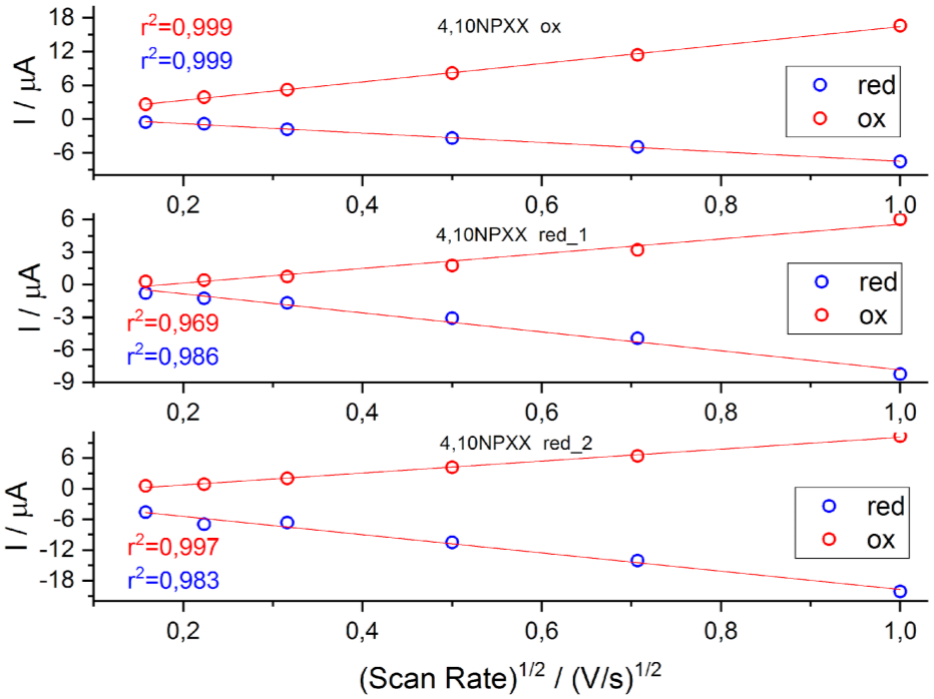

Figure S7. Linear dependence between anodic or cathodic peak currents and scan rate$^{1/2}$

Cyclic Voltammetry of 1,9-diaza peri-xanthenoxanthene

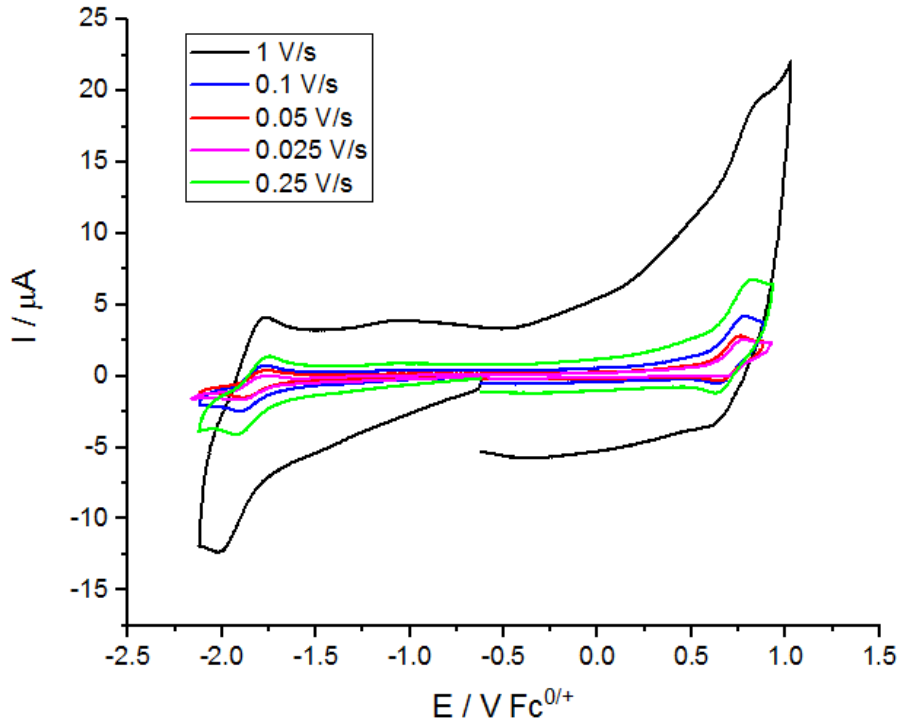

Figure S8. Cyclic voltammograms of **1,9-N,N-PXX** in ODCB (ca. 0.72 mM) at different scan rates. $TBAPF_6$ (0.08 M) is used as a supporting electrolyte; ferrocene/ferrocenium redox couple (Fc/Fc^+) is used as reference.

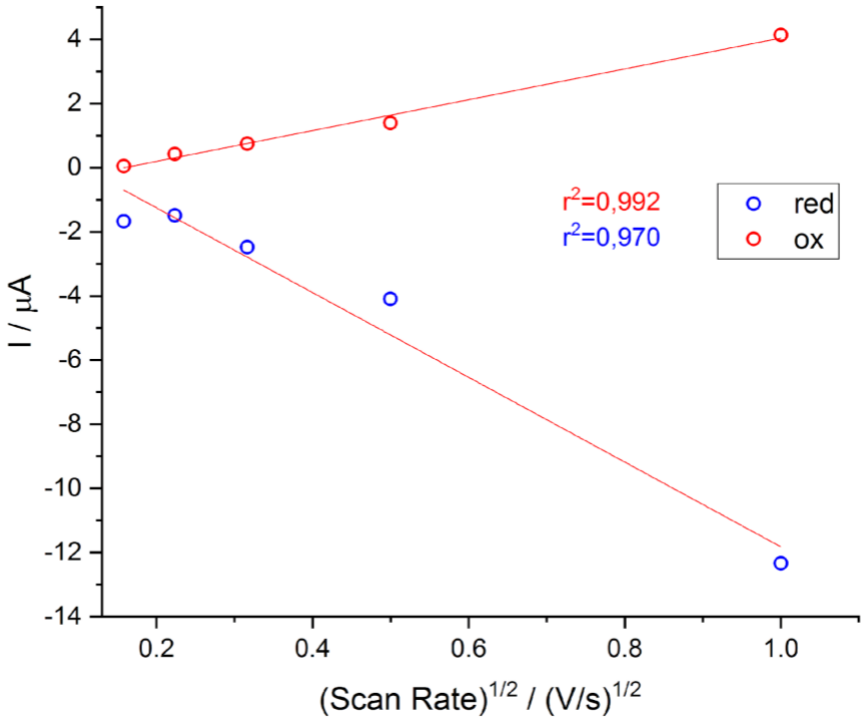

Figure S9. Linear dependence between anodic or cathodic peak currents and scan rate$^{1/2}$.

5. X-ray Data

Crystal data and structure refinement of 1,7-diaza peri-xanthenoxanthene (1985339) 1,7-N,N-PXX

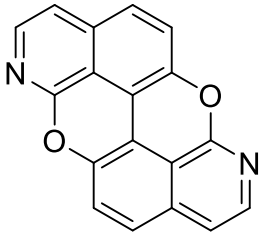

1,7-N,N-PXX

Empirical formula	$C_{18}H_8N_2O_2$	
Formula weight	284.26	
Temperature	150(2) K	
Wavelength	0.71073 Å	
Crystal system	Monoclinic	
Space group	P $2_1/c$	
Unit cell dimensions	a = 4.3819(9) Å	α = 90°.
	b = 13.469(3) Å	β = 97.073(19)°.
	c = 10.1801(18) Å	γ = 90°.
Volume	596.3(2) $Å^3$	
Z	2	
Density (calculated)	1.583 mg/m^3	
Absorption coefficient	0.106 mm^{-1}	
F(000)	292	
Crystal size	0.221 x 0.080 x 0.072 mm^3	
Theta range for data collection	3.025 to 29.488°.	
Index ranges	-6<=h<=4, -15<=k<=18, -13<=l<=13	
Reflections collected	2815	
Independent reflections	1409 [R(int) = 0.0352]	
Completeness to theta = 25.242°	99.9 %	
Refinement method	Full-matrix least-squares on F^2	
Data / restraints / parameters	1409 / 0 / 100	
Goodness-of-fit on F^2	1.010	
Final R indices [I>2sigma(I)]	R1 = 0.0684, wR2 = 0.1879	
R indices (all data)	R1 = 0.1359, wR2 = 0.2422	
Extinction coefficient	n/a	
Largest diff. peak and hole	0.394 and -0.358 e•$Å^{-3}$	

Crystal data and structure refinement of 3,9-diaza peri-xanthenoxanthene (1985342)

3,9-N,N-PXX

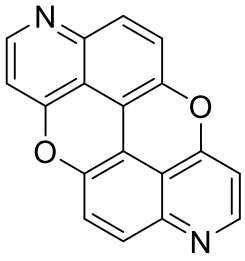

3,9-N,N-PXX

Empirical formula	$C_{18}H_{12}N_2O_4$	
Formula weight	320.30	
Temperature	100(2) K	
Wavelength	0.700 Å	
Crystal system	Monoclinic	
Space group	P $2_1/c$	
Unit cell dimensions	a = 7.557(2) Å	α = 90°.
	b = 3.668(1) Å	β = 95.85(3)°.
	c = 23.856(3) Å	γ = 90°.
Volume	657.8(2) $Å^3$	
Z	2	
Density (calculated)	1.617 mg/m^3	
Absorption coefficient	0.111 mm^{-1}	
F(000)	332	
Theta range for data collection	1.69 to 29.53°.	
Index ranges	-10<=h<=10, -5<=k<=5, -33<=l<=3	
Reflections collected	6108	
Independent reflections	1887	
Completeness to theta = 67.684°	98.1 %	
Refinement method	Full-matrix least-squares on F^2	
Data / restraints / parameters	1887 / 3 / 115	
Goodness-of-fit on F^2	1.068	
Final R indices [I>2sigma(I)]	R1 = 0.0706, wR2 = 0.2095	
R indices (all data)	R1 = 0.095, wR2 = 0.2346	
Extinction coefficient	n/a	
Largest diff. peak and hole	0.377 and -0.556 e•$Å^{-3}$	

Crystal data and structure refinement of molecule 3 (2151478)

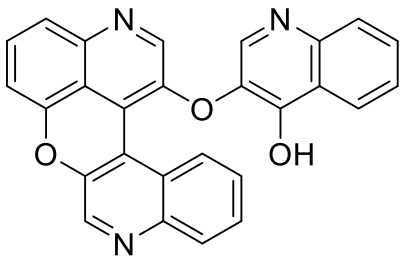

3

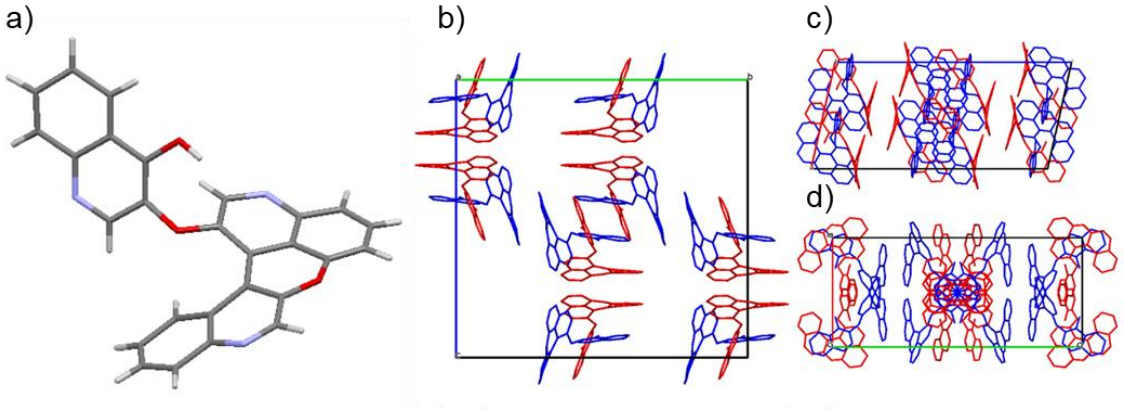

Figure S10. a) Single-crystal X-ray structure of molecule 3, solvent for crystallisation: MeOH. Coordinated solvent molecules omitted for clarity. b) Unit cell view along axis a, c) unit cell view along axis b, d) unit cell view along axis c. Enantiomer P in blue and enantiomer M in red.

Empirical formula	$C_{27}H_{24.75}N_3O_{7.88}$	
Formula weight	517.25	
Temperature	100(2) K	
Wavelength	0.700 Å	
Crystal system	Monoclinic	
Space group	C 2/*c*	
Unit cell dimensions	a = 12.826(3) Å	α = 90°.
	b = 28.416(6) Å	β = 101.61(3)°.
	c = 27.470(6) Å	γ = 90°.
Volume	9807(4) $Å^3$	
Z	16	
Density (calculated)	1.401 mg/m^3	
Absorption coefficient	0.100 mm^{-1}	
F(000)	4332	
Theta range for data collection	1.41 to 22.75°.	
Index ranges	-13<=h<=13, -31<=k<=31, -30<=l<=30	
Reflections collected	24718	
Independent reflections	6786	
Completeness to theta = 67.684°	97.6 %	
Refinement method	Full-matrix least-squares on F^2	

Data / restraints / parameters	6786 / 0 / 683
Goodness-of-fit on F^2	0.992
Final R indices [I>2sigma(I)]	R1 = 0.1006, wR2 = 0.2516
R indices (all data)	R1 = 0.2453, wR2 = 0.3480
Extinction coefficient	n/a
Largest diff. peak and hole	0.605 and -0.313 e•Å^{-3}

Crystal data and structure refinement 4,10-diaza peri-xanthenoxanthene (1985344) 4,10-N,N-PXX

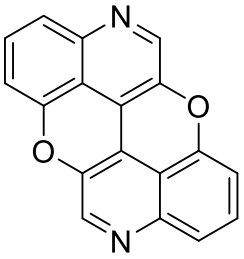

4,10-N,N-PXX

Empirical formula	$C_{18}H_8N_2O_2$	
Formula weight	284.26	
Temperature	150(2) K	
Wavelength	1.54184 Å	
Crystal system	Monoclinic	
Space group	P $2_1/n$	
Unit cell dimensions	a = 11.589(3) Å	α = 90°.
	b = 3.7599(12) Å	β = 112.54(3)°.
	c = 14.384(3) Å	γ = 90°.
Volume	578.9(3) Å^3	
Z	2	
Density (calculated)	1.631 mg/m^3	
Absorption coefficient	0.891 mm^{-1}	
F(000)	292	
Crystal size	0.469 x 0.044 x 0.031 mm^3	
Theta range for data collection	4.195 to 76.679°.	
Index ranges	-14<=h<=14, -4<=k<=4, -17<=l<=17	
Reflections collected	4883	
Independent reflections	1171 [R(int) = 0.0748]	
Completeness to theta = 67.684°	99.9 %	
Refinement method	Full-matrix least-squares on F^2	
Data / restraints / parameters	1171 / 0 / 100	

Goodness-of-fit on F^2	1.011
Final R indices [I>2sigma(I)]	R1 = 0.0899, wR2 = 0.2405
R indices (all data)	R1 = 0.1251, wR2 = 0.2993
Extinction coefficient	n/a
Largest diff. peak and hole	0.579 and -0.347 e•Å^{-3}

Crystal data and structure refinement of 3,9-diaza peri-xanthenoxanthene and 1,4-diiodo-2,3,5,6-tetrafluoroiodobenzene (2133475) 3,9-N,N-PXX•DITFB

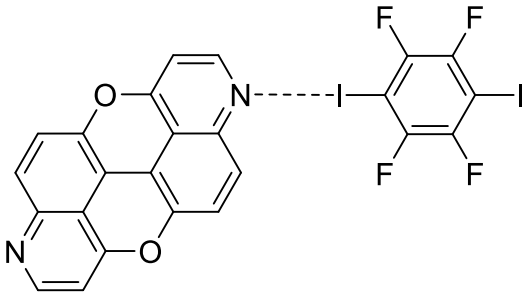

3,9-N,N-PXX · DITFB

Empirical formula	$C_{24}H_8F_4I_2N_2O_2$	
Formula weight	686.12	
Temperature	100(2) K	
Wavelength	0.6889 Å	
Crystal system	Triclinic	
Space group	P-1	
Unit cell dimensions	a = 4.2046(2) Å	α = 94.632(3)°.
	b = 6.7216(2) Å	β = 93.684(3)°.
	c = 18.2394(5) Å	γ = 99.922(3)°.
Volume	504.50(3) Å^3	
Z	1	
Density (calculated)	2.258 mg/m^3	
Absorption coefficient	3.182 mm^{-1}	
F(000)	324	
Crystal size	0.020 x 0.017 x 0.005 mm^3	
Theta range for data collection	1.089 to 35.929°.	
Index ranges	-7<=h<=6, -11<=k<=10, -24<=l<=30	
Reflections collected	7689	
Independent reflections	4100 [R(int) = 0.0615]	
Completeness to theta = 67.684°	95.9 %	
Refinement method	Full-matrix least-squares on F^2	
Data / restraints / parameters	4100 / 0 / 154	
Goodness-of-fit on F2	0.957	

Final R indices [I>2sigma(I)]	R1 = 0.0514, wR2 = 0.1171
R indices (all data)	R1 = 0.0775, wR2 = 0.1271
Extinction coefficient	n/a
Largest diff. peak and hole	1.721 and -1.428 e•Å^{-3}

Crystal data and structure refinement of 4,10-diaza peri-xanthenoxanthene and 1,4-diiodo-2,3,5,6-tetrafluoroiodobenzene (2133474) 4,10-N,N-PXX•DITFB

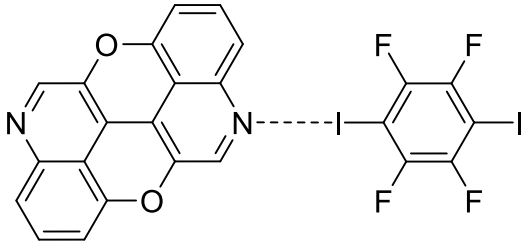

4,10-N,N-PXX · DITFB

Empirical formula	$C_{24}H_8F_4I_2N_2O_2$	
Formula weight	686.12	
Temperature	200(2) K	
Wavelength	0.71073 Å	
Crystal system	Triclinic	
Space group	P-1	
Unit cell dimensions	a = 4.1848(3) Å	α = 92.097(5)°.
	b = 7.7399(5) Å	β = 90.002(5)°.
	c = 16.2513(11) Å	γ = 99.199(5)°.
Volume	519.25(6) Å^3	
Z	1	
Density (calculated)	2.194 mg/m^3	
Absorption coefficient	3.091 mm^{-1}	
F(000)	324	
Crystal size	0.390 x 0.122 x 0.080 mm^3	
Theta range for data collection	3.730 to 29.760°.	
Index ranges	-5<=h<=5, -9<=k<=8, -20<=l<=17	
Reflections collected	4071	
Independent reflections	2460 [R(int) = 0.0338]	
Completeness to theta = 67.684°	99.7 %	
Refinement method	Full-matrix least-squares on F^2	
Data / restraints / parameters	2460 / 0 / 154	
Goodness-of-fit on F2	1.035	
Final R indices [I>2sigma(I)]	R1 = 0.0407, wR2 = 0.063	
R indices (all data)	R1 = 0.0546, wR2 = 0.0703	
Extinction coefficient	n/a	

Largest diff. peak and hole	0.934 and -0.685 e•Å^{-3}

6. Computational details

The structural and optoelectronic properties of the molecules have been computed using density functional theory (DFT) and linear response time dependent density functional theory (TDDFT) as implemented in Gaussian09. The results presented in the paper are obtained with the B3LYP exchange and correlation functional and the 6-311+g* basis set. In Fig. S10 and Fig. S11 and Table S1 there is the comparison with other functionals and basis sets for the molecules that have been synthesised in this paper. Overall, the trends depend very little on the functionals, and B3LYP shows the most pronounced redshift. The B3LYP functional has previously been used and discussed for the PXX molecule.[5] The basis set used in this work provides results very similar to the ones obtained with more precise and computational expensive basis sets.

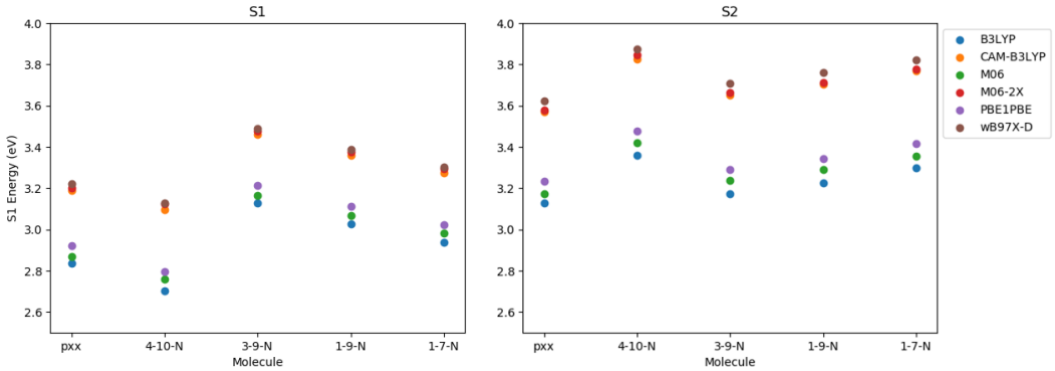

Figure S11 - DFT functional dependence on first and second singlet vertical excitation energies of example nPXX molecules at the B3LYP/6-311+G* geometry

Table S1 - Ground state total DFT energies of select regioisomers with changing basis - B3LYP

	Basis				
Molecule	3-21G	6-31+G*	6-311++G**	6-31G	aug-cc-pVTZ
1-7-N	-945.467637	-950.747531	-950.759990	-950.441304	-951.043275
1-9-N	-945.465349	-950.744065	-950.756500	-950.439368	-951.038927
3-9-N	-945.463362	-950.740849	-950.753259	-950.437760	-951.034904
4-10-N	-945.455952	-950.729220	-950.741654	-950.428375	-951.023574
pxx	-913.578507	-918.661096	-918.677043	-918.397982	-918.946746

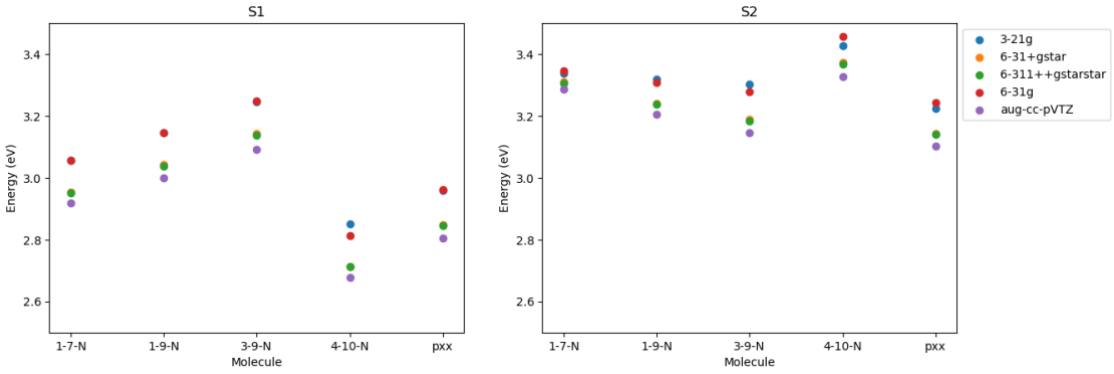

Figure S12 – Basis set dependence of first and second singlet vertical excitation energies of example nPXX molecules at the B3LYP/6-311+G* optimised geometry

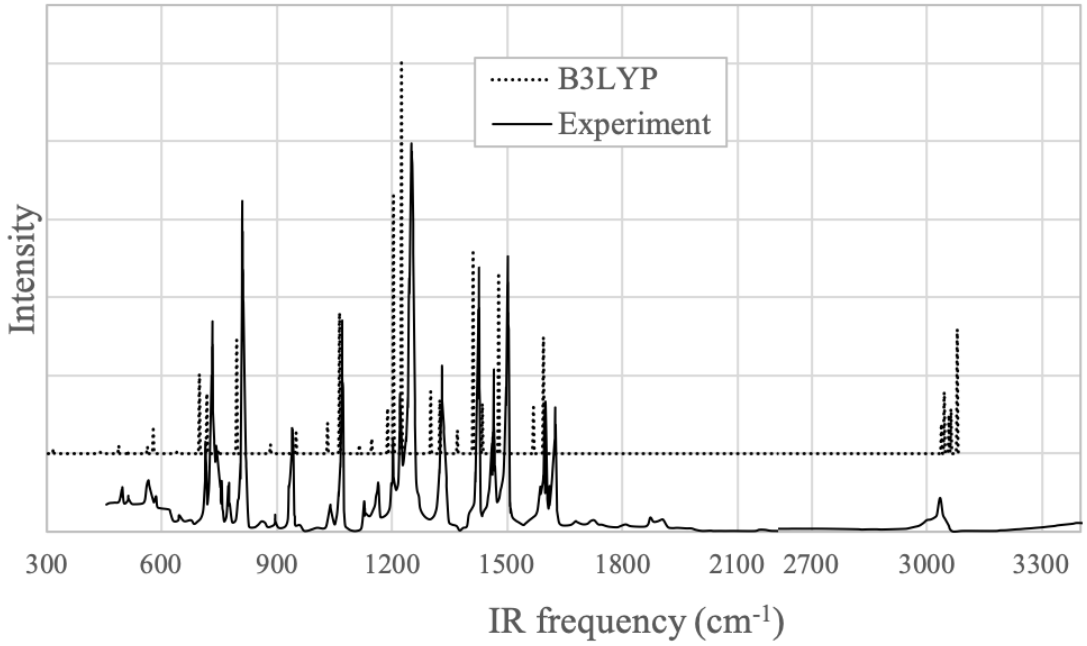

Figure S13 - PXX calculated vibrational spectra from Hessian calculation and experimental IR spectra (REF).

As shown in Fig. 12 the vibrational properties of the PXX molecule are well described by the ab initio modelling. In addition, our results well reproduce the emission and the absorption spectra of the synthetized molecules.

In Tables S2 and S3 we report the numerical values for the ab initio Franck-Condon and in Fig. S13 there are the ab initio spectra. Our results tend to underestimate the Stokes shifts. This is related to the fact that the scaffold of these molecules is rigid and we find little relaxation. In addition, there is no modelling of solvent effects here.

Table S2 – Absorption and emission maxima energies and intensities from (adiabatic Hessian type) Franck-Condon calculations calculated at the TD-B3LYP/6-31+G* level

	Absorption maxima (nm)	Intensity (Molar absorption coefficient (in dm^3.mol^-1.cm^-1))	Emission maxima (nm)	Emitted intensity (in microJ.mol^-1)	Stokes shift (nm)
PXX	484.503	34968.8	484.997	698.6	0.494
1-7-N	464.863	44563.9	465.267	993.0	0.404
1-9-N	451.339	46200.3	451.768	1107.1	0.428
3-9-N	438.907	48298.8	439.396	1109.0	0.489
4-10-N	511.919	17276.6	512.435	290.9	0.516

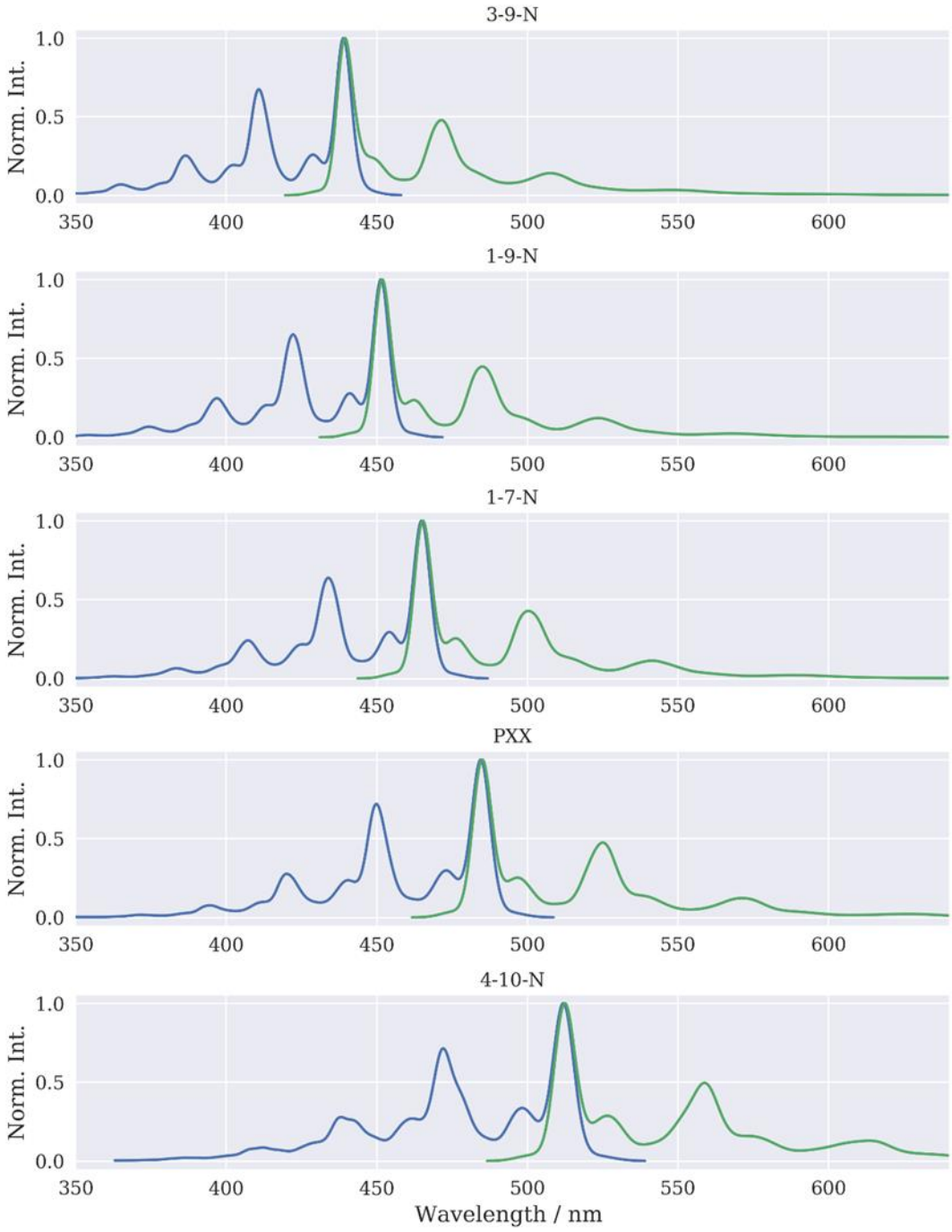

Figure S14 - Franck-Condon spectral lineshapes calculated at the B3LYP/6-31+G* level for synthesised N,N-PXX regioisomers and PXX. Both absorption (blue) and emission (green) have been normalised.

To rationalize the optoelectronic properties of the molecules we have focussed on the charge redistribution in the absorption process. In particular, we have qualitatively analysed the behaviour of the CHELPG partial atomic charges. The comparison of different pictorial representations is shown in Fig. S14.

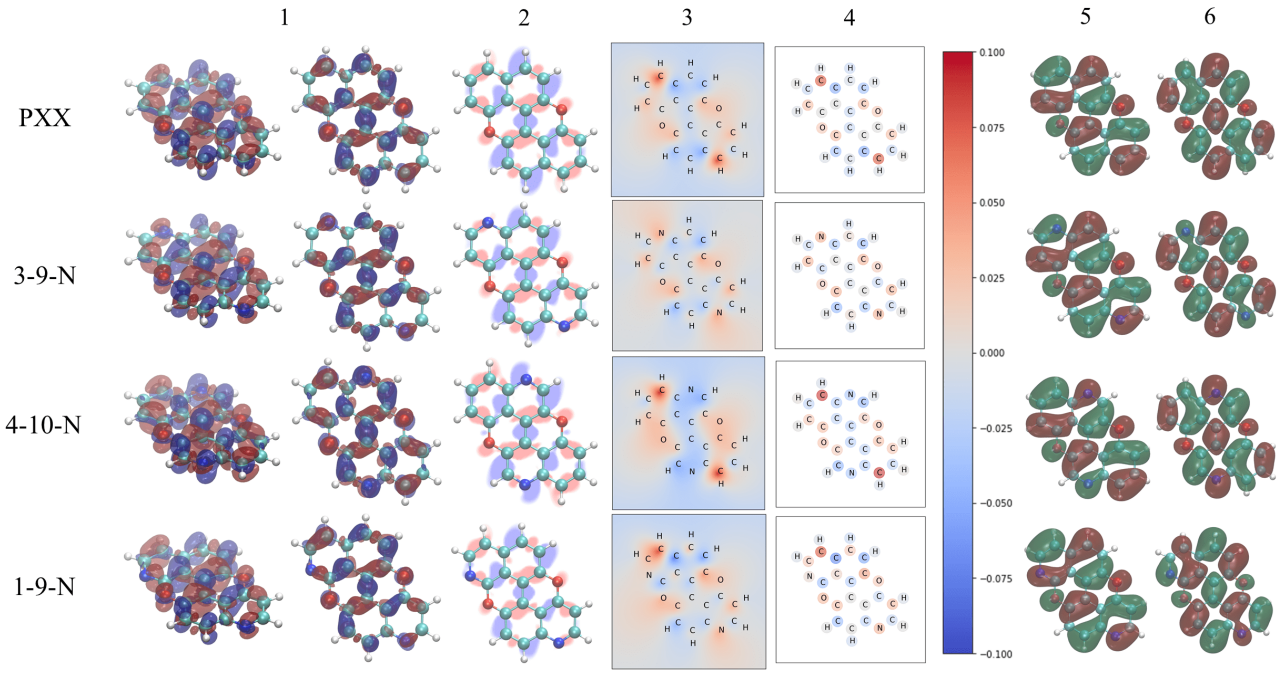

Figure S15 - 1) Charge density difference between the excited and the ground state (isometric and above), 2) z-axis average of the charge density difference, 3) interpolated difference in excited and ground state CHELPG charges, 4) difference in excited and ground state CHELPG charges, 5) highest occupied molecular orbital, 6) lowest unoccupied molecular orbital. Level of theory is TD-B3LYP/6-311+G*.

Figure S14 shows the efficacy of the charge redistribution maps used in the main text. The density difference maps are highly physical, stemming directly from the DFT and TDDFT calculations, however they obscure the effect of the doping position. Only through employing atomic charges (here using CHELPG), where the electron density around atoms is integrated over, is it possible to examine the influence of dopant position on electron transfer (3) and 4) in Figure S14). These maps closely mirror the z-axis average of the density difference.

Table S3: Ab initio results for the set of molecules discussed in the paper. Level of theory is TD/B3LYP/6-311+G*.

Molecule	HOMO (eV)	LUMO (eV)	S1 energy (eV)	Dip. (Debye)	Oscillator strength
PXX	-5.061	-1.763	2.834	2.270	0.158
1-11-N	-5.576	-2.388	2.799	2.716	0.186
1-10-N	-5.686	-2.489	2.827	1.969	0.136
1-9-N	-5.669	-2.278	3.027	2.697	0.200
1-8-N	-5.629	-2.267	2.916	2.387	0.171
1-7-N	-5.663	-2.297	2.938	2.734	0.197
2-11-N	-5.545	-2.368	2.766	2.444	0.166
2-10-N	-5.661	-2.468	2.814	1.717	0.118
2-9-N	-5.632	-2.250	2.995	2.121	0.156
2-8-N	-5.607	-2.237	2.907	2.043	0.146
3-11-N	-5.578	-2.371	2.865	2.685	0.189
3-10-N	-5.695	-2.461	2.918	1.895	0.136
3-9-N	-5.676	-2.252	3.126	2.680	0.205

4-11-N	-5.598	-2.557	2.687	2.014	0.133
4-10-N	-5.702	-2.688	2.702	1.429	0.095
5-11-N	-5.486	-2.431	2.673	2.782	0.182

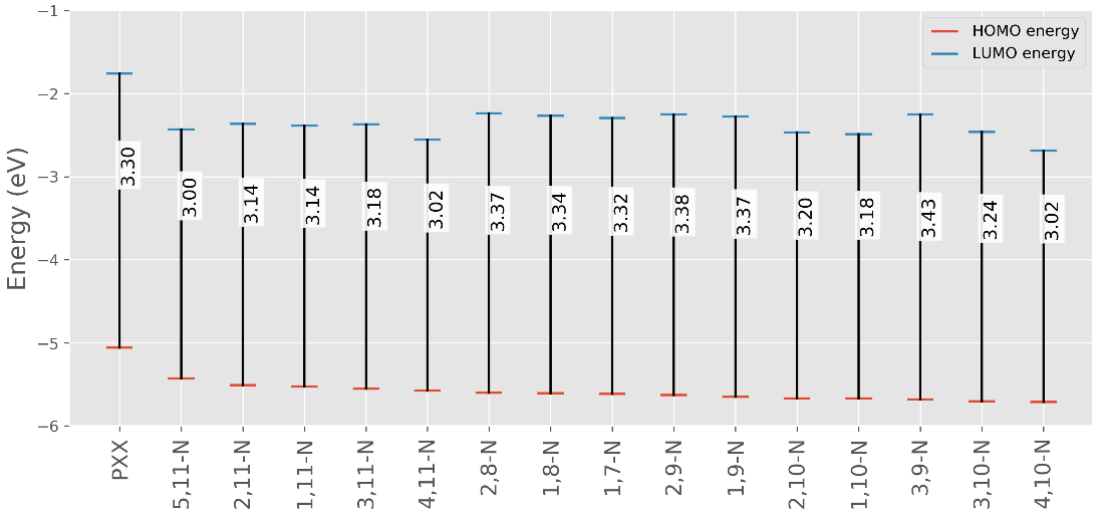

Figure S16 – DFT/B3LYP/6-311+G* HOMO and LUMO eigenvalues and gaps for PXX and nPXX regioisomers ordered by decreasing HOMO energy.

Table S4: DFT/B3LYP/6-311+G* HOMO and LUMO eigenvalues and gaps for PXX and N-PXX regioisomers.

MOLECULE	HOMO (eV)	LUMO (eV)	Kohn-Sham gap (eV)
PXX	-5.061	-1.763	3.298
5-11-N	-5.431	-2.431	3.000
2-11-N	-5.512	-2.368	3.144
1-11-N	-5.527	-2.388	3.139
3-11-N	-5.555	-2.371	3.184
4-11-N	-5.578	-2.557	3.020
2-8-N	-5.604	-2.237	3.368
1-8-N	-5.605	-2.267	3.338
1-7-N	-5.616	-2.297	3.319
2-9-N	-5.629	-2.250	3.379
1-9-N	-5.652	-2.278	3.373
2-10-N	-5.667	-2.468	3.200
1-10-N	-5.667	-2.489	3.178
3-9-N	-5.683	-2.252	3.431
3-10-N	-5.706	-2.461	3.245
4-10-N	-5.712	-2.688	3.024

Semiempirical calculations using the Huckel tight-binding Hamiltonian of the set of regioisomers were carried out using the Hulis package.[3–5] These values are generated by setting β = 3.39 eV for all calculations. This value is chosen to give the correct vertical excitation energy for PXX, and is similar to those used in previous studies.

Table S5 - TDDFT/B3LYP/6-311+G* excitation data and orbital eigenvalues for Anthanthrene derivatives. Comparison of these data to PXX results (Table **S3**) shows that addition of oxygen heteroatoms makes the optical excitation significantly more susceptible to manipulation

	S_1 excitation energy (eV)	Osc. Str.	HOMO (eV)	LUMO (eV)	Gap (eV)
Anthanthrene	2.807	0.310	-5.215	-2.340	2.875
3-9-N Anthanthrene	2.818	0.267	-5.872	-2.908	2.964
4-10-N Anthanthrene	2.819	0.302	-5.908	-2.986	2.922
1-7-N Anthanthrene	2.881	0.293	-5.693	-2.797	2.897

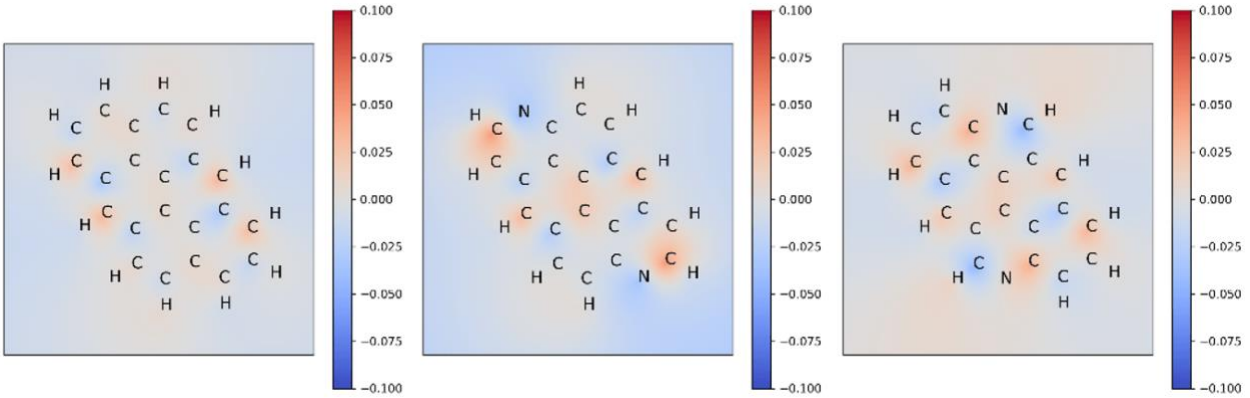

Figure S17 – Excitation charge redistribution maps for Anthanthrene (left), 3-9-N Anthanthrene (middle), and 4-10-N Anthanthrene (right). In general, the coloration here is less intense than PXX and its derivatives, suggesting less charge redistribution (transfer) and less tunability through doping position control.

7. Appendix

Characterisation of [8,8'-biisoquinoline]-7,7'-diol 2

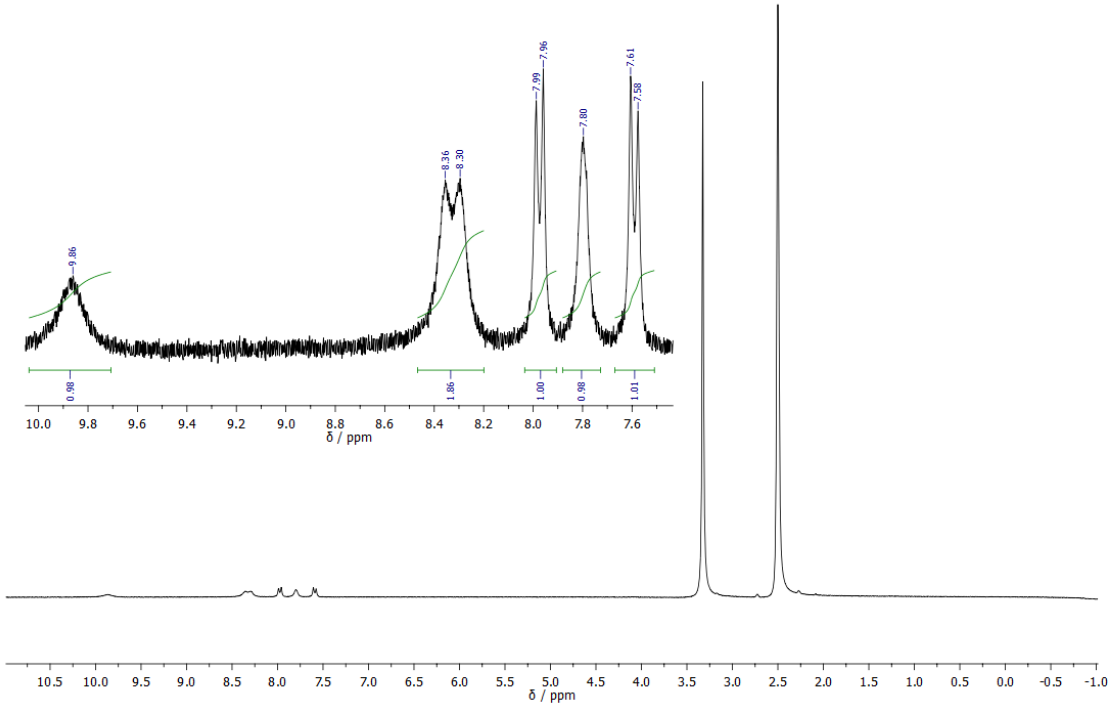

Figure SA1. ^{1}H-NMR, 500 MHz, DMSO-d_6

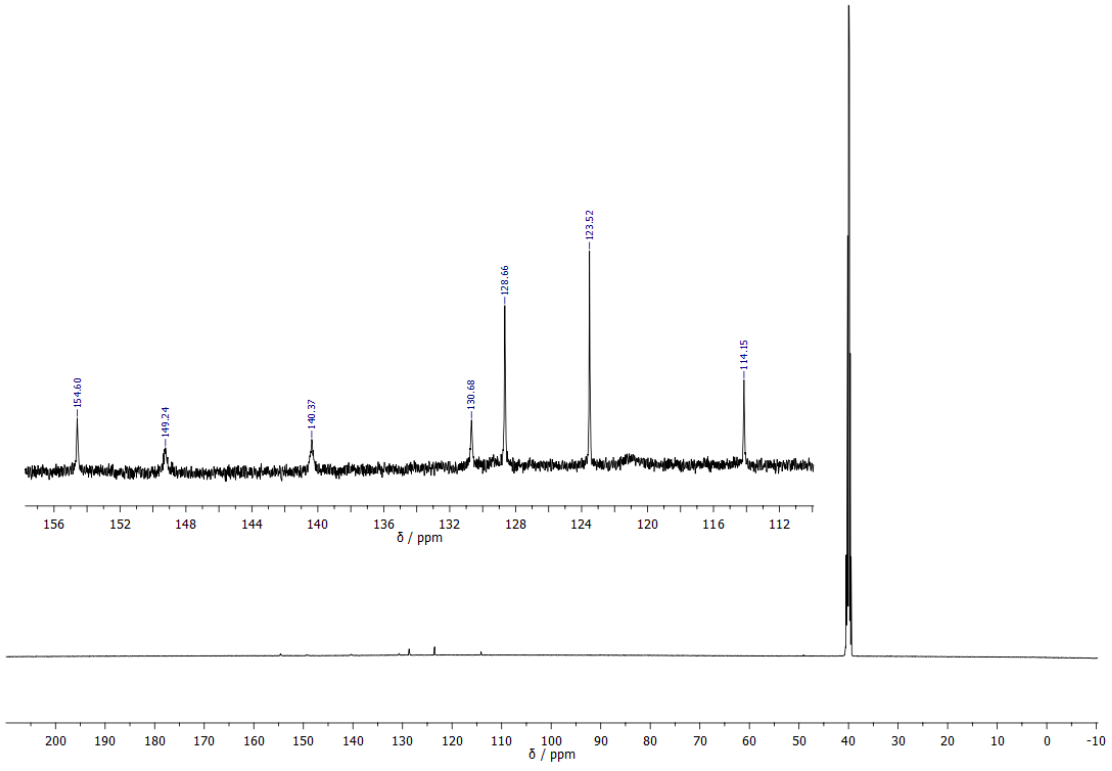

Figure SA2. ^{13}C-NMR, 125 MHz, DMSO-d_6

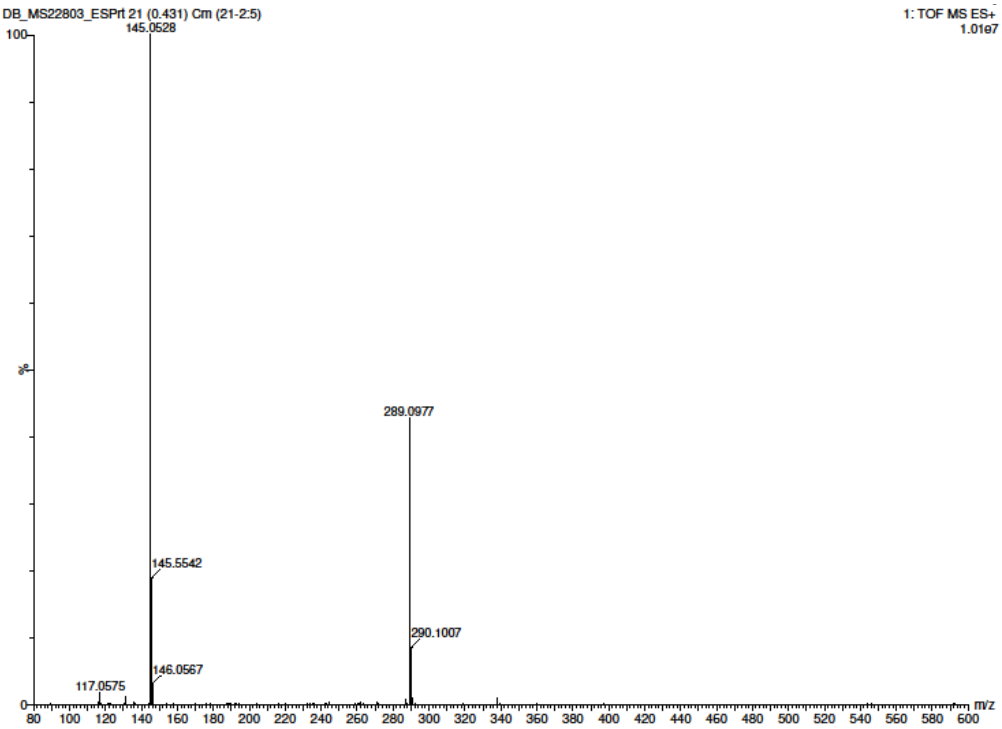

Figure SA3. HR-MS, ESI-TOF.

Elemental Composition Report **Page 1**

Single Mass Analysis
Tolerance = 10.0 PPM / DBE: min = -1.5, max = 100.0
Element prediction: Off
Number of isotope peaks used for i-FIT = 3

Monoisotopic Mass, Odd and Even Electron Ions
4 formula(e) evaluated with 1 results within limits (up to 50 closest results for each mass)
Elements Used:
C: 0-18 H: 0-13 N: 0-2 O: 0-2

Minimum:				-1.5				
Maximum:		5.0	10.0	100.0				
Mass	Calc. Mass	mDa	PPM	DBE	i-FIT	Norm	Conf(%)	Formula
289.0977	289.0977	0.0	0.0	13.5	159.1	n/a	n/a	C18 H13 N2 O2

Figure SA2. Elemental Composition Report.

Characterisation of 1,7-diaza peri-xanthenoxanthene

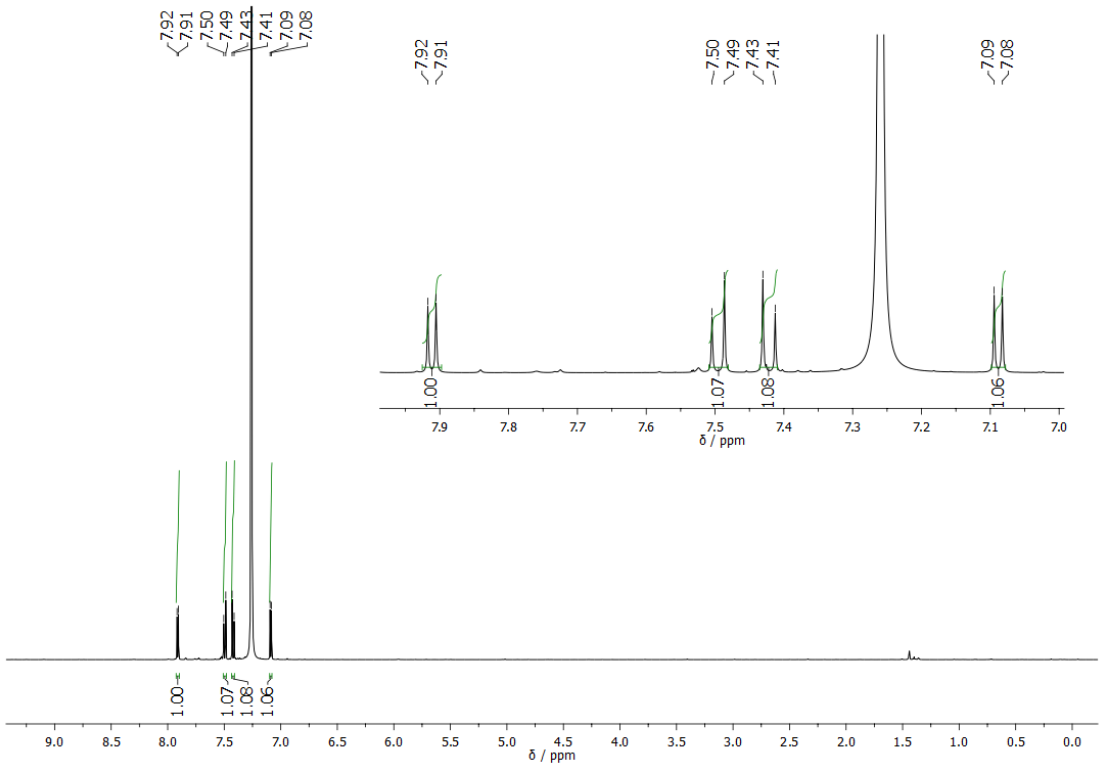

Figure SA4. ^{1}H-NMR, 500 MHz, $CDCl_3$

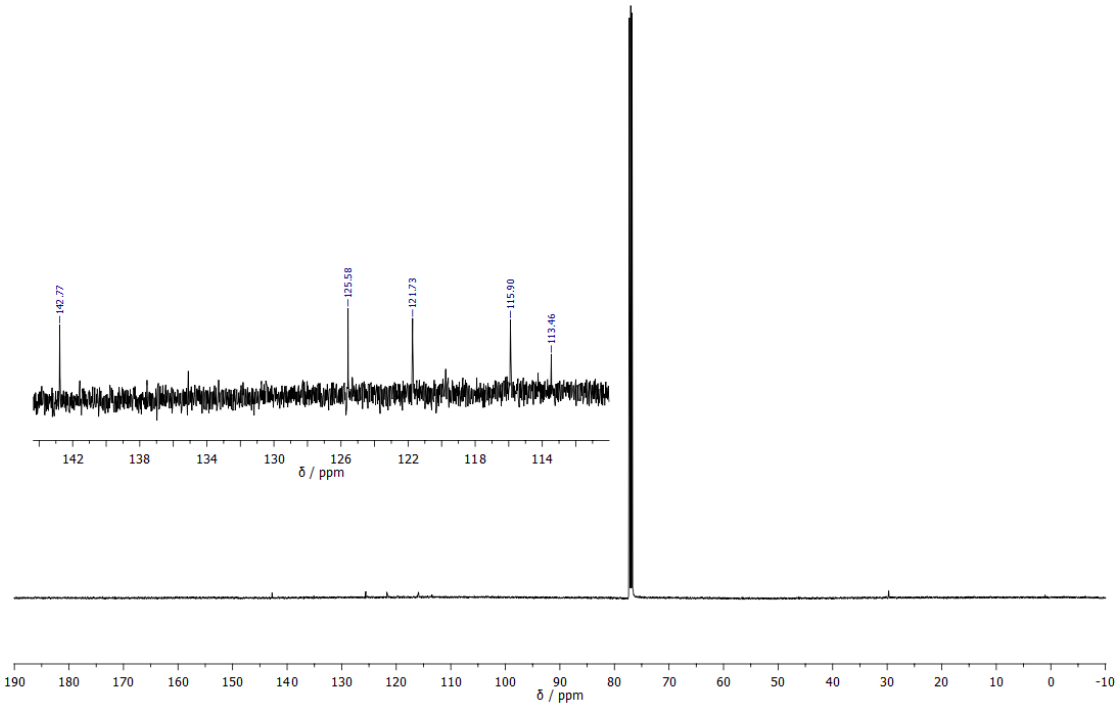

Figure SA5. ^{13}C-NMR, 125 MHz, $CDCl_3$

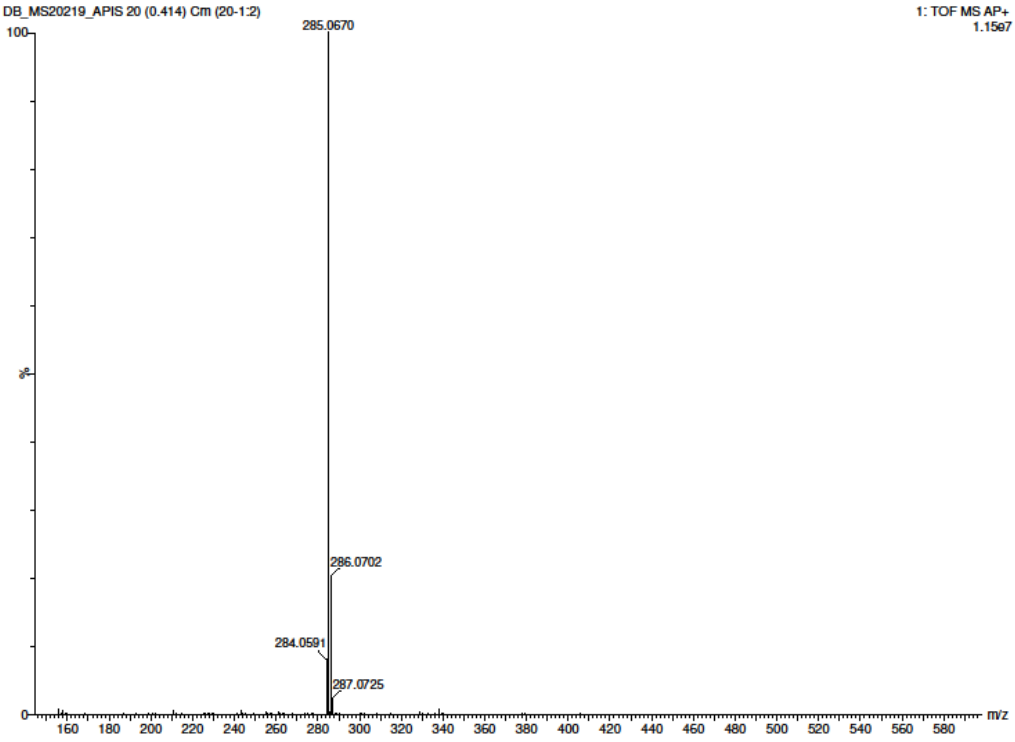

Figure SA6. HR-MS, AP-TOF.

Elemental Composition Report **Page 1**

Single Mass Analysis
Tolerance = 5.0 PPM / DBE: min = -1.5, max = 100.0
Element prediction: Off
Number of isotope peaks used for i-FIT = 3

Monoisotopic Mass, Odd and Even Electron Ions
4 formula(e) evaluated with 1 results within limits (up to 50 best isotopic matches for each mass)
Elements Used:
C: 0-18 H: 0-9 N: 0-2 O: 0-2

Minimum:				-1.5				
Maximum:		5.0	5.0	100.0				
Mass	Calc. Mass	mDa	PPM	DBE	i-FIT	Norm	Conf(%)	Formula
285.0670	285.0664	0.6	2.1	15.5	831.9	n/a	n/a	C18 H9 N2 O2

Figure SA7. Elemental Composition Report.

Characterisation of [5,5'-biquinoline]-6,6'-diol 1

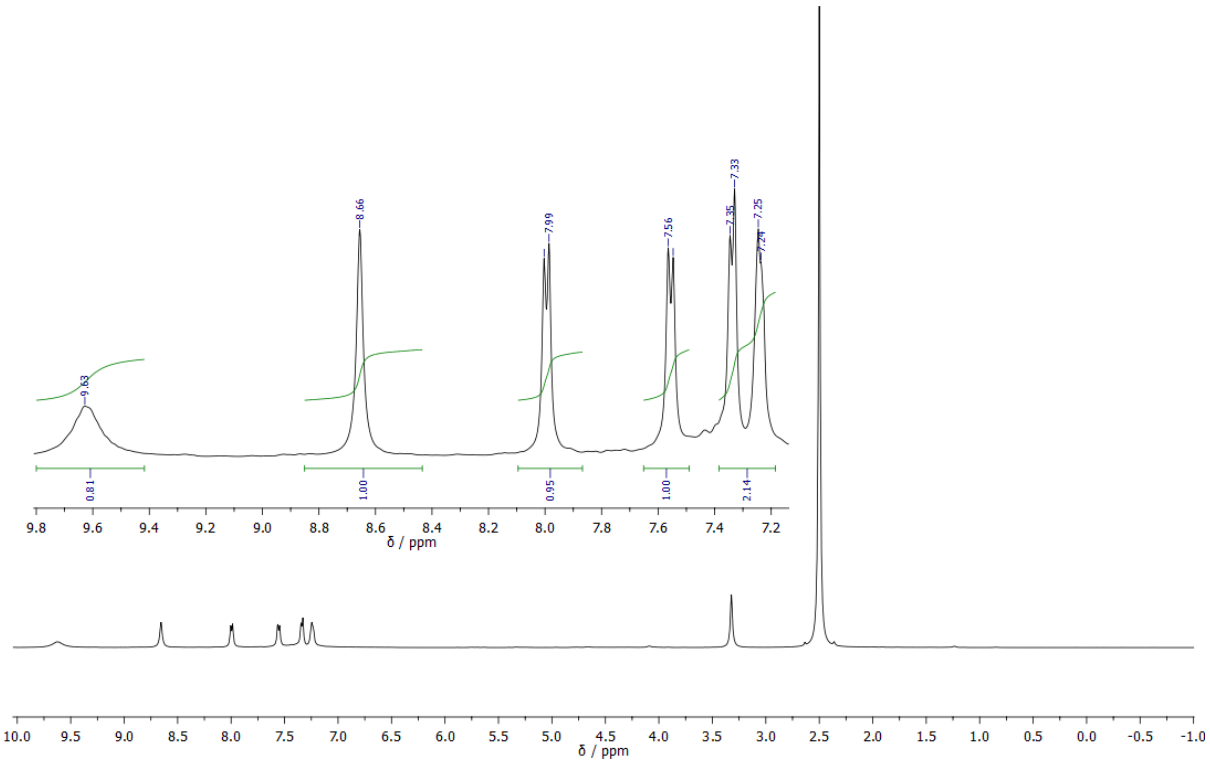

Figure SA8. ^{1}H-NMR, 500 MHz, DMSO-d_6

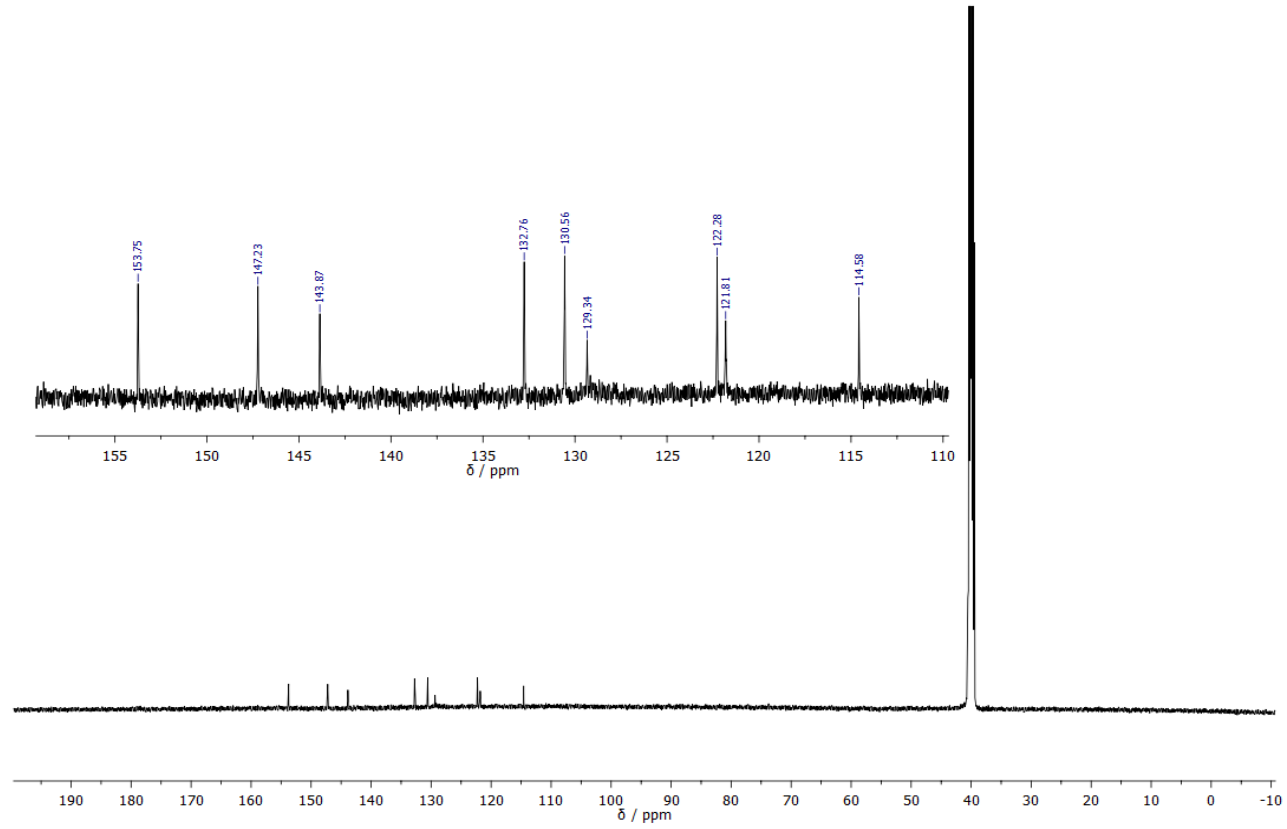

Figure SA9. ^{13}C-NMR, 125 MHz, DMSO-d_6

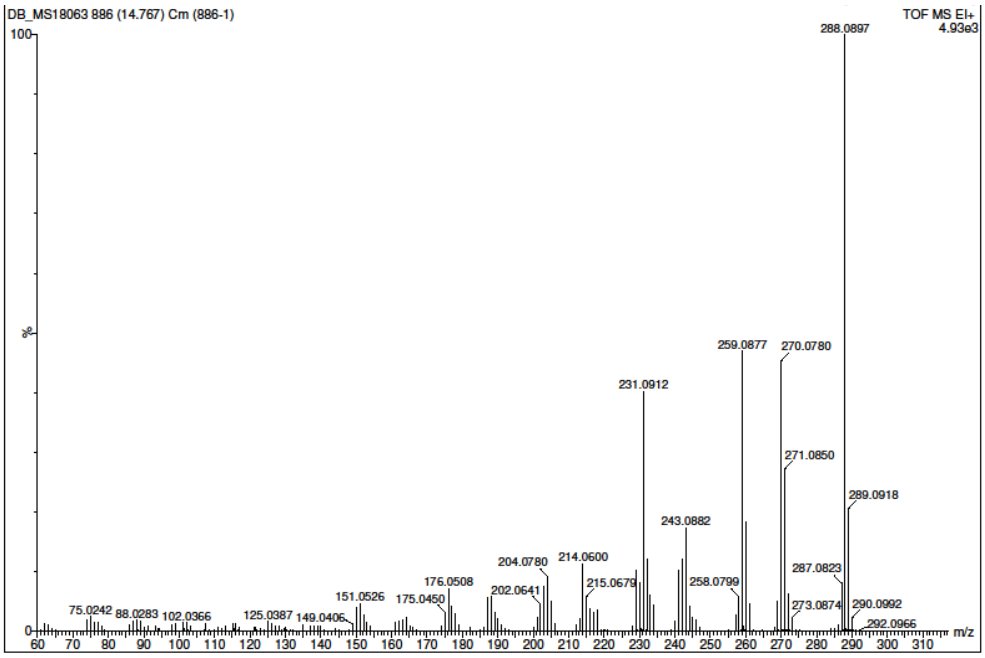

Figure SA10. HR-MS, EI-TOF.

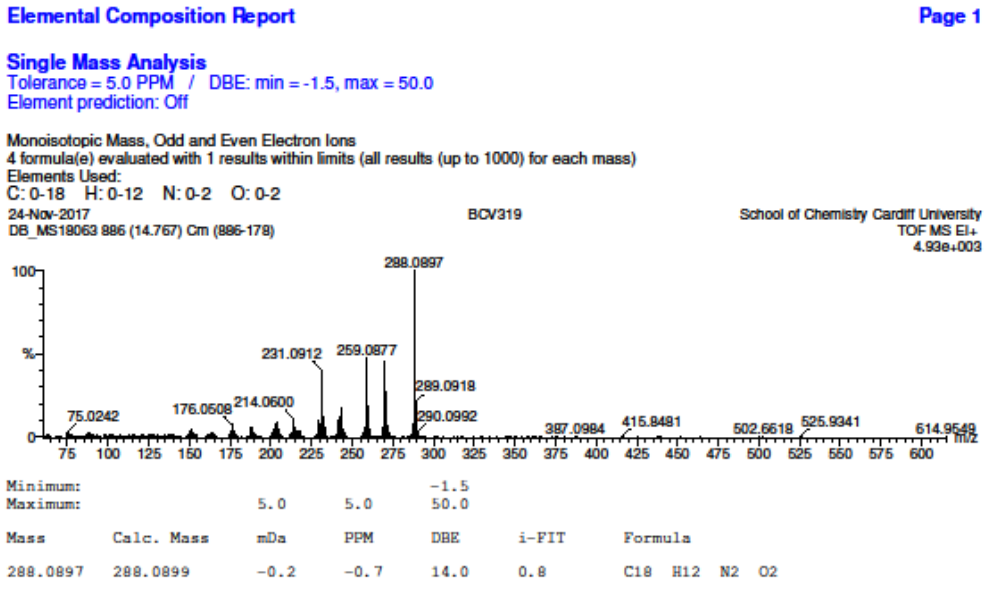

Figure SA11. Elemental Composition Report.

Characterisation of 3,9-diaza peri-xanthenoxanthene

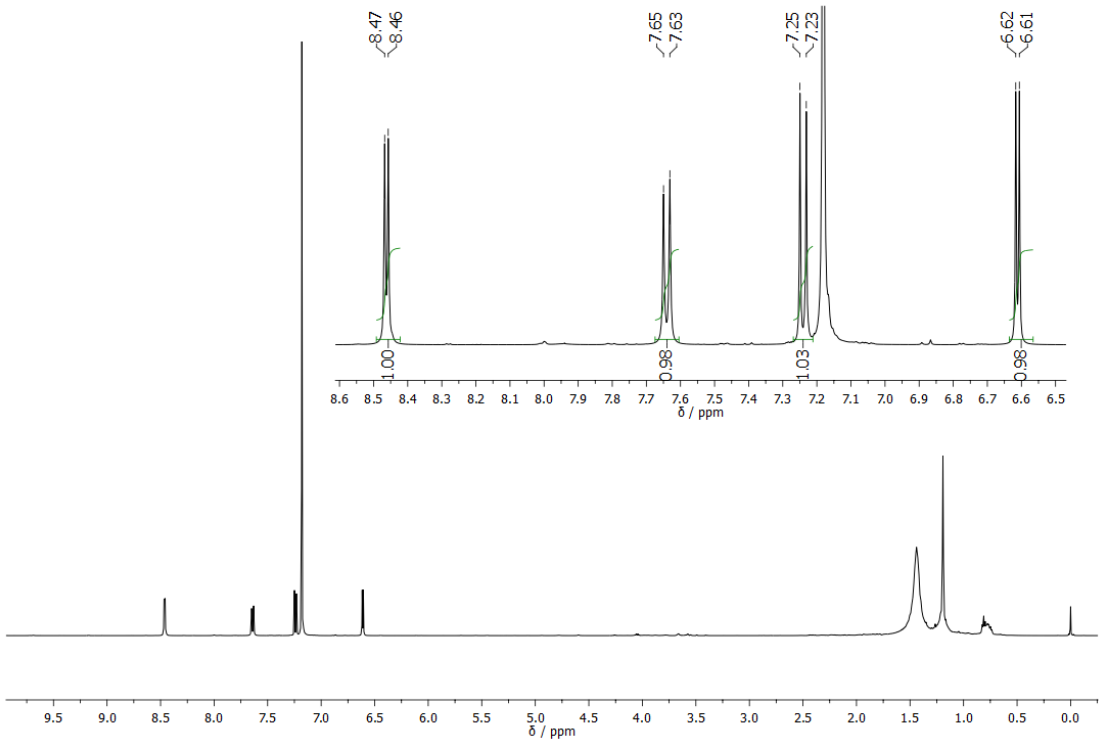

Figure SA12. ^{1}H-NMR, 500 MHz, $CDCl_3$

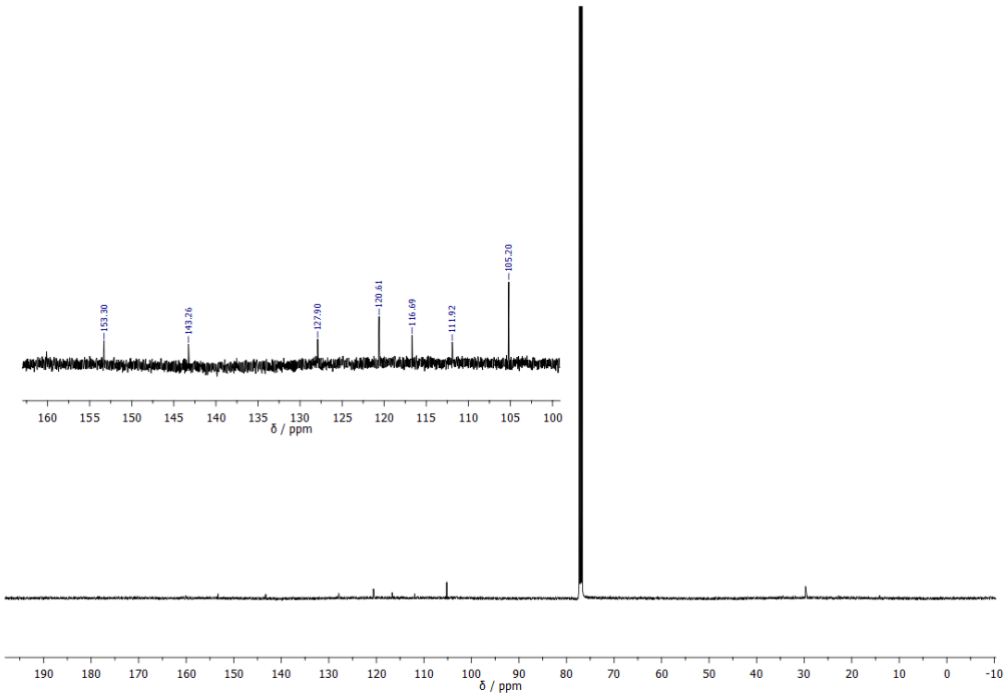

Figure SA13. ^{13}C-NMR, 125 MHz, $CDCl_3$

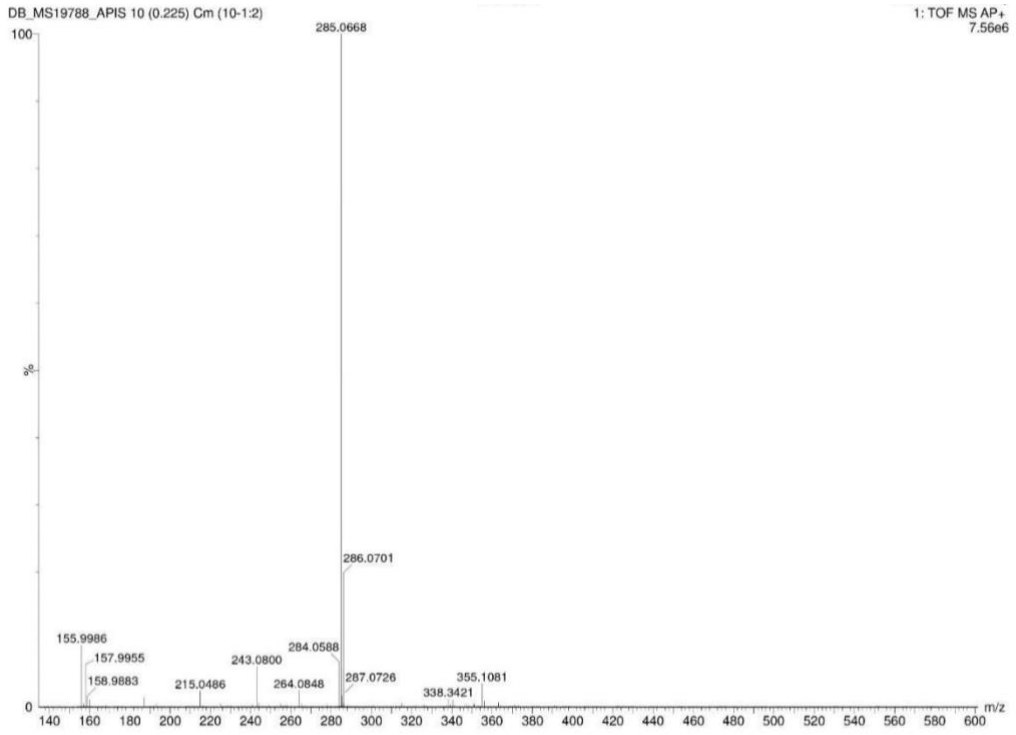

Figure SA14. HR-MS, AP-TOF.

Elemental Composition Report **Page 1**

Single Mass Analysis
Tolerance = 5.0 PPM / DBE: min = -1.5, max = 50.0
Element prediction: Off
Number of isotope peaks used for i-FIT = 3

Monoisotopic Mass, Odd and Even Electron Ions
4 formula(e) evaluated with 1 results within limits (up to 50 best isotopic matches for each mass)
Elements Used:
C: 0-18 H: 0-9 N: 0-2 O: 0-2

Minimum:				-1.5				
Maximum:		5.0	5.0	50.0				
Mass	Calc. Mass	mDa	PPM	DBE	i-FIT	Norm	Conf(%)	Formula
285.0668	285.0664	0.4	1.4	15.5	795.7	n/a	n/a	C18 H9 N2 O2

Figure SA15. Elemental Composition Report.

Characterisation of Quinolin-3-yl diethylcarbamate 4

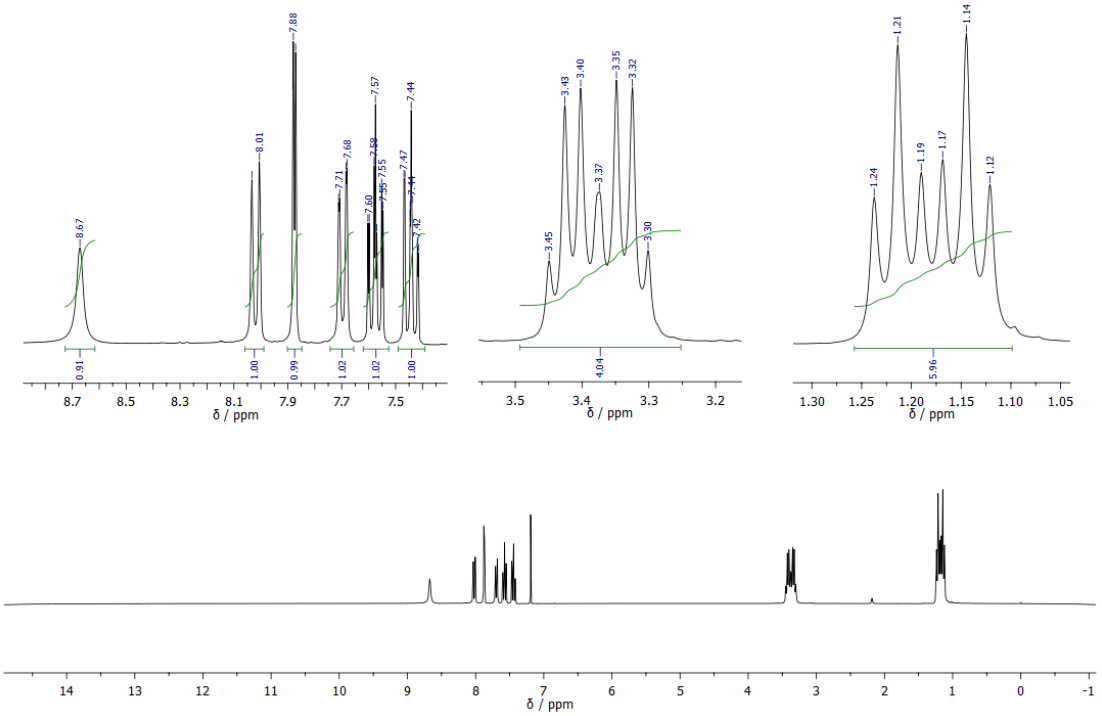

Figure SA16. ^{1}H-NMR, 300 MHz, $CDCl_3$

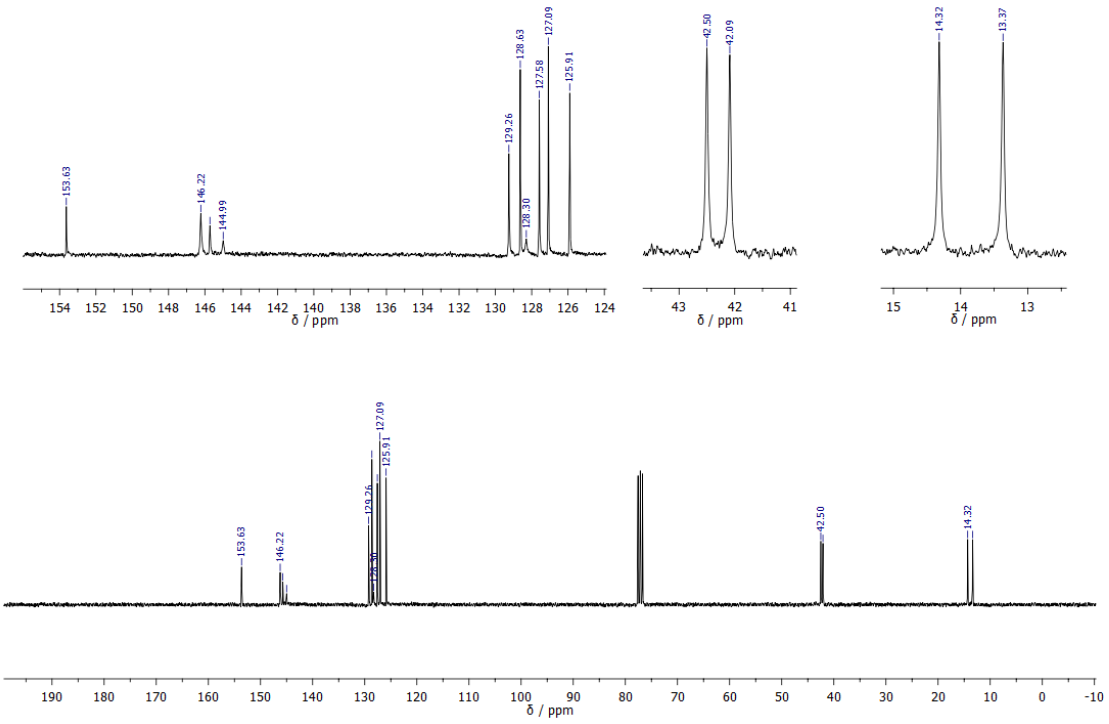

Figure SA17. ^{13}C-NMR, 75 MHz, $CDCl_3$

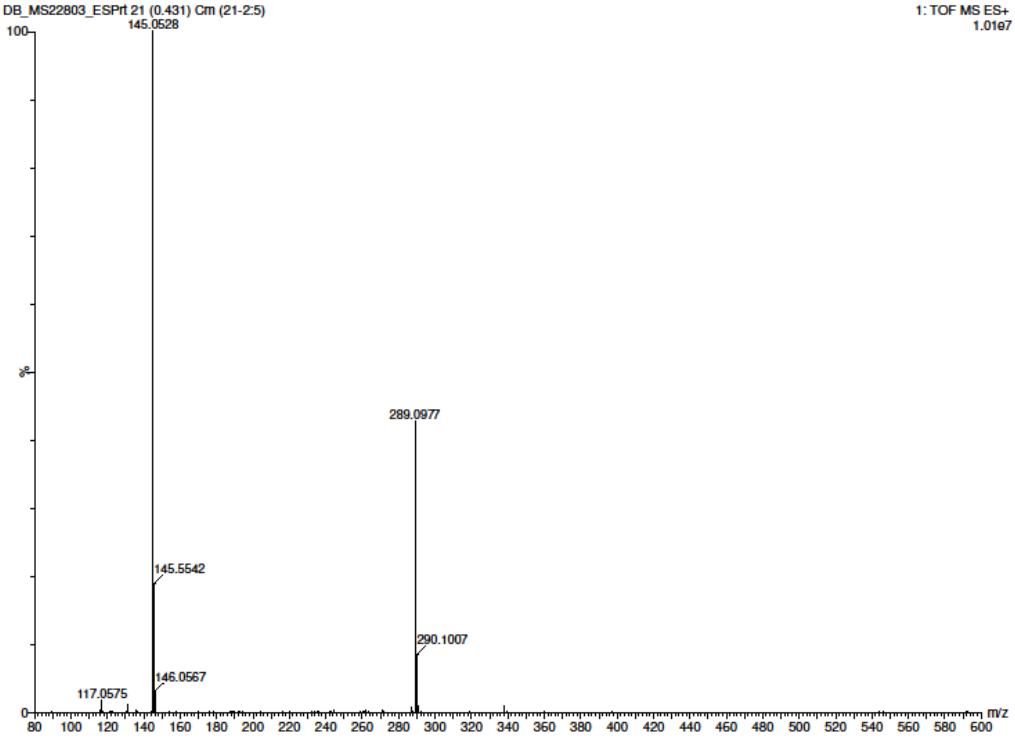

Figure SA18. HR-MS, ES-TOF.

Elemental Composition Report **Page 1**

Single Mass Analysis
Tolerance = 10.0 PPM / DBE: min = -1.5, max = 100.0
Element prediction: Off
Number of isotope peaks used for i-FIT = 3

Monoisotopic Mass, Odd and Even Electron Ions
4 formula(e) evaluated with 1 results within limits (up to 50 closest results for each mass)
Elements Used:
C: 0-18 H: 0-13 N: 0-2 O: 0-2

Minimum:				-1.5				
Maximum:		5.0	10.0	100.0				
Mass	Calc. Mass	mDa	PPM	DBE	i-FIT	Norm	Conf(%)	Formula
289.0977	289.0977	0.0	0.0	13.5	159.1	n/a	n/a	C18 H13 N2 O2

Figure SA19. Elemental Composition Report.

Characterisation of [4,4'-biquinoline]-3,3'-diyl bis(diethylcarbamate) 5

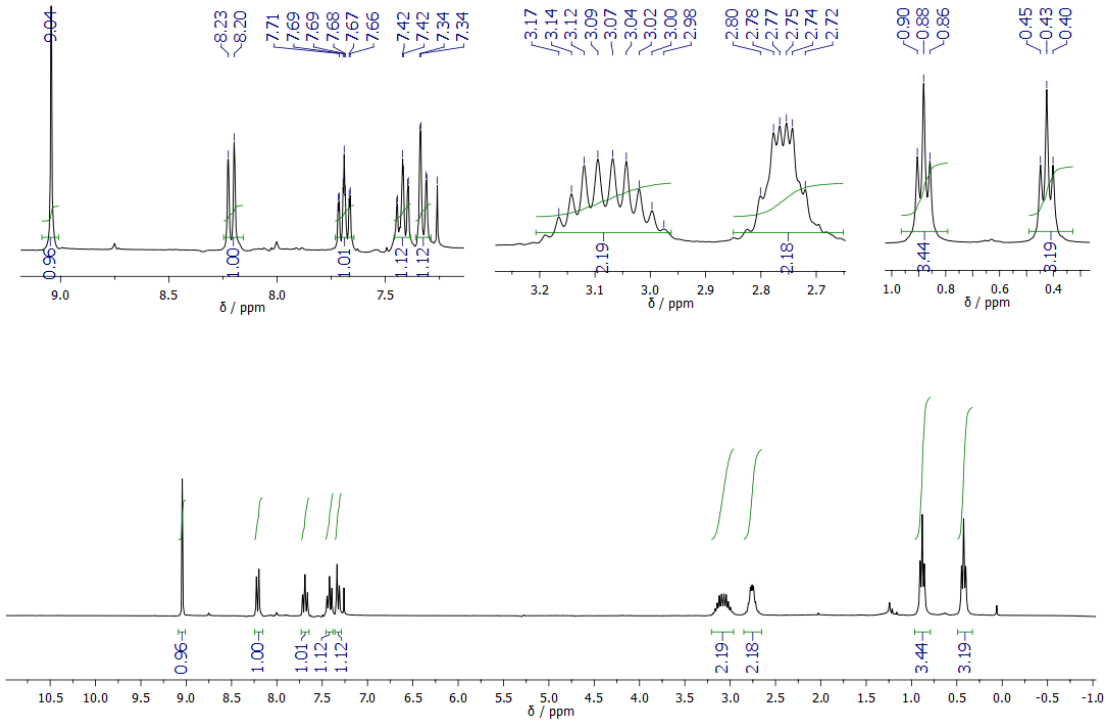

Figure SA20. ^{1}H-NMR, 300 MHz, $CDCl_3$

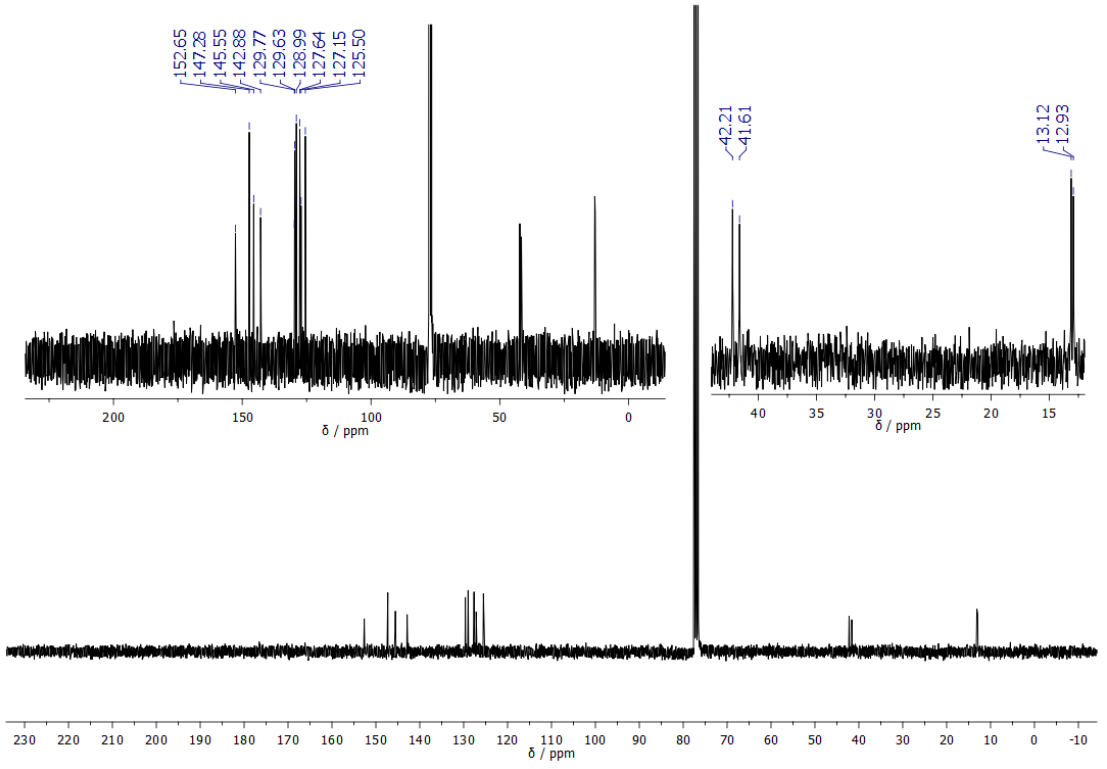

Figure SA21.^{13}C-NMR, 75 MHz, $CDCl_3$

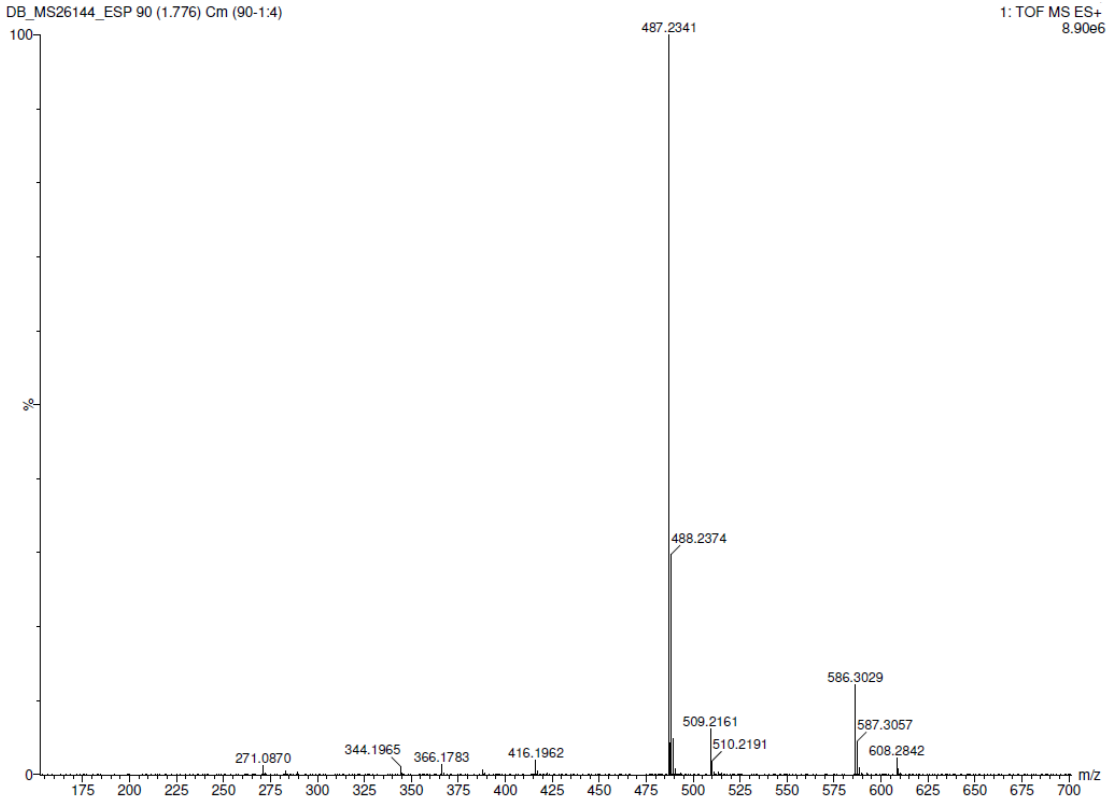

Figure SA22. HR-MS, ES-TOF.

Elemental Composition Report **Page 1**

Single Mass Analysis
Tolerance = 5.0 PPM / DBE: min = -1.5, max = 200.0
Element prediction: Off
Number of isotope peaks used for i-FIT = 3

Monoisotopic Mass, Odd and Even Electron Ions
20 formula(e) evaluated with 1 results within limits (up to 50 closest results for each mass)
Elements Used:
C: 0-28 H: 0-31 N: 0-4 O: 0-4

Minimum:				-1.5				
Maximum:		5.0	5.0	200.0				
Mass	Calc. Mass	mDa	PPM	DBE	i-FIT	Norm	Conf(%)	Formula
487.2341	487.2345	-0.4	-0.8	15.5	304.5	n/a	n/a	C28 H31 N4 O4

Figure SA23. Elemental Composition Report.

Characterisation of [4,4'-biquinoline]-3,3'-diol 6

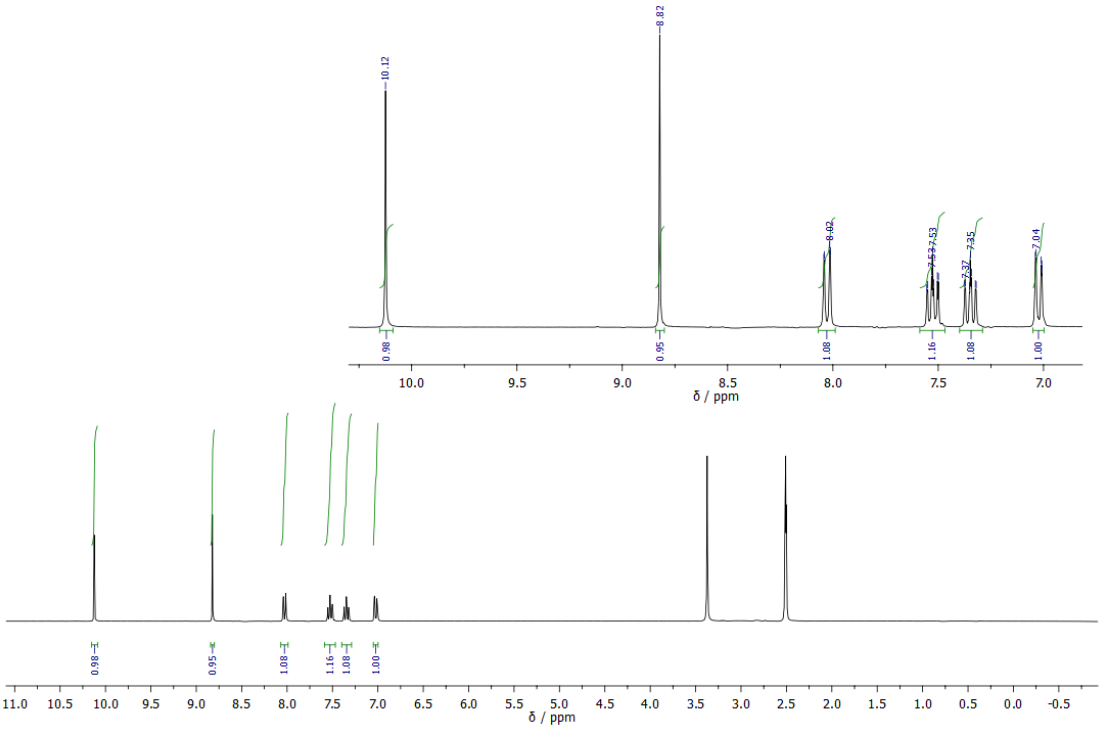

Figure SA24. ^{1}H-NMR, 500 MHz, DMSO-d_6

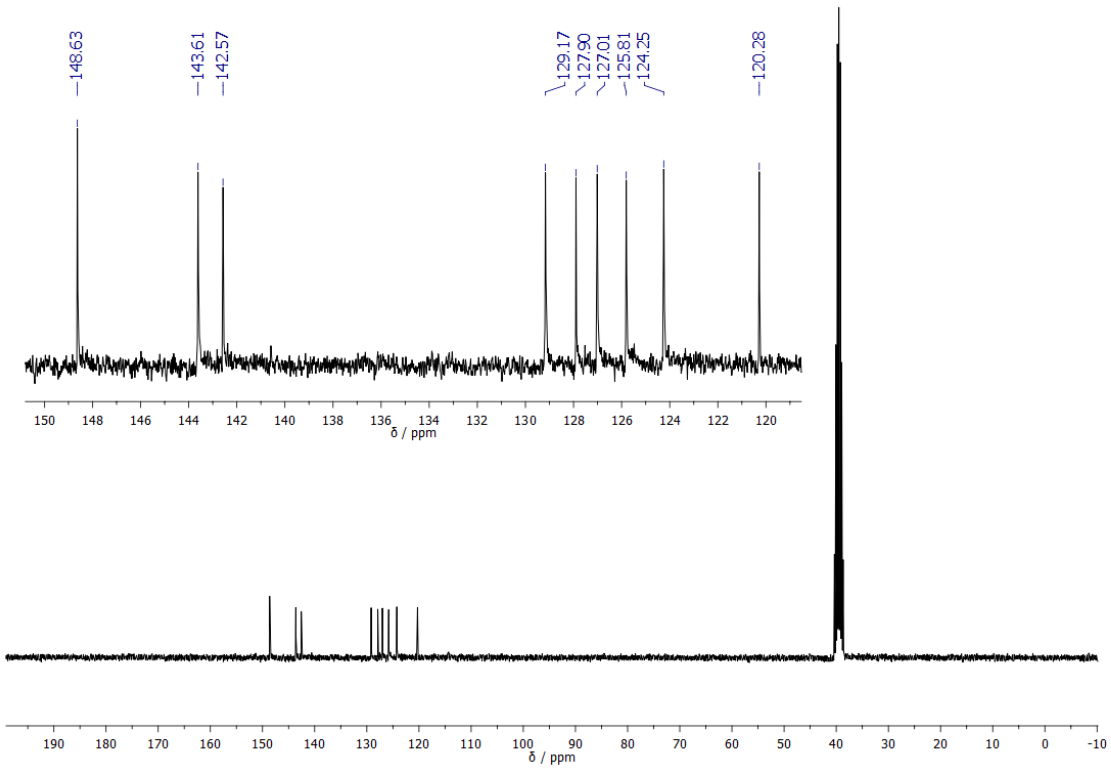

Figure SA25. ^{13}C-NMR, 125 MHz, DMSO-d_6

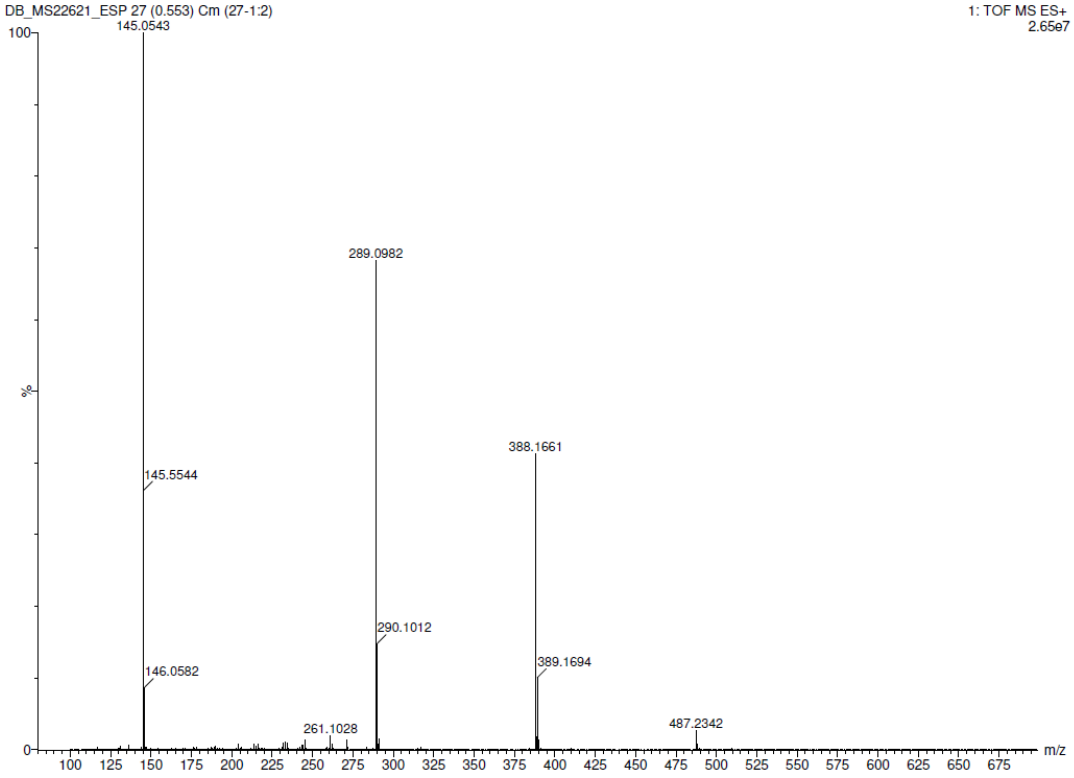

Figure SA26.HR-MS, ES-TOF.

Elemental Composition Report **Page 1**

Single Mass Analysis
Tolerance = 5.0 PPM / DBE: min = -1.5, max = 100.0
Element prediction: Off
Number of isotope peaks used for i-FIT = 3

Monoisotopic Mass, Odd and Even Electron Ions
4 formula(e) evaluated with 1 results within limits (up to 50 best isotopic matches for each mass)
Elements Used:
C: 0-18 H: 0-13 N: 0-2 O: 0-2

Minimum:				-1.5				
Maximum:		5.0	5.0	100.0				
Mass	Calc. Mass	mDa	PPM	DBE	i-FIT	Norm	Conf(%)	Formula
289.0982	289.0977	0.5	1.7	13.5	680.5	n/a	n/a	C18 H13 N2 O2

Figure SA27. Elemental Composition Report.

Characterisation of 4,10-diaza peri-xanthenoxanthene

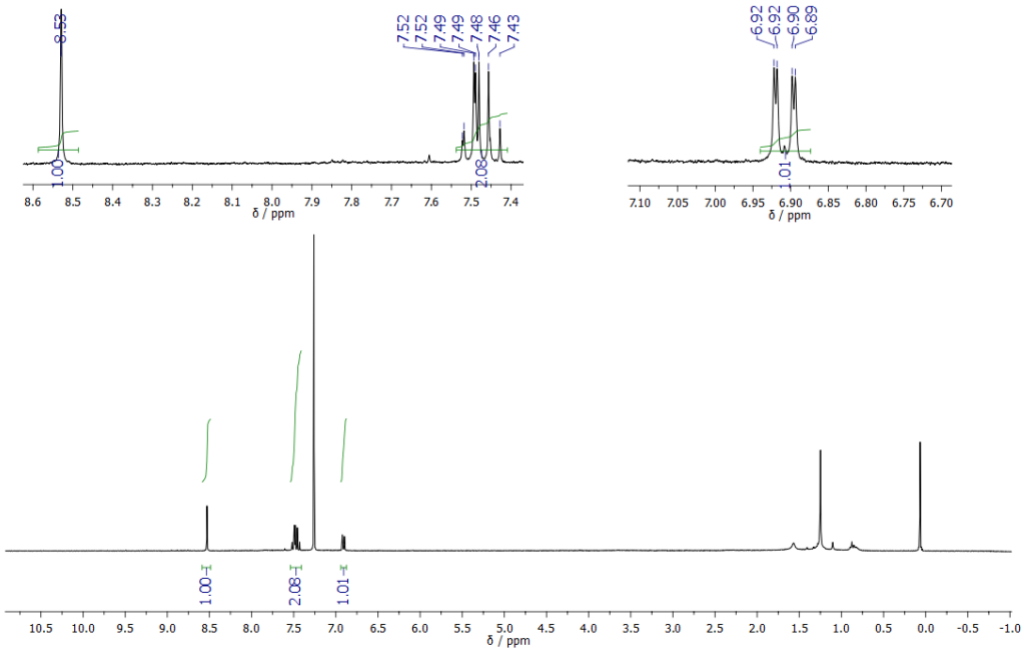

Figure SA28. ^{1}H-NMR, 500 MHz, $CDCl_3$

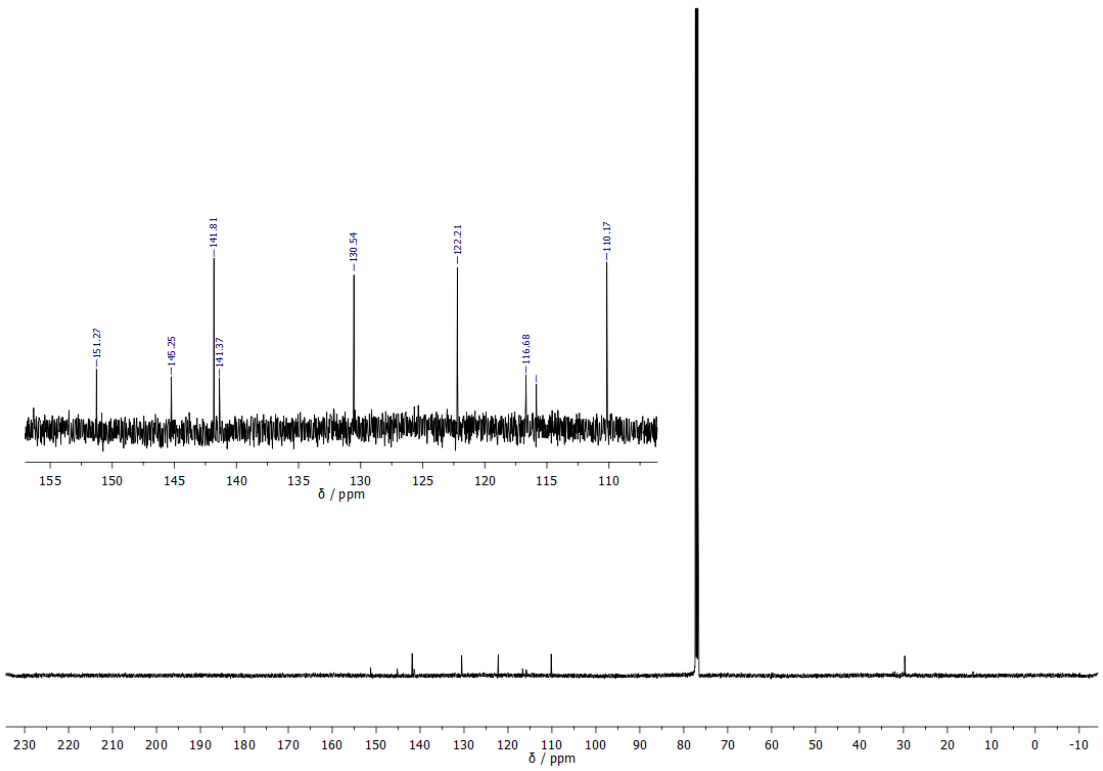

Figure SA29. ^{13}C-NMR, 125 MHz, $CDCl_3$

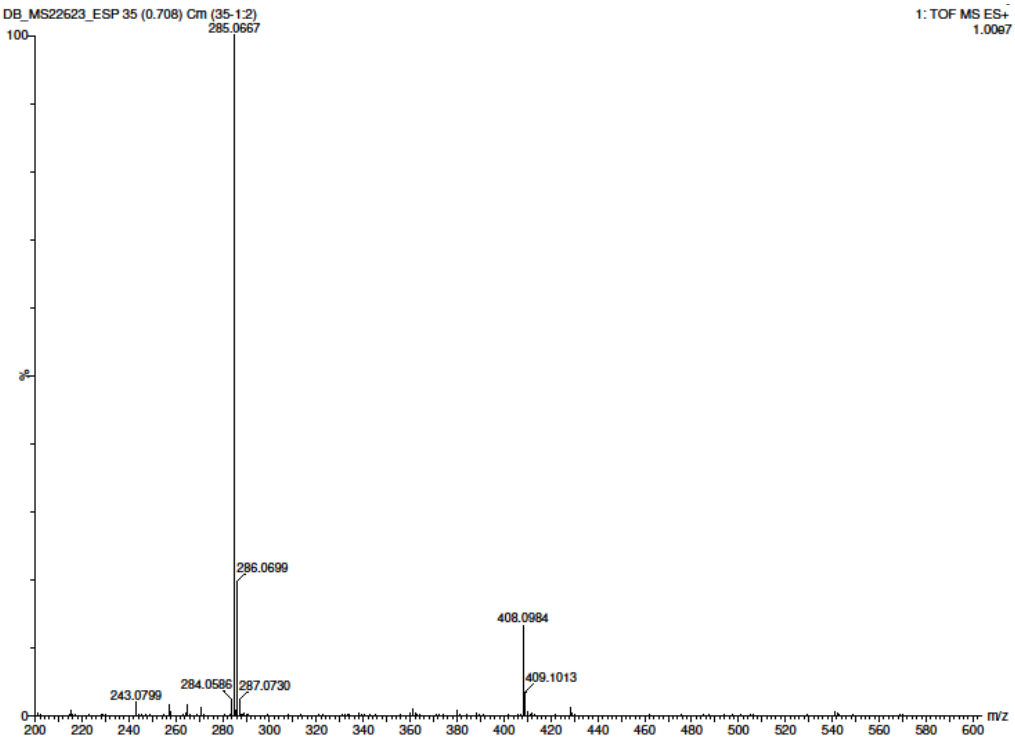

Figure SA30. HR-MS, ES-TOF.

Elemental Composition Report Page 1

Single Mass Analysis
Tolerance = 5.0 PPM / DBE: min = -1.5, max = 100.0
Element prediction: Off
Number of isotope peaks used for i-FIT = 3

Monoisotopic Mass, Odd and Even Electron Ions
4 formula(e) evaluated with 1 results within limits (up to 50 best isotopic matches for each mass)
Elements Used:
C: 0-18 H: 0-9 N: 0-2 O: 0-2

Minimum:				-1.5				
Maximum:		5.0	5.0	100.0				
Mass	Calc. Mass	mDa	PPM	DBE	i-FIT	Norm	Conf(%)	Formula
285.0667	285.0664	0.3	1.1	15.5	556.3	n/a	n/a	C18 H9 N2 O2

Figure SA31. Elemental Composition Report.

Characterisation of isoquinolin-3-yl diethylcarbamate 8

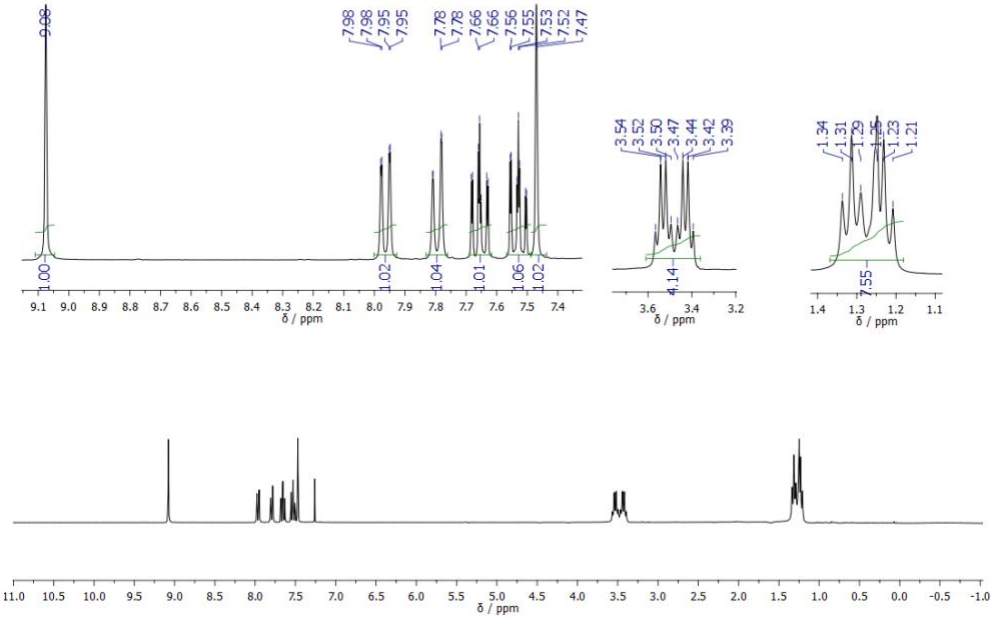

Figure SA32. ^{1}H-NMR, 300 MHz, $CDCl_3$

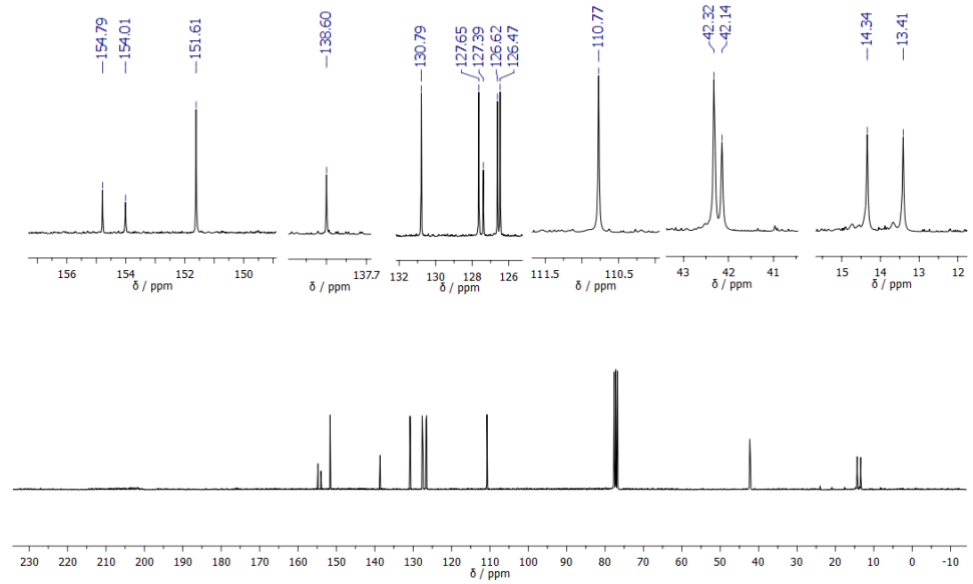

Figure SA33. ^{13}C-NMR, 75 MHz, $CDCl_3$

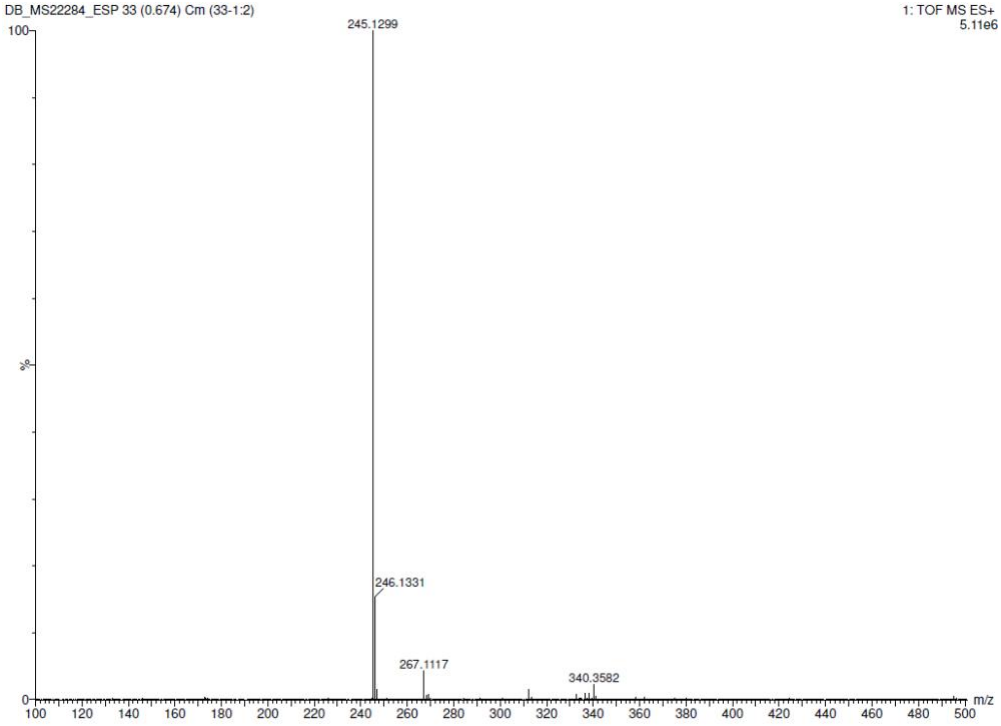

Figure SA34. HR-MS, ES-TOF.

Elemental Composition Report **Page 1**

Single Mass Analysis
Tolerance = 5.0 PPM / DBE: min = -1.5, max = 100.0
Element prediction: Off
Number of isotope peaks used for i-FIT = 3

Monoisotopic Mass, Odd and Even Electron Ions
7 formula(e) evaluated with 1 results within limits (up to 50 best isotopic matches for each mass)
Elements Used:
C: 0-14 H: 0-17 N: 0-2 O: 0-2

Minimum:				-1.5				
Maximum:		5.0	5.0	100.0				
Mass	Calc. Mass	mDa	PPM	DBE	i-FIT	Norm	Conf(%)	Formula
245.1299	245.1290	0.9	3.7	7.5	534.9	n/a	n/a	C14 H17 N2 O2

Figure SA35. Elemental Composition Report.

Characterisation of [4,4'-biisoquinoline]-3,3'-diyl bis(diethylcarbamate) 9

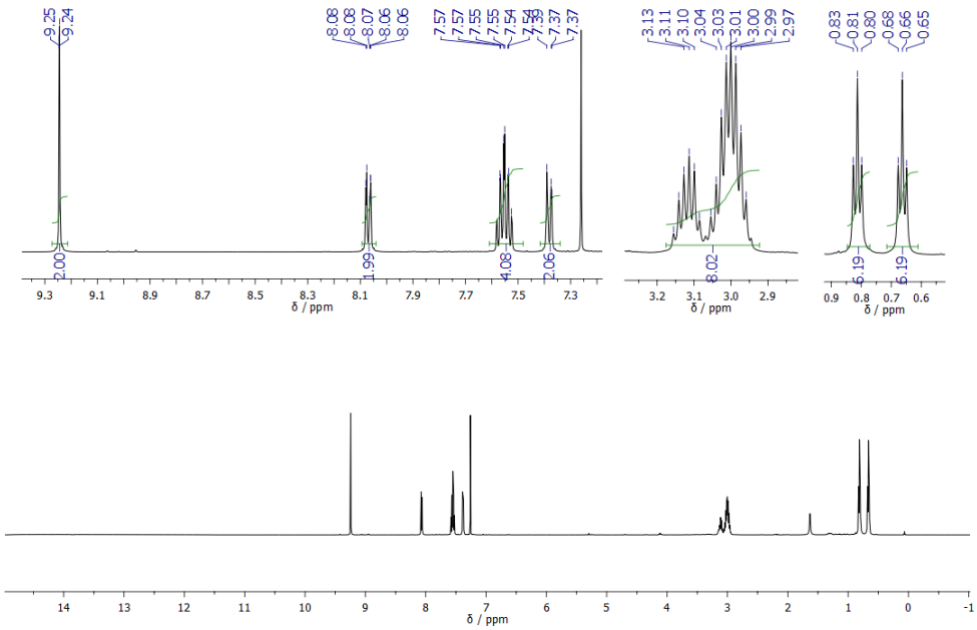

Figure SA36. ^{1}H-NMR, 300 MHz, $CDCl_3$

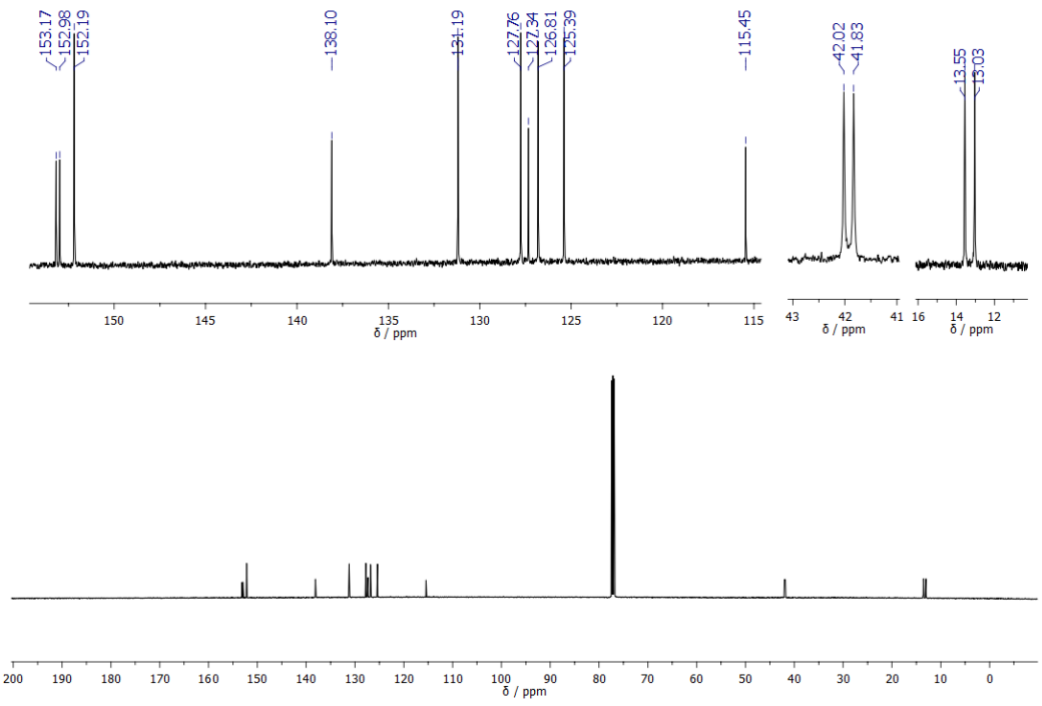

Figure SA37. ^{13}C-NMR, 75 MHz, $CDCl_3$

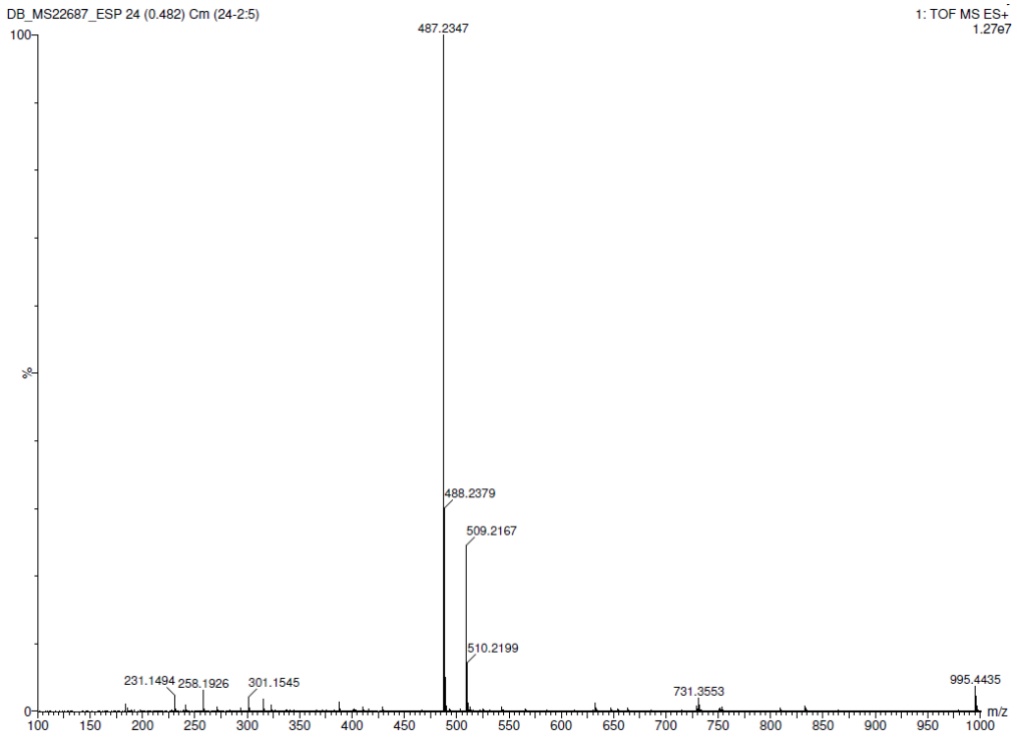

Figure SA38. HR-MS, ES-TOF.

Elemental Composition Report **Page 1**

Single Mass Analysis
Tolerance = 5.0 PPM / DBE: min = -1.5, max = 100.0
Element prediction: Off
Number of isotope peaks used for i-FIT = 3

Monoisotopic Mass, Odd and Even Electron Ions
20 formula(e) evaluated with 1 results within limits (up to 50 best isotopic matches for each mass)
Elements Used:
C: 0-28 H: 0-31 N: 0-4 O: 0-4

Minimum:				-1.5				
Maximum:		5.0	5.0	100.0				
Mass	Calc. Mass	mDa	PPM	DBE	i-FIT	Norm	Conf(%)	Formula
487.2347	487.2345	0.2	0.4	15.5	608.9	n/a	n/a	C28 H31 N4 O4

Figure SA39. Elemental Composition Report.

Characterisation of [4,4'-biisoquinoline]-3,3'-diol 10

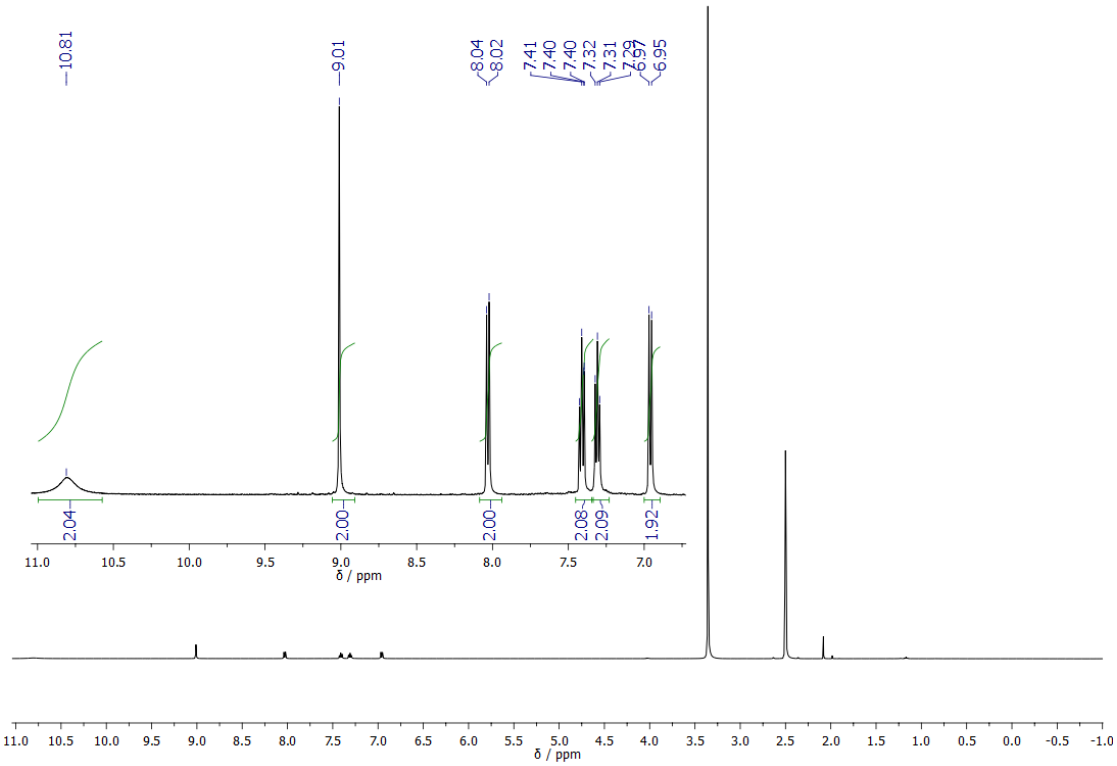

Figure SA40. ^{1}H-NMR, 500 MHz, DMSO-d_6

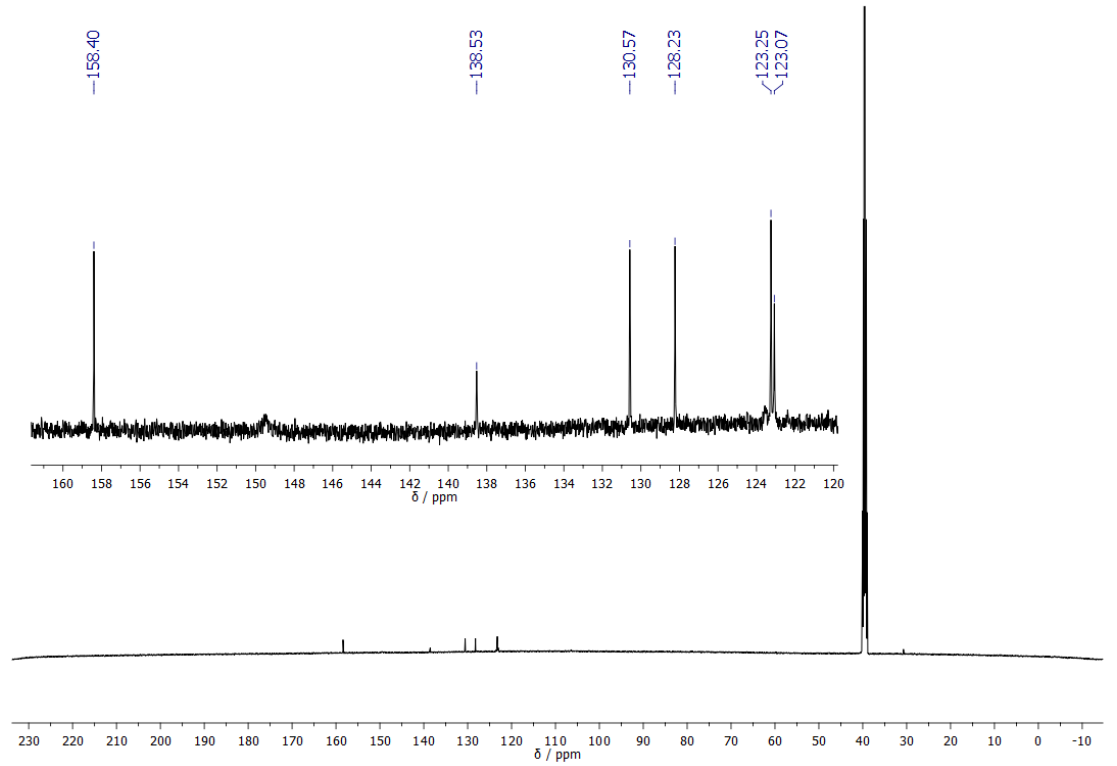

Figure SA41. ^{13}C-NMR, 125 MHz, DMSO-d_6

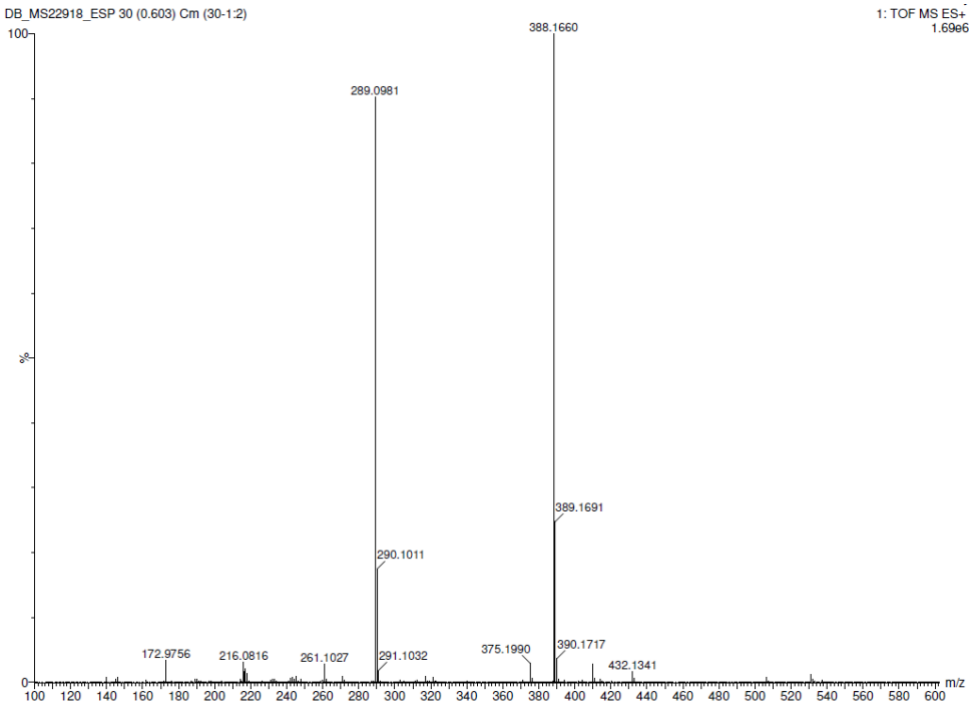

Figure SA42. HR-MS, ES-TOF.

Elemental Composition Report Page 1

Single Mass Analysis
Tolerance = 5.0 PPM / DBE: min = -1.5, max = 100.0
Element prediction: Off
Number of isotope peaks used for i-FIT = 3

Monoisotopic Mass, Odd and Even Electron Ions
4 formula(e) evaluated with 1 results within limits (up to 50 closest results for each mass)
Elements Used:
C: 0-18 H: 0-13 N: 0-2 O: 0-2

Minimum:				-1.5				
Maximum:		5.0	5.0	100.0				
Mass	Calc. Mass	mDa	PPM	DBE	i-FIT	Norm	Conf(%)	Formula
289.0981	289.0977	0.4	1.4	13.5	200.5	n/a	n/a	C18 H13 N2 O2

Figure SA43. Elemental Composition Report.

Characterisation of quinolin-3-yl diethylcarbamate 12

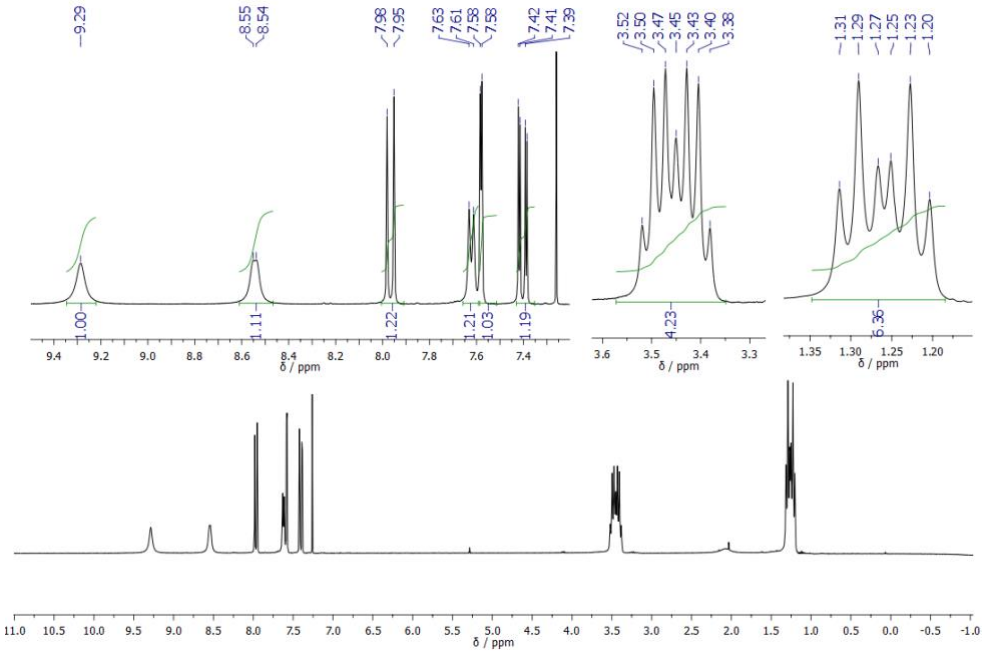

Figure SA44. ^{1}H-NMR, 300 MHz, $CDCl_3$

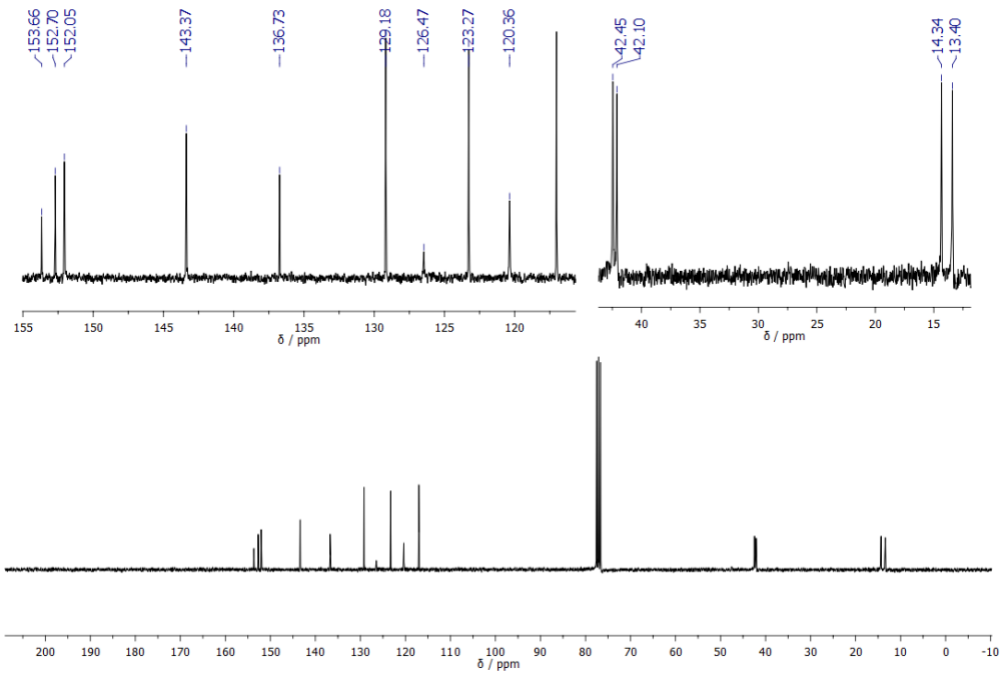

Figure SA45. ^{13}C-NMR, 75 MHz, $CDCl_3$

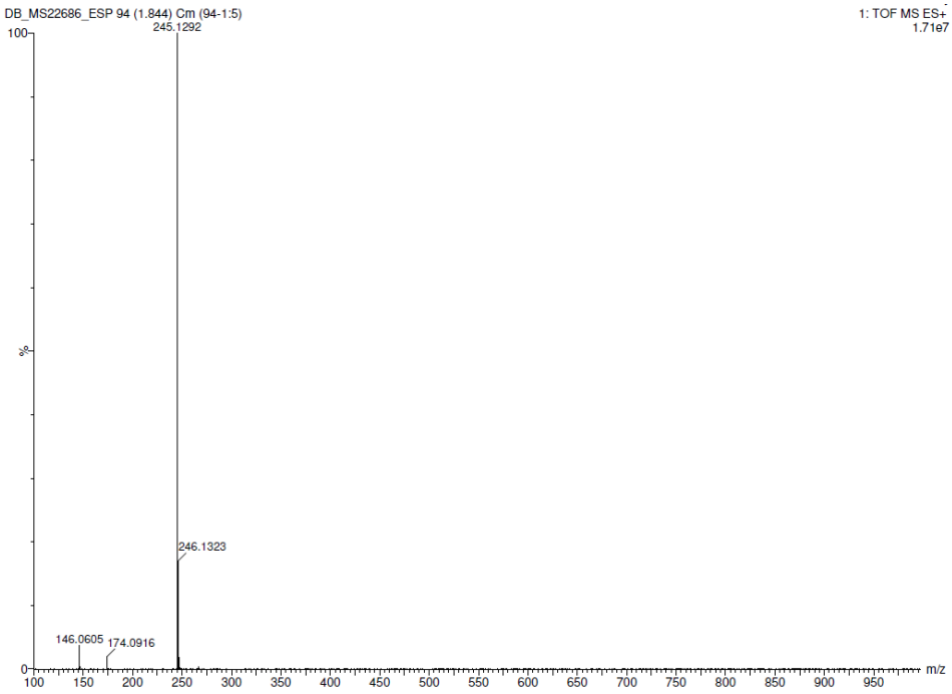

Figure SA46. HR-MS, ES-TOF.

Elemental Composition Report **Page 1**

Single Mass Analysis
Tolerance = 5.0 PPM / DBE: min = -1.5, max = 100.0
Element prediction: Off
Number of isotope peaks used for i-FIT = 3

Monoisotopic Mass, Odd and Even Electron Ions
7 formula(e) evaluated with 1 results within limits (up to 50 best isotopic matches for each mass)
Elements Used:
C: 0-14 H: 0-17 N: 0-2 O: 0-2

Minimum:				-1.5				
Maximum:		5.0	5.0	100.0				
Mass	Calc. Mass	mDa	PPM	DBE	i-FIT	Norm	Conf(%)	Formula
245.1292	245.1290	0.2	0.8	7.5	519.8	n/a	n/a	C14 H17 N2 O2

Figure SA47. Elemental Composition Report.

Characterisation of 5-hydroxyisoquinolin-6-yl diethylcarbamate 14

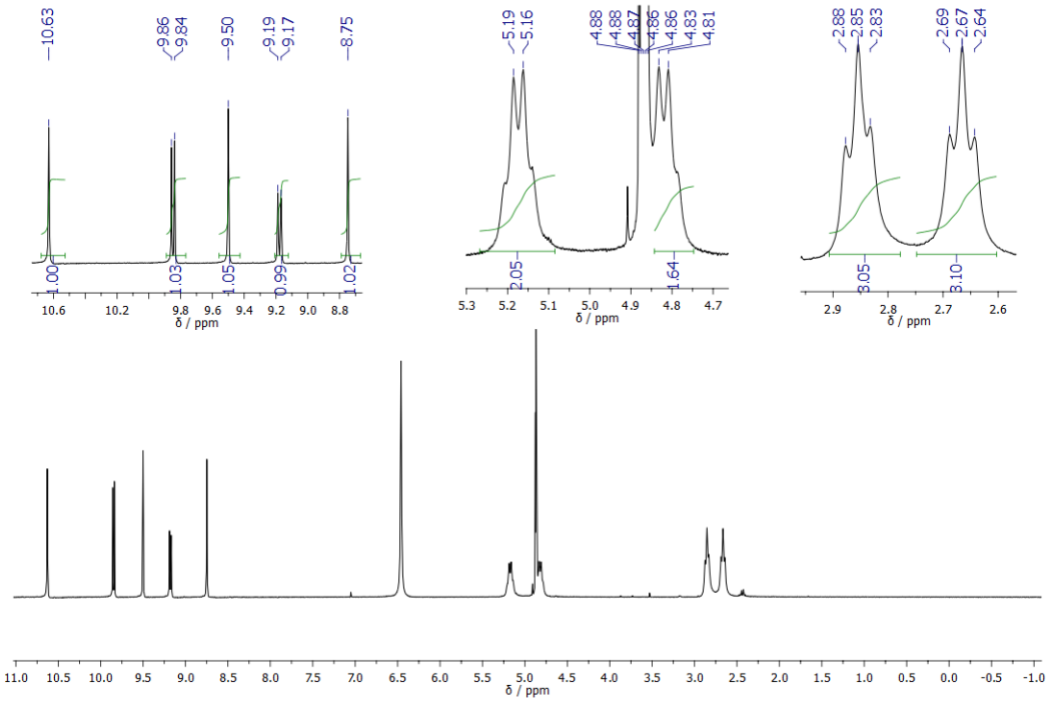

Figure SA48. ^{1}H-NMR, 300 MHz, CD_3OD

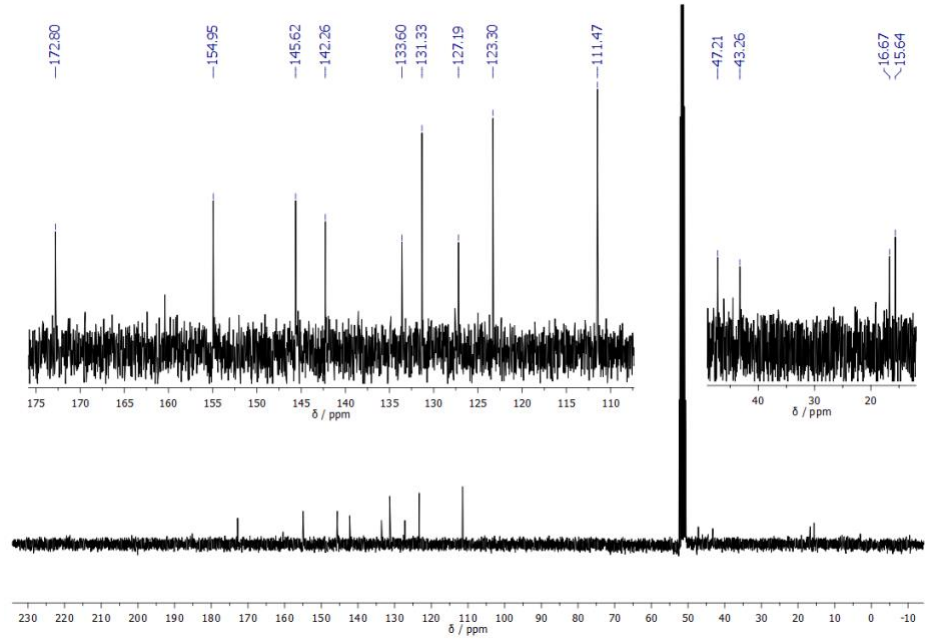

Figure SA49. ^{13}C-NMR, 75 MHz, CD_3OD

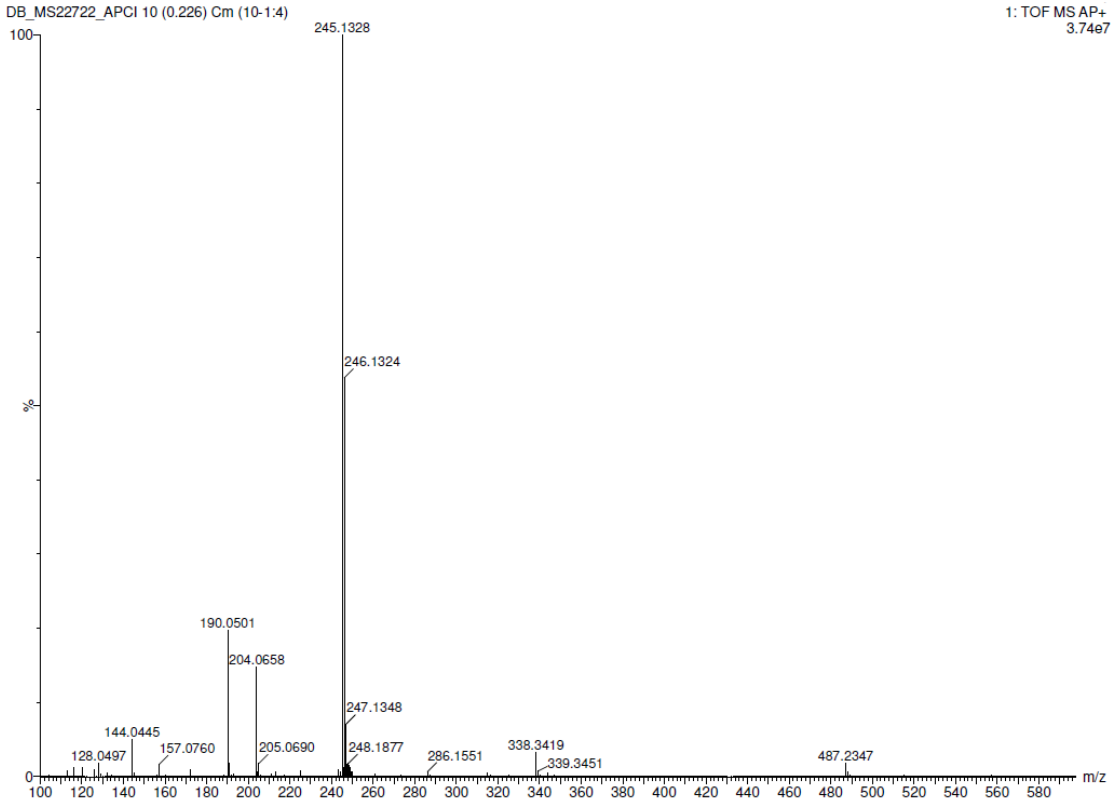

Figure SA50. HR-MS, AP-TOF.

Elemental Composition Report **Page 1**

Single Mass Analysis
Tolerance = 5.0 PPM / DBE: min = -1.5, max = 100.0
Element prediction: Off
Number of isotope peaks used for i-FIT = 3

Monoisotopic Mass, Odd and Even Electron Ions
40 formula(e) evaluated with 1 results within limits (up to 50 best isotopic matches for each mass)
Elements Used:
C: 0-28 H: 0-31 N: 0-4 O: 0-4 S: 0-1

Minimum:				-1.5				
Maximum:		5.0	5.0	100.0				
Mass	Calc. Mass	mDa	PPM	DBE	i-FIT	Norm	Conf(%)	Formula
487.2347	487.2345	0.2	0.4	15.5	335.7	n/a	n/a	C28 H31 N4 O4

Figure SA51. Elemental Composition Report.

Characterisation of 1,9-diaza peri-xanthenoxanthene

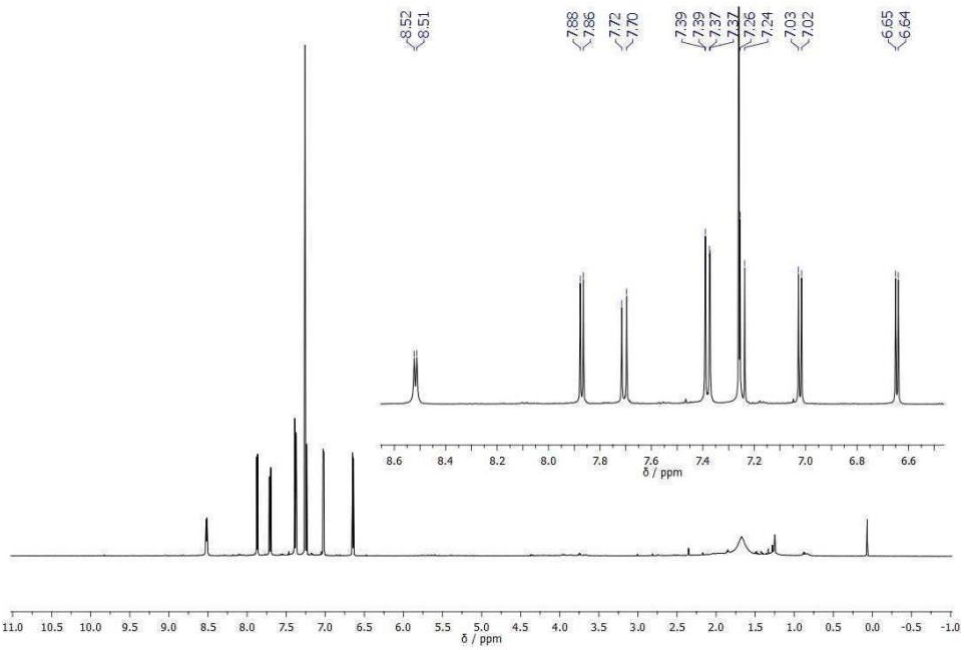

Figure SA52. ^{1}H-NMR, 500 MHz, $CDCl_3$

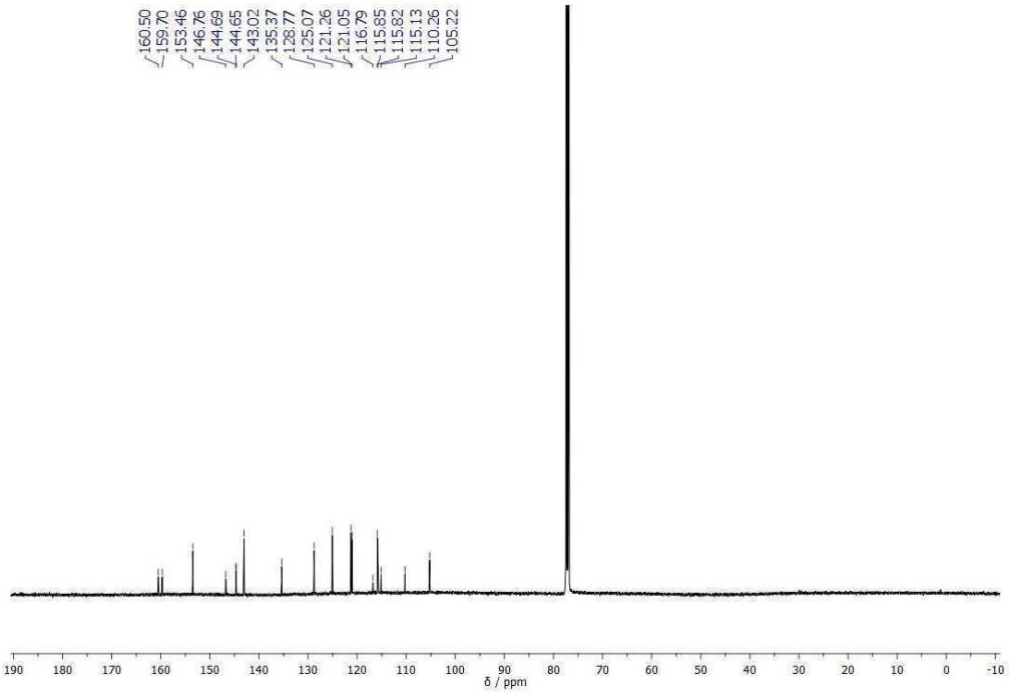

Figure SA53. ^{13}C-NMR, 125 MHz, $CDCl_3$

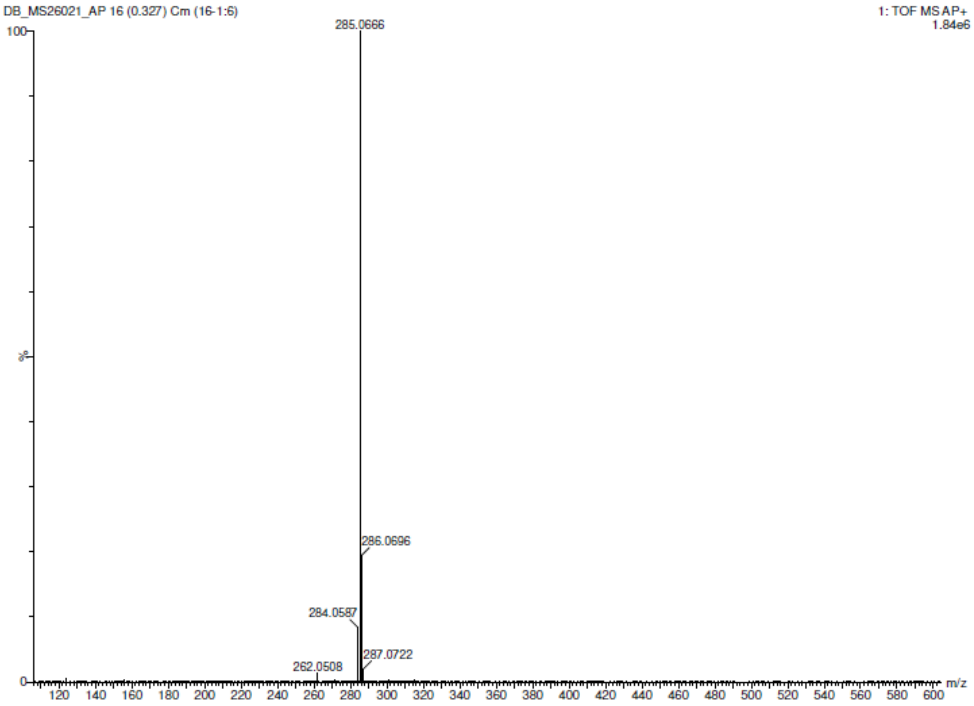

Figure SA54.: HR-MS, AP-TOF.

Elemental Composition Report **Page 1**

Single Mass Analysis
Tolerance = 5.0 PPM / DBE: min = -1.5, max = 200.0
Element prediction: Off
Number of isotope peaks used for i-FIT = 3

Monoisotopic Mass, Odd and Even Electron Ions
4 formula(e) evaluated with 1 results within limits (up to 50 closest results for each mass)
Elements Used:
C: 0-18 H: 0-9 N: 0-2 O: 0-2

Minimum:				-1.5				
Maximum:		5.0	5.0	200.0				
Mass	Calc. Mass	mDa	PPM	DBE	i-FIT	Norm	Conf(%)	Formula
285.0666	285.0664	0.2	0.7	15.5	269.7	n/a	n/a	C18 H9 N2 O2

Figure SA55. Elemental Composition Report.

Characterisation of molecule 3

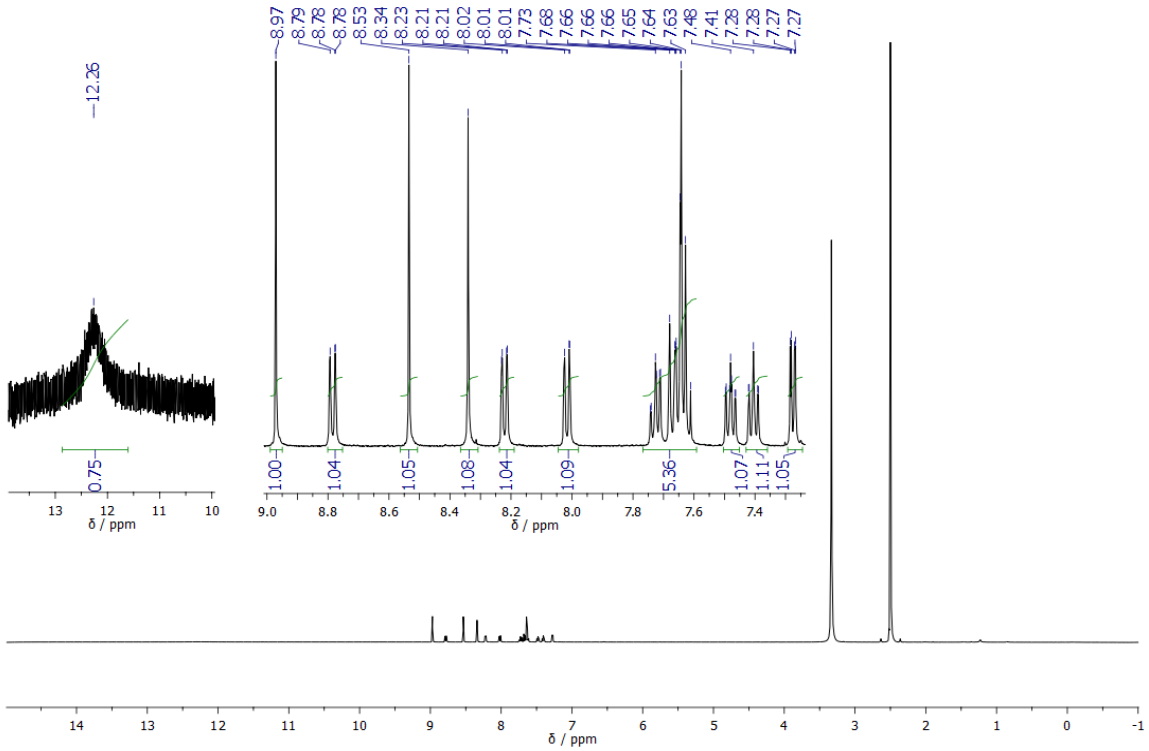

Figure SA56. ^{1}H-NMR, 500 MHz, $CDCl_3$

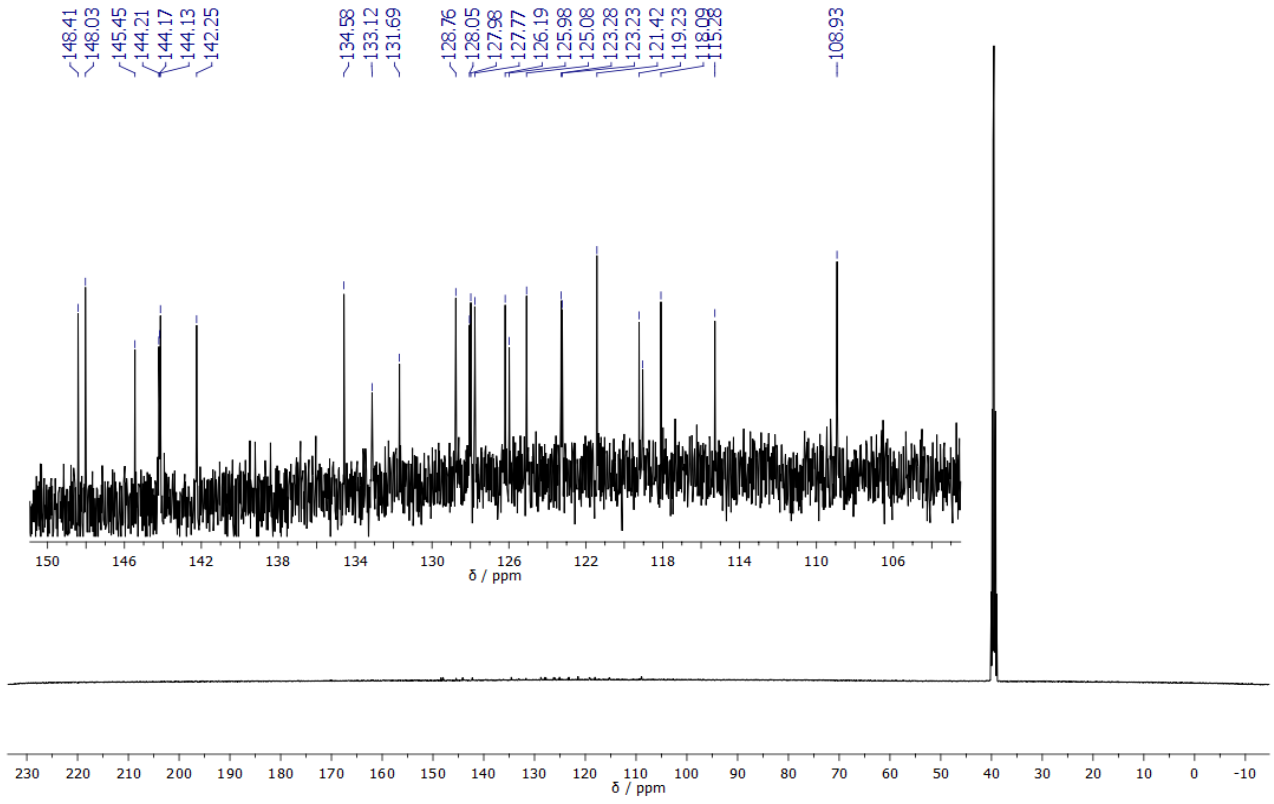

Figure SA57. ^{13}C-NMR, 125 MHz, $CDCl_3$

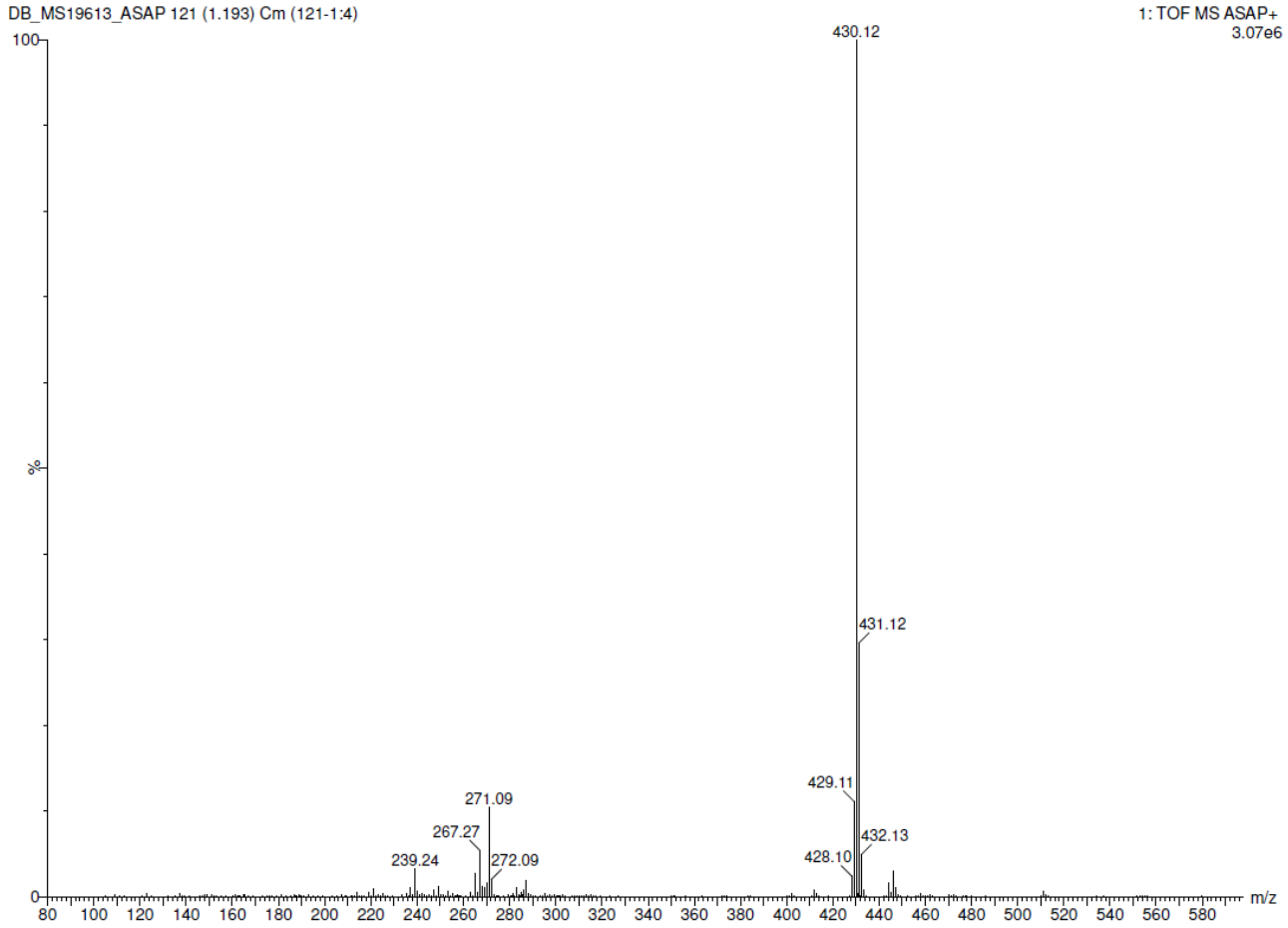

Figure SA58.: LR-MS, ASAP-TOF.

8. References

1 G. A. Crosby and J. N. Demas, *J. Phys. Chem.*, 1971, **75**, 991–1024.

2 Y. X. Chen, L. W. Yang, Y. M. Li, Z. Y. Zhou, K. H. Lam, a S. Chan and H. L. Kwong, *Chirality*, 2000, **12**, 510–513.

3 Y. Carissan, D. Hagebaum-Reignier, N. Goudard and S. Humbel, *J. Phys. Chem. A*, 2008, **112**, 13256–13262.

4 Y. Carissan, Hagebaum-Reignier, D. N. Goudard and S. Humbel, 2008, http://www.hulis.free.fr.

5 D. A. Bahnick, *J. Chem. Educ.*, 1994, **71**, 171–173.